THE FORMATION OF ENDOSYMBIOTIC MEMBRANE COMPARTMENTS: MEMBRANE IDENTITY MARKERS AND THE REGULATION OF VESICLE TRAFFICKING

Sergey Ivanov

Thesis committee

Thesis supervisor
Prof. dr. T. Bisseling
Professor of Molecular Biology
Wageningen University

Thesis co-supervisors
Dr. E.E. Fedorova,
Researcher, Laboratory of Molecular Biology, Wageningen University
Dr. ir. E.H.M. Limpens
Assistant professor, Laboratory of Molecular Biology, Wageningen University

Other members
Prof. dr. ir. J. Bakker, Wageningen University
Prof. dr. ir. F.P.M. Govers, Wageningen University
Dr. E.T. Kiers, VU University Amsterdam
Prof. dr. F. Krajinski, Max Planck Institute of Molecular Plant Physiology, Potsdam, Germany

This research was conducted under the auspices of the graduate School of Experimental Plant Sciences

The formation of endosymbiotic membrane compartments: membrane identity markers and the regulation of vesicle trafficking

Sergey Ivanov

Thesis
submitted in fulfillment of the requirements for the degree of doctor
at Wageningen University
by the authority of Rector Magnificus
Prof. dr. M.J. Kropff,
in the presence of the
Thesis Committee appointed by the Academic Board
to be defended in public
on Thursday 6 September 2012
at 11 a.m. in the Aula

Contents

Outline

Plants as sessile organisms have limited access to vital elements like nitrogen and phosphorus. The evolutionary pressure to improve access to such nutrients is well underlined by the success of certain endosymbiotic interactions. Plants acquired the ability to form a symbiotic relation with certain fungal species like arbuscular mycorrizae (AM) fungi which facilitate phosphorus uptake. The importance of this endosymbiosis is well illustrated by the fact that 80% of current higher plants have maintained this symbiosis that first evolved about 450 million years ago. The availability of a nitrogen source that can be used by plants especially depends on the process of biological nitrogen fixation by microbes. These microbes have the ability to transform atmospheric nitrogen into ammonia. The endosymbiosis of *Rhizobium* bacteria and plants of the legume family results in one of the most efficient biological nitrogen fixing systems. This symbiosis evolved about 60 million years ago shortly after the rise of legume plant family.

In both symbiotic interactions the microbes are hosted in an intracellular membrane compartment made by the host. These membrane compartments form the heart of these endosymbiotic interactions as it controls the exchange of compounds between host and its microsymbiont. In the model legume *Medicago truncatula* (*Medicago*) AM fungi form highly branched hyphae inside root cortical cells. These hyphae are called arbuscules and are surrounded by a periarbuscular membrane made by the host. *Medicago* can also establish a symbiosis with *Rhizobium* bacteria. In this symbiosis, bacteria are internalized into cells of new plant organ, root nodule. Root nodules are formed as a result of this plant-bacterium interaction. Intracellular bacteria are surrounded by a membrane, called symbiosome membrane and this membrane compartment and bacterium form a nitrogen-fixing organelle-like structure, which is named symbiosome. As *Medicago* can establish both symbiotic interactions, it is a good model system to study and compare these interactions. The main questions I addressed in this thesis concerned the molecular and cellular mechanisms by which symbiotic (periarbuscular and symbiosome) membranes are formed. I have used identity markers of plant cellular endomembrane system to unravel molecular and cell biological mechanisms that are involved in symbiotic membrane formation.

In chapter one, we describe the state of the art concerning the role of endo- and exocytotic-like processes in symbiosome formation. As the formation of symbiosomes primarily involves exocytosis, we discussed the role of secretory mechanisms in a broader perspective comparing the *Rhizobium* symbiosis with plants interacting with symbiotic and pathogenic biotrophic fungi, respectively.

To study the previously postulated endocytotic nature of symbiosome formation, we used in chapter two a set of molecular membrane identity markers. These markers are small GTPases belonging to the Rab family and SNARE (*s*oluble *N*-ethylmaleimide sensitive factor *a*ttachment protein *re*ceptor) proteins which prime and execute fusion of membranes, respectively. A default endocytotic pathway consists of several subsequent steps. It starts from engulfing molecules or larger particles by inward membrane budding. The formed membrane vesicles, that are named early endosomes, mature into late endosomes which in their turn ultimately fuse with vacuoles. To test whether the mechanism controlling release of rhizobia from the infection thread (symbiosome formation) is derived from endocytosis

we studied whether an identity marker of early endosomes (SNARE MtSYP41) and one of late endosome (GTPase MtRab5) occur at symbiosome membranes. Neither of these two identity markers could at any stage of development be detected on symbiosomes. So our studies strongly suggest that symbiosome formation is not derived from the endocytotic pathway. However, symbiosomes are labeled by the vacuolar marker MtRab7 when they reach an elongated stage. As this indicates that symbiosomes might have a vacuolar nature, we tested whether vacuolar SNAREs are present on symbiosomes. This showed that neither SNAREs localized on the target membrane (t-SNARE: MtSYP22, MtSYP52, MtVTI11) nor those of transport vesicles (v-SNARE: MtVAMP711) are present on functional symbiosomes. However, they do appear on symbiosome membranes at the onset of senescence. This explains that during senescence homotypic fusion of symbiosomes and fusion with vacuoles take place that triggers symbiosomes to be turned into a lytic compartment. In addition, we tested an identity marker of the plasma membrane (t-SNARE MtSYP132). We showed that this SNARE is present on symbiosomes at all stages of development. Hence, we hypothesized that an exocytotic pathway is involved in symbiosome formation and this hypothesis was tested in chapter three.

In chapter three, we described the function of SNAREs belonging to the VAMP72 group, which are involved in exocytosis to the plasma membrane via the trans-Golgi network compartment. We have identified six *MtVAMP72* genes in *Medicago*. Functional analysis of the *MtVAMP72* genes using an RNAi approach showed that two genes, *MtVAMP72d* and *MtVAMP721e*, are essential in establishing symbiosis. They are essential for release of the *Rhizobium* bacteria inside host cells as well as for symbiosome division. In the AM symbiosis they are also essential for intracellular accommodation of the fungus (arbuscule formation). Using GFP fusions as well as antibodies against these symbiotic MtVAMP72s we showed that MtVAMP-positive vesicles accumulate at the site of rhizobial release and periarbuscular membrane. So we identified an exocytotic pathway essential for symbiotic membrane formation in both symbioses and we postulated that this pathway was co-opted by the *Rhizobium* symbiosis from the more ancient AM fungal symbiosis.

In chapter four, we have extended the studies on the function of the symbiotic MtVAMP72s to early steps of microbial infection of the root. We used real time confocal imaging to determine changes in MtVAMP72 accumulation upon perifungal membrane formation. This membrane structure is formed when the fungus penetrates root epidermal and outer cortical cells intracellularly. Root colonization starts when hyphopodia (swollen hyphal tips also referred as appresoria) adhere to the host root epidermis. It triggers the formation of a prepenetration apparatus, a large column of cytoplasm, packed with cytoskeleton, endoplasmic reticulum, Golgi apparatus, mitochondria and secretory vesicles between the nucleus and the contact point. The fungal hypha penetrates the epidermal cell through the track laid down by the prepenetration apparatus and becomes surrounded by invagination of the host plasma membrane (perifungal membrane). We expressed MtVAMP72 with a relatively strong heterologous promoter and showed that GFP tagged MtVAMP721d/e accumulates at the tip of growing hyphae, the site of perifungal membrane formation. Furthermore, components of the secretory machinery including endoplasmic reticulum and Golgi apparatus accumulate at the site of perifungal membrane formation in all steps of trans-cellular live style of fungus.

In chapter five (concluding remarks) we discussed the data obtained in this thesis as well as recent literature on the formation of symbiotic interfaces. We especially discussed the nature of the endosymbiotic compartments and their evolution.

Chapter 1

Intracellular plant microbe associations: secretory pathways and the formation of perimicrobial compartments

Sergey Ivanov, Elena Fedorova and Ton Bisseling

Laboratory of Molecular Biology, Graduate School Experimental Plant Science, Wageningen University, Droevendaalsesteeg 1, 6708PB Wageningen, The Netherlands

Plants can establish intracellular interactions with symbiotic as well as pathogenic microbes. Such intracellular accommodation of microbes always involves the formation of a host membrane compartment – the interface between the cytoplasm of the host and the microbe. These are the so-called perimicrobial compartments. In this review we will focus on the *Rhizobium*-legume symbiosis in which the microbes are hosted in organelle-like compartments, which are named symbiosomes. The signaling events leading to infection and symbiosome formation are discussed. Further the role of the host cell endomembrane system in symbiosome formation is described and compared with the processes involved in arbuscule and haustorium formation during the interaction of plants and biotrophic fungi.

Introduction

Higher plants are able to interact with microbes in various ways. These interactions can be pathogenic or beneficial and can vary from extracellular associations to intracellular accommodation of microorganisms. In this review, we will focus on intracellularly hosted microbes. A well studied example is the symbiosis of rhizobial bacteria and legume plants that leads to the formation of N_2-fixing root nodules. We will focus on this interaction and will compare it with the interaction of biotrophic fungi/oomycetes that also can establish an intracellular interaction with plants.

Establishing these intracellular interactions involves two major steps: (a) the microbe enters the plant to reach its target cells; (b) target cells are infected and in these cells specialized membrane compartments enclosing the microbes are made by the host cells (Fig. 1). These so-called perimicrobial membranes form an interface between host cytoplasm and microbe and facilitate, for example, exchange of nutrients. We will briefly describe the signaling events and cell biological changes in host cells when microbes infect their host plant and subsequently induce the formation of perimicrobial compartments.

Cell biology of infection and formation of perimicrobial compartments

In general, rhizobia enter the root epidermis by intracellular infection threads (ITs). These are tube-like structures that direct bacteria to their target cells (Gage, 2004; Brewin, 2004), which are newly formed nodule primordium cells produced by mitotic activation of cortical cells. IT initiation involves root hair curling, which entraps the bacteria. There, the cell wall is degraded in a local manner and this brings bacteria into contact with the root hair plasma membrane. By vesicle targeting to this site a new inward growing IT is formed that guides the bacteria to the base of root hair cells. Subsequently, rhizobia are released into the apoplast and a new IT is formed in the adjacent cortical cell layer. This process is repeated till the nodule primordium is reached. There ITs penetrate primordial cells and subsequently, bacteria are released into the host cells. The release is preceded by formation of the so-called unwalled droplet, where the cell wall of the IT is absent and bacteria come in close contact with the IT membrane (Fig. 1*A*). At such local entry points, bacteria enter the cytoplasm of the plant by an endocytosis-like process. In this way, bacterium becomes surrounded by a host cell derived membrane, the peribacteroid membrane (PBM). PBM and enclosed bacteria form the symbiosome (SB). SBs subsequently divide and differentiate into their N_2-fixing stage and can markedly enlarge. These SBs ultimately completely fill the infected cells (Fig. 2).

In addition to rhizobia, *Frankia* actinomycetes can also establish an N_2-fixing nodular symbiosis. Their host plants (e.g. *Alnus* and *Casuarina*) form nodules where actinorhizal symbionts occupy cells by forming intracellular hyphae surrounded by a perimicrobial membrane of host origin (Guan *et al*., 1998).

Arbuscular mycorrhizas (AM) are symbiotic biotrophic fungi that enter the root epidermis and cross the outer cortex intracellularly. In the inner root cortex cells hyphae either grow intercellularly (in legumes) or remain intracellular (Genre *et al*., 2008). Despite these differences intracellular penetration of inner cortex cells leads to arbuscule formation in both cases (Fig. 1*B*). Arbuscules are highly branched intracellular hyphae that
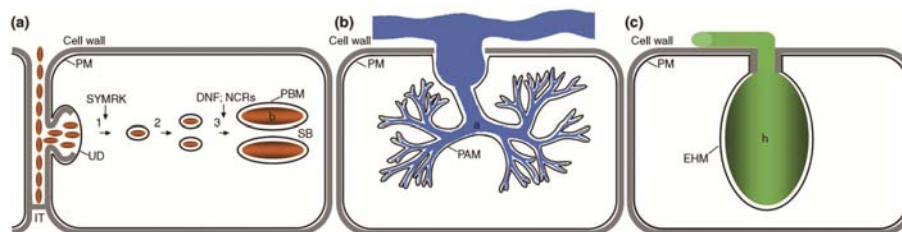
Figure 1. Schematic representation of intracellular membrane compartments formed by microorganism during plant infection. (*A*) In most legumes the release of rhizobia into the host cytoplasm is preceded by the formation of so-called unwalled droplets (*UD*); at these sites the bacteria are released (*1*) from infection threads (*IT*) and (for example in *Lotus* and *Medicago*) each bacterium becomes surrounded by a host membrane, the peribacteroid membrane (*PBM*). The bacterium and surrounding PBM undergo synchronic division (*2*) and growth (*3*). Once the bacterium stops dividing it terminally differentiate into its symbiotic nitrogen-fixing form called bacteroid (*b*) and with its surrounding PBM it forms the symbiosome (*SB*). Some host genes that are known to control a certain step of symbiosome development have been indicated. (*B*) During the interaction with arbuscular micorrhizal (AM) fungi intercellular hypha form side branches which penetrate cortical cells, arbuscules (*a*). These form multiple thin branches surrounded by a host membrane (periarbuscular membrane, PAM). (*C*) Haustoria (*h*) are formed from a terminal side branch of a hypha of a biotrophic pathogenic fungus and surrounded by an extrahaustorial membrane (*EHM*) formed by the host.

are surrounded by a host membrane which is named periarbuscular membrane (PAM) (Parniske, 2008).

Pathogenic biotrophic fungi/oomycetes can colonize the host plant in various ways (O'Connel and Panstruga, 2006) before they form intracellular feeding structures. In obligate biotrophs side branches of hyphae that terminate in the penetrated host cell form the haustoria (Fig. 1*C*). Haustoria are surrounded by a plant membrane, extrahaustorial membrane (EHM). Hemibiotrophs and some obligate biotrophs form filamentous intracellular hyphae which can penetrate from cell to cell (O'Connel and Panstruga, 2006). So in all cases microbes are surrounded by a membrane of plant origin in their intracellular stage. In this way nutrients can be exchanged in a controlled manner.

Signaling events inducing infection

When microbes enter a host cell this is preceded by the formation of a preinfection structure by the host at the site of entry. It is a cytoplasmic aggregation formed by cytoskeletal elements, the repositioning of the nucleus, endoplasmic reticulum and Golgi apparatus and facilitates the targeting of vesicles to the site of microbial entry. This is the case for symbiotic and pathogenic biotrophic fungi as well as rhizobia (Genre *et al*., 2005; Hardham *et al*., 2007). Therefore it is very likely that the microbe signals its host by which changes are induced in the host endomembrane processes.

In the *Rhizobium*-legume symbiosis the bacterial Nod factor (NF) plays a pivotal role in the induction of the infection process and accompanying changes in endomembrane biology. These lipochito-oligosaccharides are perceived in the root epidermis by LysM domain receptor kinases (Limpens *et al*., 2003; Madsen *et al*., 2003) that share homology with the chitin receptor (Gimenez-Ibanez *et al*., 2009). The NF signaling cascade that is activated by these receptors has recently been reviewed in detail (Oldroyd and Downie, 2008;

Den Herder and Parniske, 2009). Among others this cascade involves a leucine-rich receptor-like kinase located in the plasma membrane (SymRK), putative calcium-activated potassium channels located in the nuclear envelope (*Lotus japonicus* CASTOR and POLLUX; *Medicago truncatula* DMI1,) and a calcium/calmodulin-dependent protein kinase (CCamK). These NF signaling components do result in the activation of transcription regulators like NSP1/NSP2, NIN and ERN.

SymRK, DMI1 and CCamK have initially been identified as essential components for rhizobial NF-induced infection. Surprisingly, these host factors were also shown to be essential for the infection of root cells by AM fungi (Parniske, 2008) as well as for haustorium formation in roots by the hemibiotrophic pathogenic fungus *Colle-*

Figure 2. *Medicago truncatula* root nodule cell filled with symbiosomes. The peribacteroid membrane (arrow) of the symbiosomes is visualized by GFP-Rab7. v, vacuole. (Scale bar, 10 μm).

totrichum (Genre *et al.*, 2009). SymRK and CCamK were also shown to be essential for a touch response upon a physical trigger (Genre *et al.*, 2009). Therefore all these intracellular infection processes seem to have recruited a focal secretion mechanism from a common touch sensing mechanism. However this touch related focal secretion is not required for all biotrophic fungi/oomycetes as powdery mildews can form haustoria on leaves of SymRK and CCamK mutants (Mellersh and Parniske, 2006).

In legumes the sites of initial penetration and the formation of perimicrobial compartment are well separated in time and space as the rhizobia are accommodated in *de novo* formed organs. This facilitates studies (e.g. by nodule specific knock-down experiments) on the signaling mechanism underlying the formation of perimicrobial compartments. In *Medicago*, *SymRK* is expressed in the zone of the nodule where rhizobia are released from the infection threads and SBs are first formed. Nodule specific knock down of *SymRK* expression in *Medicago* as well as in *Sesbania rostrata* showed that it blocked SB formation, whereas IT formation in the nodule was not affected (Fig. 1A) (Limpens *et al.*, 2005; Capoen *et al.*, 2005). Recently, a nodule specific remorin of *Medicago* (MtSYMREM1) was identified that interacts with SymRK (Lefebvre *et al.*, 2010). Remorins are plant-specific plasma membrane-associated proteins which have been described as components of lipid rafts (Mongrand *et al.*, 2004). Knock-down of *MtSYMREM1* leads to a similar block of SB formation as the *SymRK* knock-down, hence MtSYMREM1 might control the location of SymRK in subdomains of the host membrane. The involvement of such subdomains is further supported by the fact that flotillin, other lipid rafts associated protein (Doherty and McMahon, 2009), as recently shown to play a role in the initial IT formation (Haney and Long, 2010).

In a more indirect manner it was shown that CCamK is also required for SB formation as complementation of the *Medicago CCamK* mutant with the rice ortholog leads to a
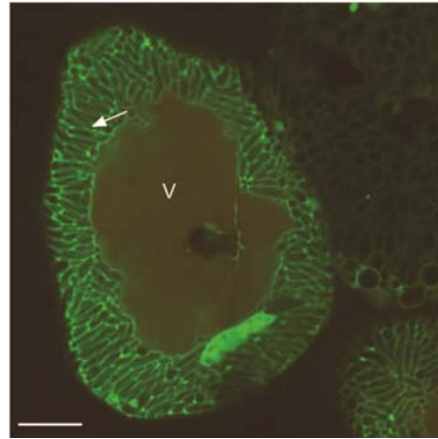
restored ability to form nodules but SB formation is blocked (Godfroy *et al.*, 2006). Whether these NF signaling components are activated by NF or another stimulus remains to be demonstrated.

Mutations in *SymRK* and *CCamK* also block penetration of the epidermis during AM infection (Genre *et al.*, 2005; 2009). Whether these NF signaling genes are also required for arbuscule formation is less clear. When the *SymRK* expression level is markedly reduced in an RNAi experiment, a few hyphae can still reach the inner cortex and there they do form arbuscules. This suggests that SymRK is not essential for PAM formation or that a low level of it is sufficient (Morandi *et al.*, 2005; Gherbi *et al.*, 2008). Although perimicrobial compartment formation is blocked by mutations in *SymRK* and *CCamK* in the interaction with *Colletotrichum*, it remains to be demonstrated in which steps precisely they are involved (Genre *et al.*, 2009).

Formation of perimicrobial compartments and endo- and exocytosis

The mature perimicrobial membranes have distinct features that are required for their function. For example, phosphate and ammonia transporters are present on the PAM facilitating the transfer of phosphate and ammonia from the AM fungus to the plant (Pumplin and Harrison, 2009; Guether *et al.*, 2009), whereas a putative cation channel capable of NH_4^+ transport and a dicarboxylate carrier are present on the PBM of the SB (White *et al.*, 2007). However, how the formation of these perimicrobial membrane compartments evolved from major endomembrane processes like exo- and endocytosis is unclear. The availability of membrane identity markers (Samaj et al., 2005) involved in these processes allows now to address such questions.

Small GTPases of the Rab family and SNARE (*N*-ethylmaleimide-sensitive factor attachment protein receptor) proteins are such membrane identity markers (Behnia and Munro, 2005; Pfeffer, 2007). Rab GTPases control the transport and docking of vesicles to their target membrane compartment. Subsequently, a vesicle-associated SNARE (v-SNARE) protein forms a complex with cognate SNARE proteins in the target compartment (t-SNARE) which drives the membrane fusion. Proteomics analysis of PBMs indicated several years ago the presence of an endocytosis identity marker, Rab7, on this membrane (Wienkoop and Salbach, 2003). However, the timing of acquiring such a marker during SB formation and a more detailed comparison with the endocytotic pathway has only recently been described (Limpens *et al.*, 2009). This showed that the *Medicago* early endosomal marker SYP4 (t-SNARE) and the (late) endosomal marker Rab5 do not occur on SBs during their development. In contrast, the PBM does acquire the late endosomal/vacuolar marker Rab7 when SBs have stopped dividing (Fig. 2). However, the vacuolar t-SNAREs SYP22 and VTI11 are absent till the senescence stage. At the start of senescence SBs obtain these vacuolar SNAREs and they fuse to form a large lytic compartment. The unknown mechanism by which a SB with a late endosomal identity marker can block the acquisition of vacuolar identity (leading to the killing of the microbe) seems at the heart of how an intracellular association can be maintained. So although it is text book knowledge that rhizobia enter the cell by an endocytotic-like process, at the molecular level no support for a relation between endocytosis and early SB formation is available. In contrast, exocytosis seems to play a key role. Namely, it was shown that the plasma membrane t-SNARE

SYP132 is present on PBM (Limpens *et al.*, 2009; Catalano *et al.*, 2007) directly from release from IT up to the senescence stage (Limpens *et al.*, 2009).

The involvement of exocytosis in SB development is underlined by the *Medicago dnf1* mutant. This mutant does form SBs, but these get arrested after SB division (so they remain short rods; Fig. 1A). DNF1 was shown to be a nodule specific variant of a subunit of the signal peptidase complex. This is an early component of the protein secretory pathway in the endoplasmic reticulum where it cleaves off signal peptides (Wang *et al.*, 2010). DNF1 was also shown to be essential for the targeting of nodule-specific cysteine-rich peptides which serve as antimicrobial compounds (Alunni *et al.*, 2007; Brogden, 2005). These peptides do induce the differentiation into the markedly enlarged SBs. At least in part, it explains why SBs in *dnf1* mutant arrest at an early stage of development (Mergaert *et al.*, 2006; Van de Velde *et al.*, 2010).

PAM and EHM form a continuum with the plasma membrane of the host. It has been postulated that the EHM is formed by 'stretching and invagination' of the plasma membrane of the host or by *de novo* synthesis of the perimicrobial compartment (Koh *et al.*, 2005). The first mechanism implies that already present plasma membrane of the host cell stretches and invaginates around the growing haustorium and this is compensated by vesicle insertion in the host cell periphery. In this model the neckband, which is formed by callose deposition at the site of penetration acts as a 'sieve' to allow certain membrane components to enter the EHM while excluding others (Koh *et al.*, 2005). Membranes can only stretch 2–3% (Apodaca, 2002) and so it is unlikely that this plays a role. So it means exocytosis drives the growth of the perimicrobial compartment either by insertion of vesicles at a distance (cell periphery) or directly in the growing perimicrobial compartment. The latter seems far more likely as by targeting of vesicles with the right cargo a membrane with properties different from that of the plasma membrane can be formed. In contrast, it is very hard to understand how insertion of vesicles in the cell periphery could result in the specific accumulation of certain proteins in the EHM and PAM (Pumplin and Harrison, 2009; Wang *et al.*, 2009) or how several plasma membrane proteins could be absent in the EHM (Koh *et al.*, 2005).

The involvement of exocytosis in basal host defense against non-adapted pathogens is much better understood than its involvement in the formation of haustoria in a compatible interaction. The *Arabidopsis thaliana* t-SNARE PEN1/SYP121 is essential for this defense and it accumulates in microdomains in the host plasma membrane at the site where the fungus tries to enter the host (Assaad *et al.*., 2004; Bhat *et al.*, 2005). By forming SNARE complexes with the SNAP33 adaptor and v-SNAREs VAMP721/22 (Kwon *et al.*, 2008) it facilitates the fusion with vesicles that have the v-SNAREs VAMP721 and VAMP722 at their surface and a possible cargo with antimicrobial compounds (Kusumawati *et al.*, 2008). The v-SNAREs VAMP721 and VAMP722 do play a role in normal exocytosis and have been co-opted to serve in basal immune defense. Reduced levels of VAMP721/722 and loss of function mutations of PEN1 block this defense response but increase the level of fungal entry and haustoria formation (Kwon *et al.*, 2008). This shows that different exocytotic pathways have to be used in basal host defense and EHM formation.

Conclusion

Studies on the different intracellular plant microbe associations have revealed that exocytosis related pathways play an important role in the formation of perimicrobial compartments, the infection process, as well as the basal defense response against non-adapted pathogens. These studies have markedly contributed to the insight that multiple exocytotic pathways have to be operational in plants. Interactions with various pathogens might even use different pathways as it is shown that defense against *Pseudomonas* requires SYP132, whereas the SNAREs SYP121 and VAMP721/722 are essential in defense against powdery mildew (Kwon *et al.*, 2008; Kalde *et al.*, 2007). The formation of haustoria seems to exploit even other pathway(s) as mutations in these SNAREs do not block but stimulate haustorium formation. Interestingly, SB formation in the *Rhizobium*-legume symbiosis does also involve SYP132 (Limpens *et al*., 2009; Catalano *et al*., 2007) and further *Medicago* homologs of the *Arabidopsis* VAMP72 are essential for SB formation (S. Ivanov, E. Limpens, E. Fedorova, T. Bisseling, unpublished).

Although studies on the mechanisms by which secretory pathways have been co-opted to serve in plant microbe interactions are still in their infancy it needs to become clear how these pathways deliver vesicles specifically to the new target membrane and how the cargos are modified to fulfill their specific functions in the specific plant-microbe interaction.

References

Alunni B, Kevei Z, Redondo-Nieto M, Kondorosi A, Mergaert P, Kondorosi E (2007). Genomic organization and evolutionary insights on GRP and NCR genes, two large nodule-specific gene families in *Medicago truncatula*. *Mol Plant Microbe Interact* **20**:1138-1148.

Apodaca G (2002). Modulation of membrane traffic by mechanical stimuli. *Am J Physiol Renal Physiol* **282**:179-190.

Assaad FF, Qiu JL, Youngs H, Ehrhardt D, Zimmerli L, Kalde M, Wanner G, Peck SC, Edwards H, Ramonell K, Somerville CR, Thordal-Christensen H (2004). The PEN1 syntaxin defines a novel cellular compartment upon fungal attack and is required for the timely assembly of papillae. *Mol Biol Cell* **15**:5118-129.

Behnia R, Munro S (2005). Organelle identity and the signposts for membrane traffic. *Nature* **438**:597-604.

Bhat RA, Miklis M, Schmelzer E, Schulze-Lefert P, Panstruga R (2005). Recruitment and interaction dynamics of plant penetration resistance components in a plasma membrane microdomain. *Proc Natl Acad Sci U S A* **102**:3135-3140.

Brewin NJ (2004). Plant cell wall remodelling in the *Rhizobium*-legume symbiosis. *Crit Rev Plant Sci* **23**:293-316.

Brogden KA (2005). Antimicrobial peptides: pore formers or metabolic inhibitors in bacteria? *Nat Rev Microbiol* **3**:238-250.

Capoen W, Goormachtig S, De Rycke R, Schroeyers K, Holsters M (2005). SrSymRK, a plant receptor essential for symbiosome formation. *Proc Natl Acad Sci USA* **102**:10369-10374.

Catalano CM, Czymmek KJ, Gann JG, Sherrier DJ (2007). *Medicago truncatula* syntaxin SYP132 defines the symbiosome membrane and infection droplet membrane in root nodules. *Planta* **225**:541-550.

Den Herder G, Parniske M (2009). The unbearable naivety of legumes in symbiosis. *Curr Op Plant Biol* **12**:491-499.

Doherty GJ, McMahon HT (2009). Mechanisms of endocytosis. *Annu Rev Biochem* **78**:857-902.

Gage DJ (2004). Infection and invasion of roots by symbiotic, nitrogen-fixing rhizobia during nodulation of temperate legumes. *Microbiol Mol Biol Rev* **68**:280-300.

Genre A, Chabaud M, Faccio A, Barker DG, Bonfante P (2008). Prepenetration apparatus assembly precedes and predicts the colonization patterns of arbuscular mycorrhizal fungi within the root cortex of both *Medicago truncatula* and *Daucus carota*. *Plant Cell* **20**:1407-1420.

Genre A, Chabaud M, Timmers T, Bonfante P, Barker DG (2005). Arbuscular mycorrhizal fungi elicit a novel intracellular apparatus in *Medicago truncatula* root epidermal cells before infection. *Plant Cell* **17**:3489-3499.

Genre A, Ortu G, Bertoldo C, Martino E, Bonfante P (2009). Biotic and abiotic stimulation of root epidermal cells reveals common and specific responses to arbuscular mycorrhizal fungi. *Plant Physiol* **149**:1424-1434.

Gherbi H, Markmann K, Svistoonoff S, Estevan J, Autran D, Giczey G, Auguy F, Péret B, Laplaze L, Franche C, Parniske M, Bogusz D. (2008). SymRK defines a common genetic basis for plant root endosymbioses with arbuscular mycorrhiza fungi, rhizobia, and *Frankia* bacteria. *Proc Natl Acad Sci USA* **105**:4928-4932.

Gimenez-Ibanez S, Ntoukakis V, Rathjen JP (2009). The LysM receptor kinase CERK1 mediates bacterial perception in *Arabidopsis*. *Plant Signal Behav* **4**:539-541.

Godfroy O, Debellé F, Timmers T, Rosenberg C (2006). A rice calcium- and calmodulin-dependent protein kinase restores nodulation to a legume mutant. *Mol. Plant Microb Interac* **19**:495-501.

Guan C, Pawlowski K, Bisseling T (1998). Interaction between *Frankia* and actinorhizal plants. *Subcell Biochem* **29**:165-189.

Guether M, Neuhäuser B, Balestrini R, Dynowski M, Ludewig U, Bonfante P (2009). A mycorrhizal-specific ammonium transporter from *Lotus japonicus* acquires nitrogen released by arbuscular mycorrhizal fungi. *Plant Physiol* **150**:73-83.

Haney CH, Long SR (2010). Plant flotillins are required for infection by nitrogen-fixing bacteria. *Proc Natl Acad Sci USA* **107**:478-483.

Hardham AR, Jones DA, Takemoto D (2007). Cytoskeleton and cell wall function in penetration resistance. *Curr Opin Plant Biol* **10**:342-348.

Kalde M, Nühse TS, Findlay K, Peck SC (2007). The syntaxin SYP132 contributes to plant resistance against bacteria and secretion of pathogenesis-related protein 1. *Proc Natl Acad Sci USA* **104**:11850-11855.

Koh S, André A, Edwards H, Ehrhardt D, Somerville S (2005). *Arabidopsis thaliana* subcellular responses to compatible *Erysiphe cichoracearum* infections. *Plant J* **44**:516-529.

Kusumawati L, Imin N, Djordjevic MA (2008). Characterization of the secretome of suspension cultures of *Medicago* species reveals proteins important for defense and development. *J Proteome Res* **7**:4508-4520.

Kwon C, Neu C, Pajonk S, Yun HS, Lipka U, Humphry M, Bau S, Straus M, Kwaaitaal M, Rampelt H, El Kasmi F, Jurgens G, Parker J, Panstruga R, Lipka V, Schulze-Lefert P. (2008). Co-option of a default secretory pathway for plant immune responses. *Nature* **451**:835-840.

Lefebvre B, Timmers T, Mbengue M, Moreau S, Hervé C, Tóth K, Bittencourt-Silvestre J, Klaus D, Deslandes L, Godiard L, Murray JD, Udvardi MK, Raffaele S, Mongrand S, Cullimore J, Gamas P, Niebel A, Ott T (2010). A remorin protein interacts with symbiotic receptors and regulates bacterial infection. *Proc Natl Acad Sci USA* **107**:2343-2348.

Limpens E, Franken C, Smit P, Willemse J, Bisseling T, Geurts R (2003). LysM domain receptor kinases regulating rhizobial Nod factor-induced infection. *Science* **302**:630-633.

Limpens E, Ivanov S, van Esse W, Voets G, Fedorova E, Bisseling T (2009). *Medicago* N2-fixing symbiosomes acquire the endocytic identity marker Rab7 but delay the acquisition of vacuolar identity. *Plant Cell* **21**:2811-2828.

Limpens E, Mirabella R, Fedorova E, Franken C, Franssen H, Bisseling T, Geurts R (2005). Formation of organelle-like N2-fixing symbiosomes in legume root nodules is controlled by DMI2. *Proc Natl Acad Sci USA* **102**:10375-10380.

Madsen EB, Madsen LH, Radutoiu S, Olbryt M, Rakwalska M, Szczyglowski K, Sato S, Kaneko T, Tabata S, Sandal N, Stougaard J (2003). A receptor kinase gene of the LysM type is involved in legume perception of rhizobial signals. *Nature* **425**:637-640.

Mellersh D, Parniske M (2006). Common symbiosis genes of *Lotus japonicus* are not required for intracellular accommodation of the rust fungus *Uromyces loti*. *New Phytol* **170**:641-644.

Mergaert P, Uchiumi T, Alunni B, Evanno G, Cheron A, Catrice O, Mausset AE, Barloy-Hubler F, Galibert F, Kondorosi A, Kondorosi E (2006). Eukaryotic control on bacterial cell cycle and differentiation in the *Rhizobium*-legume symbiosis. *Proc Natl Acad Sci USA* **103**:5230-5235.

Mongrand S, Morel J, Laroche J, Claverol S, Carde JP, Hartmann MA, Bonneu M, Simon-Plas F, Lessire R, Bessoule JJ (2004). Lipid rafts in higher plant cells: purification and characterization of Triton X-100-insolublemicrodomains from tobacco plasma membrane. *J Biol Chem* **279**:36277-36286.

Morandi D, Prado E, Sagan M, Duc G (2005). Characterisation of new symbiotic *Medicago truncatula* (Gaertn.) mutants, and phenotypic or genotypic complementary information on previously described mutants. *Mycorrhiza* **15**:283-289.

O'Connell RJ, Panstruga R (2006). Tete a tete inside a plant cell: establishing compatibility between plants and biotrophic fungi and oomycetes. *New Phytol* **171**:699-718.

Oldroyd GED, Downie JA (2008). Coordinating nodule morphogenesis with rhizobial infection in legumes. *Annu Rev Plant Biol* **58**:519-546.

Parniske M (2008). Arbuscular mycorrhiza: the mother of plant root endosymbioses. *Nature Rev Microbiol* **6**:763-775.

Pfeffer S (2007). Unsolved mysteries in membrane traffic. *Annu Rev Plant Biol* **76**:629-645.

Pumplin N, Harrison MJ (2009). Live-cell imaging reveals periarbuscular membrane domains and organelle location in *Medicago truncatula* roots during arbuscular mycorrhizal symbiosis. *Plant Physiol* **151**:809-819.

Samaj J, Read ND, Volkmann D, Menzel D, Baluska F (2005). The endocytic network in plants. *Trends Cell Biol* **15**:425-433.

Van de Velde W, Zehirov G, Szatmari A, Debreczeny M, Ishihara H, Farkas A, Mikulass K, Nagy A, Tiricz H, Satiat-Jeunemaître B, Alunni B, Bourge M, Kucho K, Abe M, Kereszt A, Maroti G, Uchiumi T, Kondorosi E, Mergaert P (2010). Nodule specific peptides govern terminal differentiation of bacteria in symbiosis. *Science* **327**:1122-1126.

Wang D, Griffitts L, Starker C, Fedorova E, Limpens E, Ivanov S, Bisseling T, Long S (2010). A nodule specific protein secretory pathway required for nitrogen-fixing symbiosis. *Science*, **327**:1126-1129.

Wang W, Wen Y, Berkey R, Xiao S (2009). Specific targeting of the *Arabidopsis* resistance protein RPW8.2 to the interfacial membrane encasing the fungal haustorium renders broad-spectrum resistance to powdery mildew. *Plant Cell* **21**:2898-2913.

White J, Prell J, James EK, Poole P (2007). Nutrient sharing between symbionts. *Plant Physiol* **144**:604-614.

Wienkoop S, Saalbach G (2003). Proteome analysis. Novel proteins identified at the peribacteroid membrane from *Lotus japonicus* root nodules. *Plant Physiol* **131**:1080-1090.

.

Chapter 2

Medicago N$_2$-fixing symbiosomes acquire the endocytic identity marker Rab7 but delay the acquisition of vacuolar identity

Erik Limpens, Sergey Ivanov, Wilma van Esse, Guido Voets, Elena Fedorova and Ton Bisseling

Laboratory of Molecular Biology, Graduate School Experimental Plant Science, Wageningen University, Droevendaalsesteeg 1, 6708PB Wageningen, The Netherlands

Rhizobium **bacteria form N$_2$-fixing organelles, called symbiosomes, inside the cells of legume root nodules. The bacteria are generally thought to enter the cells via an endocytosis-like process. To examine this, we studied the identity of symbiosomes in relation to the endocytic pathway. We show that in *Medicago truncatula*, the small GTPases Rab5 and Rab7 are endosomal membrane identity markers, marking different (partly overlapping) endosome populations. Although symbiosome formation is considered to be an endocytosis-like process, symbiosomes do not acquire Rab5 at any stage during their development, nor do they accept the trans-Golgi network identity marker SYP4, presumed to mark early endosomes in plants. By contrast, the endosomal marker Rab7 does occur on symbiosomes from an early stage of development when they have stopped dividing up to the senescence stage. However, the symbiosomes do not acquire vacuolar SNAREs (SYP22 and VTI11) until the onset of their senescence. By contrast, symbiosomes acquire the plasma membrane SNARE SYP132 from the start of symbiosome formation throughout their development. Therefore, symbiosomes appear to be locked in a unique SYP132- and Rab7-positive endosome stage and the delay in acquiring (lytic) vacuolar identity (e.g., vacuolar SNAREs) most likely ensures their survival and maintenance as individual units.**

Introduction

Legume plants have the unique ability to host N_2-fixing *Rhizobium* bacteria inside cells of a newly formed organ, the so-called root nodule. The bacteria are thought to enter nodule cells through an endocytosis-like process and are maintained as host membrane-bound compartments, called symbiosomes (SBs), that each contain one (or a few) bacterium (Roth and Stacey, 1989). By multiplication, ultimately thousands of individual N_2-fixing SBs are present in an infected nodule cell. Endocytosis is a ubiquitous cellular process involving vesicle mediated transport of extracellular material from the plasma membrane to a lytic compartment, lysosomes in animal cells, and vacuoles in plants. This transport is performed by distinct membrane structures, so-called early and late endosomes, which are involved in subsequent steps of transport. Upon endocytosis, vesicles are first targeted to early endosomes where material that needs to be degraded is sorted and transported further to late endosomes that finally fuse with lysosomes or the lytic vacuole (Pelham, 2002; Perret *et al.*, 2005; Samaj *et al.*, 2005; Geldner and Jurgens, 2006; Mo *et al.*, 2006; Jaillais *et al.*, 2008; Robinson *et al.*, 2008; Ebine and Ueda, 2009).

The endocytic-like entry of rhizobia into nodule cells shows some similarity to phagocytosis of bacteria into animal cells. In general, this process involves a maturation of the plasma membrane-derived bacterium-containing endosome/phagosome to eventually fuse with a lytic compartment (Vieira *et al.*, 2002). This maturation requires a sequential interaction with the different compartments of the endocytic pathway. By analogy, it is therefore of interest to determine whether SBs share properties with compartments of the plant endocytic pathway and if so how targeting to a lytic vacuole is avoided.

The different endosome compartments can be distinguished by the presence of specific membrane identity markers, such as regulatory small GTPases of the Rab family and SNARE (*N*-ethylmaleimide-sensitive factor attachment protein receptor) proteins (Sanderfoot *et al.*, 2000; Pfeffer and Aivazian, 2004; Seabra and Wasmeier, 2004; Behnia and Munro, 2005; Lipka *et al.*, 2007; Pfeffer, 2007; Sanderfoot, 2007; Bassham and Blatt 2008; Nielsen *et al.*, 2008). These proteins control the specificity of membrane fusion events at the compartments where they reside. Rab GTPases control the transport and docking of vesicles after which a vesicle-associated SNARE protein forms a complex with complementary SNARE proteins in the target compartment that drives the fusion. Well-studied identity markers of the endocytic pathway in animals and yeast are the small GTPases Rab5 and Rab7, which control early and late endosome interactions, respectively.

Several bacterial pathogens of animal cells are able to avoid the fusion of their pathogen-containing compartment with lysosomes to ensure their maintenance and multiplication (Alonso and Garcia-del Portillo, 2004). Such intracellular pathogens manipulate the endocytic pathway, with the result that their membrane compartment does not undergo the normal phagocytic maturation route (Via *et al.*, 1997; Knodler *et al.*, 2001; Brumell and Grinstein, 2004; Behnia and Munro, 2005). By manipulating the association of distinct membrane identity markers, they either stop or segregate from the default phagocytic pathway to the lysosome. For example, *Mycobacterium bovis* vacuoles retain the early endosome marker Rab5 and do not acquire the late endosomal Rab7, thereby preventing the fusion with lysosomes (Via *et al.*, 1997). So they become locked in an early endosome

stage. We hypothesized that rhizobia might similarly manipulate the endocytic pathway to maintain SBs and avoid fusion with lytic compartments.

Among the best-studied endosomal proteins in plants are the *Arabidopsis thaliana* Rab5 homologs (Ueda *et al*., 2001, 2004). *Arabidopsis* contains three Rab5 homologs: Ara7/RabF2b and Rha1/RabF2a, which are most homologous to yeast and animal Rab5s, and Ara6/RabF1, which represents a plant unique Rab5 homolog (Ueda *et al*., 2001). Ara6/RabF1 and Ara7/Rha1 have been shown to occur in distinct, yet overlapping, endosome populations in *Arabidopsis* (Ueda *et al*., 2004) that both are characterized as multivesicular bodies (MVBs) (Tse *et al*., 2004; Haas *et al*., 2007; Lam *et al*., 2007). Furthermore, the Rab5-labeled endosomes were also named prevacuolar compartments (PVCs) as they contain vacuolar sorting receptors and interfering with their function affected the proper trafficking of vacuolar proteins from the Golgi to the vacuole (Li *et al*., 2002; Paris and Neuhaus, 2002; Sohn *et al*., 2003; Surpin *et al*., 2003; Bolte *et al*., 2004; Kotzer *et al*., 2004; Tse *et al*., 2004; Foresti *et al*., 2006; Otegui *et al*., 2006). This implies that the endocytic pathway and the vacuolar biosynthetic pathway merge at Rab5 PVCs. In plants, Rab5 PVCs are considered to represent late endosome compartments as they are in yeast, whereas in animal cells, Rab5-labeled endosomes are early endosomes (Gerrard *et al*., 2000; Pelham, 2002; Jurgens, 2004; Surpin and Raikhel, 2004; Samaj *et al*., 2005; Jaillais *et al*., 2008). The trans-Golgi network (TGN) is now thought to represent the early endosome compartment in plants, similar to the situation in yeast (Dettmer *et al*., 2006; Lam *et al*., 2007a, 2007b; Chow *et al*., 2008; Robert *et al*., 2008; Robinson *et al*., 2008; Ebine and Ueda 2009). However, the exact organization of the plant TGN and the transport steps it is involved in still need to be better defined.

Rab7 GTPase generally is thought to be required for the formation of lytic compartments (Bucci *et al*., 2000). Animal and yeast cells generally contain a single Rab7 protein, which localizes to late endosomes and to lysosomes/vacuoles (Schimmoller and Riezman, 1993; Bruckert *et al*., 2000; Bucci *et al*., 2000; Pelham, 2002). By contrast, *Arabidopsis* contains eight Rab7 homologs, which suggests that they have several specialized functions possibly related to the multiple vacuole types found in plants (Rutherford and Moore, 2002; Surpin *et al*., 2003; Sanderfoot, 2007; Sanmartın *et al*., 2007; Nielsen *et al*., 2008). Rab7 proteins have been localized to the tonoplast in both *Arabidopsis* and rice (*Oryza sativa*; Saito *et al*., 2002; Nahm *et al*., 2003); however, they have not been studied much in plants. Furthermore, Rab7 proteins have been implicated in SB maintenance in soybean (*Glycine max*; Cheon *et al*., 1993; Son *et al*., 2003), and several Rab7 homologs were identified in a proteomics study of SBs in *Lotus japonicus* (Wienkoop and Saalbach, 2003). This suggests that SB formation may have hijacked the endocytic pathway to become a vacuole-like compartment (Mellor, 1989).

To test the hypothesis that SBs manipulate the endocytic machinery for their maintenance, we first mainly focused on the key endosomal Rab GTPases, Rab5 and Rab7, during SB development in the model legume *Medicago truncatula*. *Medicago* nodules have a persistent meristem at their apex by which new cells are continuously added to the nodule tissues. Therefore, these tissues are of graded age with the youngest cells adjacent to the meristem and the oldest cells near the root attachment site. The bacteria are continuously released as SBs from cell wall-bound infection threads in two to three cell layers directly adjacent to the meristem. After SBs are taken up into the cells, they start to divide and finally

differentiate into their N_2-fixing form. The zone where release and subsequent division and differentiation of SBs occur is called the infection zone. This zone is followed by the fixation zone where SBs are N_2-fixing organelles. In older nodules, senescence is induced in the basal, most proximal to the root part of the nodule (senescence zone). Senescence starts with the fusion and formation of lytic SB compartments (Vasse *et al*., 1990; Van de Velde *et al.*, 2006). The resulting age gradient provides a strong experimental system to study SB properties at subsequent stages of development in single longitudinal nodule sections.

Here, we show that SBs do not make use of the known/default endocytic pathway in *Medicago* to enter nodule cells. We show that SBs do acquire the endosomal marker Rab7 when they stop diving and that Rab7 specifically regulates the maturation of the SBs into a nitrogen-fixing organelle. Furthermore, SBs seem to be maintained as individual membrane compartments by delaying the acquisition of vacuolar SNAREs.

Results

Identification of *Medicago* Rab5 and Rab7 homologs. To study the involvement of the endocytic pathway in SB formation, we first identified markers for the endosomal compartments in *Medicago*. We initially focused on the key endosomal small GTPases of the Rab family, Rab5 and Rab7. In *Medicago*, three Rab5 homologs, Rab5A1 (TC106962), Rab5A2 (TC106963), and Rab5B (TC93994), were identified in the available genomic and cDNA sequences. All three *Medicago* Rab5 homologs are represented in nodule cDNA libraries. *Medicago* Rab5A1 and Rab5A2 are most homologous to the two conserved Rab5s of *Arabidopsis*, Ara7/RabF2b and Rha1/RabF2a, whereas *Medicago* Rab5B is most homologous to Rab5 unique for plants (e.g., *Arabidopsis* Ara6/RabF1, Ueda *et al*., 2001; see Fig. S1). *Medicago* Rab5A1 and Rab5A2 contain the C-terminal Cys-motif that is highly conserved in most Rab GTPases and represents a site for isoprenylation. By contrast, *Medicago* Rab5B lacks this C-terminal Cys motif, but it contains the N-terminal domain characteristic for Rab5 unique to plants that is most likely acylated (Ueda *et al*., 2001).

The *Medicago* genome contains at least eight *Rab7* homologs (Fig. S1). Only two Rab7 ESTs, Rab7A1 (TC101145) and Rab7A2 (TC94423), were represented in nodule cDNA libraries; therefore, we focused on these two Rab7 proteins.

The expression of the three *Rab5* and two *Rab7* genes in 10-day-old and 3-week-old nodules was verified using real-time RT-PCR and their expression level appeared largely similar to that in roots (Fig. S2). Furthermore, microarray analyses on RNA from infected cells isolated by laser capture microdissection showed that all genes that we selected in this study are active in the cells containing SBs (E. Limpens, unpublished data).

Rab5s occur on endosomes. To study whether the *Medicago* Rab5 proteins localize to endosomal membrane compartments, we generated transgenic *Medicago* roots that express green fluorescent protein (GFP) fusion constructs via *Agrobacterium rhizogenes*-mediated root transformation. Rab5A1 and RabA2 were fused to the C-terminus of GFP, while Rab5B, which is likely N-acylated, was fused to the N-terminus of GFP. The GFP Rab5 fusion constructs were expressed under control of the cauliflower mosaic virus *35S* promoter and/or the *Arabidopsis Ubiquitin3* promoter, and the subcellular localization of the
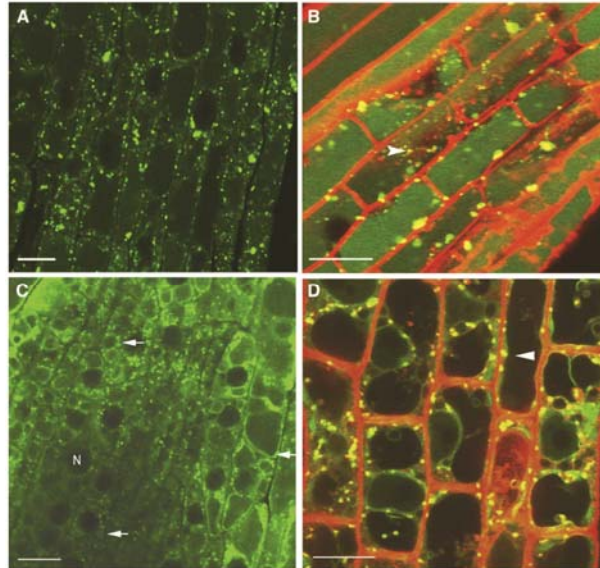
Figure 1. Rab5 and Rab7 occur on endosomes. (*A*) to (*D*) Confocal image of *p35S::GFP-Rab5A2* (*A* and *B*) and *p35S::GFP-MtRab7A2* (*C* and *D*) expressing *Medicago* roots. (*A*) GFP-MtRab5A2 marks dot-like structures. Similar localization patterns were observed for Rab5A1 and Rab5B (see Fig. S3). (*C*) GFP-Rab7A2 (as well as GFP-Rab7A1; see Fig. S3) marks dot-like structures as well as the tonoplast of small and large vacuoles (arrows). (*B*) and (*D*) Pulse chase (45 min) with the fluorescent endosomal tracer FM4-64. Yellow dots represent the co-localization of GFP and red fluorescent FM4-64 signal (arrowhead), showing that the structures are endosomes. At this time point, FM4-64 does not yet label the tonoplast. N, nucleus. (Scale bars, 10 μm.)

fusion proteins was studied by confocal microscopy in the elongation zone (Fig. 1) and root hairs.

All three Rab5 fusion proteins localized to small, highly mobile, dot-like structures within the cytoplasm (Fig. 1A; Fig. 3). These small dots are most likely endosomes as described for *Arabidopsis* (Ueda *et al*., 2001, 2004). In addition, larger structures labeled by Rab5s were observed, most likely representing clusters of endosomes. Although Ara6 and Ara7/Rha1 were shown to label distinct but overlapping endosome populations in *Arabidopsis*, we did not study to what extent the populations marked by the different Rab5s overlap in *Medicago*.

To verify that the Rab5-labeled dots represent compartments of the endocytic pathway, we performed a pulse-chase experiment with the fluorescent endosomal tracer FM4-64. FM4-64 is a lipophylic styryl dye that fluoresces upon insertion into membranes and can only enter cells through endocytic uptake (Ueda *et al*., 2001, 2004; Tse *et al*., 2004; Samaj *et al*., 2005). FM4-64 partly co-localized with GFP-Rab5 (similar for all three MtRab5s) before FM4-64 labeling of the tonoplast occurred (Fig. 1*B*; Fig. S3). This indicates that the Rab5-labeled compartments indeed represent endosomes.
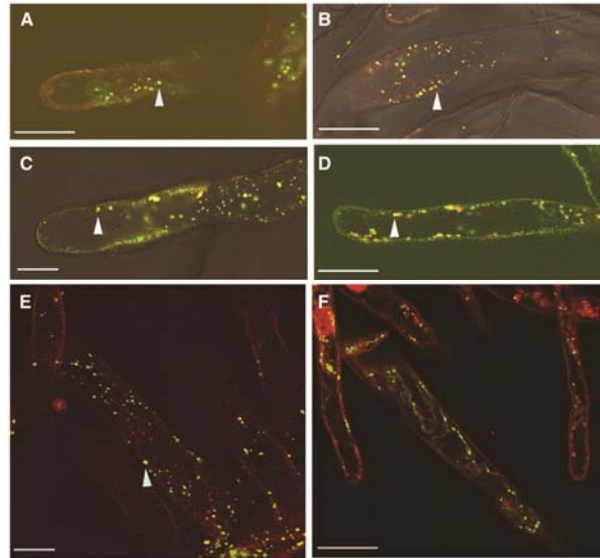
Figure 2. Rab5 marks prevacuolar compartments, while Rab7 marks different, partly overlapping endosome populations. (*A*) Immunolocalization of anti-Rab5 (anti-Ara7) (secondary antibody CY3-tagged; red) on *p35S::GFP-Rab5A2*-expressing root hairs, showing a high level of co-localization (yellow signal; arrowhead). (*B*) Immunolocalization of anti-BP-80 (secondary antibody CY3-tagged; red) on *p35S::GFP-Rab5B*-expressing root hairs. (*C*) Immunolocalization of anti-BP-80 (red) on *p35S::GFP-Rab5A2*-expressing root hairs. The high level of co-localization (yellow signal; arrowhead) in (*B*) and (*C*) indicates that the Rab5-labeled endosomes represent PVC compartments. (*D*) Immunolocalization of anti-Rab5 (anti-Ara7) (red) on *p35S::GFP-Ra*b7A1–expressing root hairs. Endosomes show partial co-localization of anti-Rab5 and GFP-Rab7 (yellow signal; arrowhead). (*E*) Double immunolocalization of anti-Rab7, detected with CY3-tagged secondary antibody (red), and anti-Rab5 (anti-Ara7) detected with Alexa488-tagged secondary antibody (green), on dot-like structures in root hairs of wild-type plants. Rab7 and Rab5 show only partial co-localization (yellow signal; arrowhead). (*F*) Immunolocalization of BP-80 (secondary Ab CY3-tagged; red) on *p35S::GFP-Rab7A2*-expressing root. Note the low level of co-localization. (Scale bars, 10 μm.)

To verify that the GFP-tagged Rab5 proteins are targeted to the same compartments as their endogenous counterparts, we performed immunolocalization studies using an antibody specific for Rab5 (anti-Ara7 from *Arabidopsis*). This showed that in transgenic *GFP-Rab5*-expressing roots, GFP and anti-Rab5 show a very high level of co-localization (Fig. 2*A*). Furthermore, in nontransgenic roots, a similar number of Rab5-containing dot-like structures are observed (recognized by anti-Ara7). So neither the use of heterologous promoters nor the presence of the GFP tag affected proper targeting of Rab5.

To determine the ultrastructural properties of Rab5-labeled compartments, the localization of the Rab5 fusion proteins was analyzed by electron microscopy (EM). EM immunogold labeling with an anti-GFP antibody was used to localize the GFP fusion proteins in the elongation zone of transgenic roots. Rab5 proteins occurred specifically on membrane compartments with a diameter of 100 to 300 nm containing internal membranes (Fig. 3*A* and *B*). So they are structurally similar to MVBs (Tse *et al.*, 2004). EM immunogold detection using a Rab5 (anti-Ara7) antibody on transgenic as well as nontransgenic roots con-
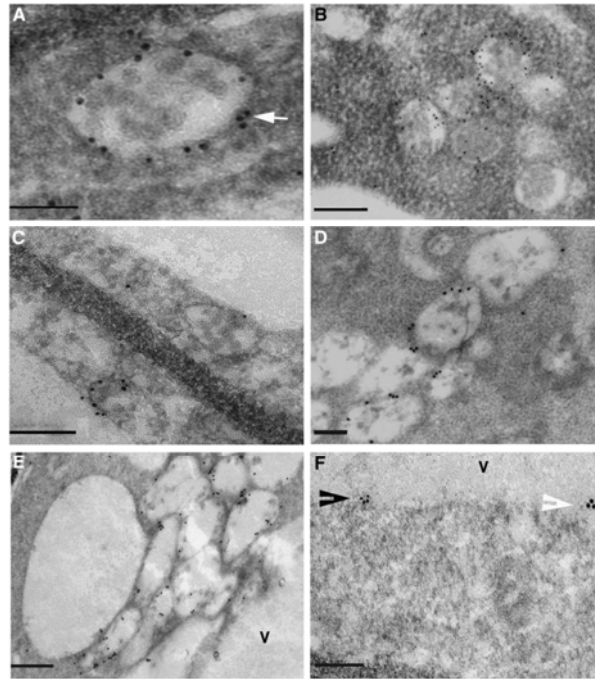
Figure 3. Rab5 and Rab7 mark differently sized MVBs. (*A*) and (*B*) EM immunogold detection (immunogold signal appears as black dots; indicated by white arrow) of anti-GFP in *p35S::GFP-Rab5A2*-expressing *Medicago* roots, showing 100- to 300-nm multivesicular endosomes, single (*A*) or in clusters (*B*). (*C*) Anti-Rab5 (anti-Ara7) EM-immunogold detection on *p35S::GFP-Rab5A2* roots shows similarly sized multivesicular endosomes. (*D*) and (*E*) EM-immunogold labeling of anti-GFP in *p35S::GFP-Rab7A2*-expressing *Medicago* roots. Immunogold signal is present over 300- to 500-nm MVBs fusing together (*D*) and with the tonoplast (*E*). (*F*) Double immunolocalization on *p35S::GFP-R*ab7A2 roots using anti-GFP detected by 15-nm gold particles (white arrowhead) and anti-Rab7 detected by 10-nm gold (black arrowhead). The signal for both GFP and Rab7 is present on the tonoplast. v, vacuole. (Scale bar, 100 nm in *A*, 200 nm in *B-D*, 500 nm in *E*, 200 nm in *F*.)

firmed the localization to MVBs with a size of 100 to 300 nm (Fig. 3*C*). This supports our conclusion that the Rab5 fusion proteins are targeted to the same endomembrane compartments (MVBs) as their endogenous counterparts.

Rab7 marks endosomes and the tonoplast. Similar to the Rab5 analyses, GFP-Rab7 fusion constructs for both Rab7A1 and Rab7A2 were expressed under the control of the *35S* promoter or *Ubiquitin3* promoter in *A. rhizogenes*–transformed roots. GFP localization was determined by confocal microscopy in the elongation zone (Fig. 1) and root hairs of these roots. GFP fluorescence occurred as mobile dot-like structures in the cytoplasm, which were often in the vicinity of the vacuoles (Fig. 1*C*; Fig. S3). In addition, small (merging) and large vacuoles were labeled (Fig. 1*C*).

EM immunolocalization of GFP-Rab7A2 (and GFP-Rab7A1), using an antibody against GFP, showed that in both cases, Rab7 associated with the membranes of MVBs ranging in size from 300 to 500 nm (Fig. 3*D* and *E*). In addition, it occurred on the tonoplasts of young (single) vacuoles and clusters of fusing small vacuoles as well as large vacuoles (Fig. 3*E* and *F*).

We verified the localization of endogenous Rab7 to these compartments using anti-*Medicago* Rab7 antibody. In nontransgenic roots, Rab7 occurred on dot-like structures (Fig. 2*E*) as well as vacuoles. Furthermore, double EM immunolocalization using anti-GFP and anti-Rab7 in the *p35S::GFP-Rab7A2* transgenic roots confirmed their co-localization (Fig. 3*F*). This implies that the GFP fusion construct can be used to identify the endomembrane compartments containing Rab7, and we conclude that Rab7A1/A2 is located on both MVBs (300 to 500 nm) and vacuoles. To determine whether the Rab7-labeled MVBs are part of the endocytic pathway, we also performed a pulse-chase experiment with FM4-64. Co-localization of GFP-Rab7A1/A2 and FM4-64 fluorescence was first seen in dot-like structures (Fig. 1*D*); from 1 h after the FM4-64 pulse co-localization, the tonoplast started to appear, and after ~3 h, the tonoplast was intensely labeled, indicating that also Rab7 MVBs are participating in endocytosis.

Rab5 and Rab7 occur on different but partly overlapping endosome populations. Both Rab5s and Rab7A1/A2 are located on endomembrane compartments (MVBs); however, the Rab7 containing compartments are markedly bigger (300 to 500 nm) than those containing Rab5 (100 to 300 nm). Therefore, it is likely that these MVBs represent distinct populations that only partly overlap. To test this, we performed immunolabeling with anti-Rab5 (anti-Ara7) on transgenic roots expressing *GFP-Rab7A1*. For analysis, we used root hairs from roots expressing *GFP-Rab7A1* as the antibody penetration is better in root hairs and the signal is easy to quantify (Fig. 2*D*). We also performed double immunolocalization with anti-Rab5 (anti-Ara7) and anti-Rab7 on nontransgenic roots (Fig. 2*E*). In both cases, ~30% of the Rab5-labeled dot-like structures co-localized with Rab7-positive structures (Fig. 2*D* and *E*). So the Rab7 endosomes appear to define a unique endocytic compartment.

In *Arabidopsis*, the endocytic pathway and vacuolar biosynthesis pathway merge at Rab5-labeled MVBs, also named PVCs as they contain vacuolar sorting receptors (Li *et al*., 2002; Paris and Neuhaus, 2002; Jurgens, 2004, Samaj *et al*., 2005; Foresti *et al*., 2006). To further characterize the Rab5 and Rab7 MVBs in *Medicago*, we used antibodies against the vacuolar sorting receptor BP-80 (from pea [*Pisum sativum*]), which is generally used as a marker for PVCs in plants (Paris and Neuhaus, 2002). BP-80 occurs in numerous small dots in the cytoplasm, a pattern similar to that of Rab5. Furthermore, in GFP-Rab5A2- or GFP-Rab5B-expressing *Medicago* roots, a high percentage (80%) of the endosomes contain both BP-80 and Rab5 (Fig. 2*B* and *C*). We also have tested the co-localization of BP-80 with Rab7MVBs in GFP-Rab7A1 roots. Rab7-positive bodies have a much lower level (<10%) of co-localization with BP-80 compared with Rab5 MVBs (Fig. 2*F*).

So the *Medicago* Rab5 MVBs are very similar to the Rab5 MVBs of *Arabidopsis* as both contain vacuolar sorting receptors. The latter suggests that also in *Medicago* the endocytic pathway and the vacuolar biosynthetic pathway merge at these compartments. Since part of the Rab7-labeled MVBs also contain Rab5, it is possible that they represent an intermediate compartment between Rab5-containing MVBs and vacuoles.
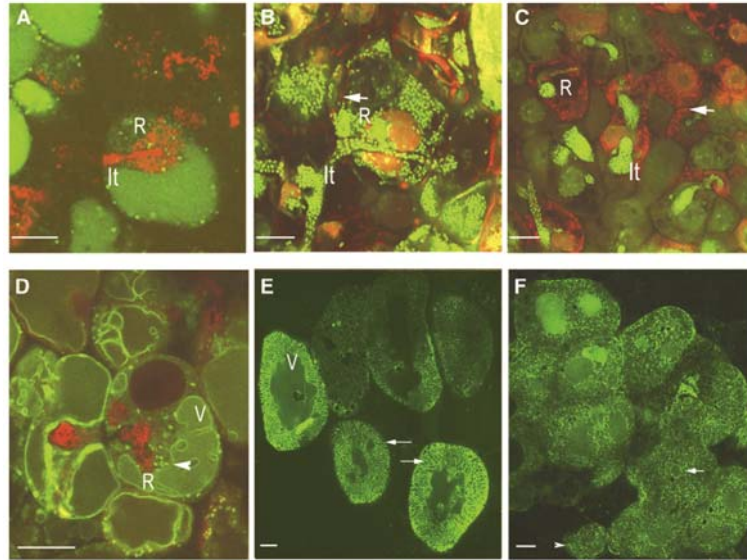
Figure 4. Rab7 occurs on SBs, but Rab5 does not. (*A*) Confocal image of *pUBQ3::GFP-Rab5A2*-expressing nodules. GFP-Rab5A2-labeled endosomes (green dots) are present in the infected cells, but no GFP signal is present on SBs after release from the infection thread (*It*). The rhizobia (*R*) are expressing monomeric red fluorescent protein (mRFP; red). (*B*) Immunolocalization of anti-Rab5 (anti-Ara7) on wild-type nodule-infected cells during SB formation in the infection zone. The signal for Rab5 is revealed as red dots (secondary antibody tagged with CY3; arrow). No co-localization of immunosignal with SBs was observed. The rhizobia are counterstained by SYTOX Green. (*C*) Immunolocalization of anti-BP80 (CY3-tagged secondary antibody, red dots; arrow) in the distal infection zone of wild-type nodules. Rhizobia (*R*) are counterstained by SYTOX Green. No co-localization of immunosignal with SBs was observed. (*D*) Confocal image of *pE12::GFP-R*ab7A2 expression in the distal part of the nodule. GFP-Rab7A2 marks both endosomes and the tonoplast (*v*, vacuole). No labeling of freshly released SBs is seen at this stage. The rhizobia (*R*) are expressing mRFP (red). (*E*) Confocal image of *pLB::GFP-Rab*7A2 expression in the infection zone of the nodule. The GFP signal is present over the SB membranes of mature SBs (arrow) and the tonoplast. Wild-type bacteria are not counterstained. (*F*) Immunolocalization of Rab7 in the fixation zone of wild-type nodules using anti-Rab7. The signal (Alexa 488-tagged secondary antibody, green) is present on SB membranes, tonoplast (arrows), and endosomes (arrowheads). (Scale bars, 10 μm.)

Rab5 does not occur on symbiosome membrane. Next, we studied the involvement of the endosomal Rab proteins in SB formation. We first tested whether the Rab5s occur on the SB membrane at any stage of its development. The cauliflower mosaic virus *35S* promoter was not suitable to visualize GFP fusion constructs during the different stages of SB development, as it is only very weakly active in nodule cells that are infected by rhizobia (Auriac and Timmers, 2007; see Fig. S4). In contrast with the report by Auriac and Timmers (2007), the *35S* promoter used in this study was active in the meristem of the nodule as well as in the uninfected cells (Fig. S4). The *Arabidopsis Ubiquitin3* promoter is active in the nodule meristem as well as in infected cells of the infection zone, although its activity markedly decreases in the most proximal part of the infection zone. To get stronger

fluorescent signal in the infected cells, we additionally used a *Medicago ENOD12* promoter and a pea leghemoglobin (*LB*) promoter to express the GFP fusions. *ENOD12* is active in the (distal part of the) infection zone, where bacteria are released from the infection threads and SBs multiply. The *LB* promoter is most active in the fixation zone containing mature, N_2-fixing SBs, but expression already starts in the infection zone. These promoters allowed us to study SBs at all developmental stages.

Rab5 occurred on MVBs in both uninfected and infected cells of root nodules (Fig. 4*A*; Fig. S3), and this was similar for all three Rab5 homologs. However, none of the three Rab5 fusion proteins co-localized with SBs at any stage of development, from release of the infection thread to mature N_2-fixing SBs. Rab5 proteins were also immunolocalized using anti-Rab5 (anti-Ara7). This confirmed that the Rab5s were present on endosomes (small dot-like structures) in infected and uninfected cells (Fig. 4*B*). However, they were not detected on the SB membrane at any stage of development. Similar results were obtained with immunolocalization of BP-80 in the nodule. Also here, no association of BP-80 with the SB membrane was observed in 14-day-old nodules, whereas BP-80-marked PVCs are present in the infected cells (Fig. 4*C*). Secondary antibody controls did not show any labeling in roots and nodules (Fig. S11). Also immuno-EM analyses of the transgenic nodules did not show any Rab5 labeling of the SB membrane, whereas a clear signal was observed over endosomes in the same cells. From these data, we conclude that the SB membrane does not acquire the key endocytic marker Rab5 during any stage of SB development.

Rab7 does occur on symbiosome membranes. In the same way, we examined the localization of Rab7A1/A2 during SB development. As in roots, GFP-Rab7A1/A2 occurs on dot-like endosomes as well as the tonoplast in (un) infected nodule cells (Fig. 4*D* and *E*; Fig. S3). No labeling of the SB membrane was observed in the distal part of the infection zone, where bacteria are released from the infection thread and SBs are dividing (Fig. 4*D*). However, in the proximal part of the infection zone, where the SBs are elongating and differentiate and in the fixation zone, GFP-Rab7A1/A2 does occur on SB membranes. Rab7 is maintained on SBs throughout the fixation zone (Fig. 4*E*). This was verified by immunolocalizing anti-Rab7 in nontransgenic nodules (Fig. 4*F*). The association of Rab7 with the SB membrane was confirmed by immuno-EM (Fig. 5*A* and *B*). This immunolocalization also confirmed that Rab7 genes are expressed in nodule cells containing SBs.

So, our localization studies with the endosomal Rabs showed that SBs do not acquire Rab5, whereas Rab7 is associated with SBs when they start to elongate. The absence of Rab5 on SBs makes it less likely that SBs mature by a sequential interaction with the different compartments of the endocytic pathway. Nevertheless, we tested whether an early endosomal marker is associated with SBs at the stage preceding the presence of Rab7.

To investigate this, we selected a *Medicago* homolog of the *Arabidopsis* SNARE SYP4 family (MtSYP41; TC96961), which have been shown to mark the TGN (Bassham *et al.*, 2000; Sanderfoot *et al.*, 2001). The TGN was recently shown to function as an early endosome in plants (Dettmer *et al.*, 2006; Robert *et al.*, 2008). We analyzed the localization of GFP-SYP4 in transgenic roots and nodules expressed under the control of the *Ubiquitin3* promoter. In transgenic roots, GFP-MtSYP4 marks numerous mobile dot-like structures (Fig. S5*A*) similar to SYP41 proteins in *Arabidopsis*. Furthermore, pulse-chase labeling with FM4-64 in GFP-SYP41 roots showed marked co-localization already within 20 to 30
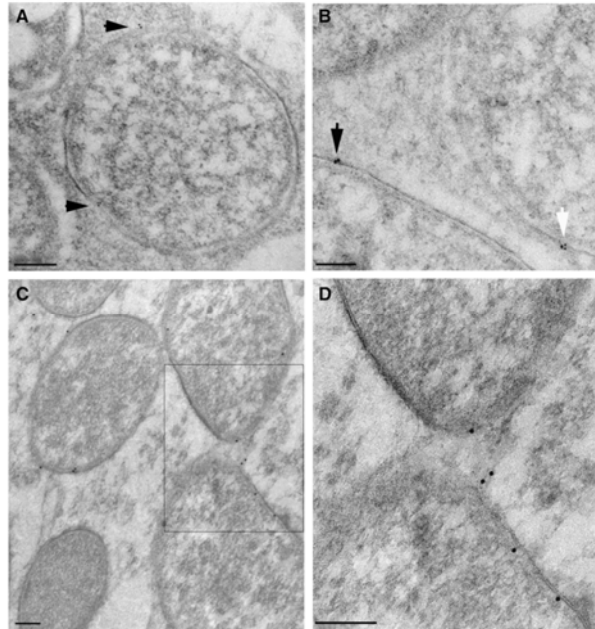
Figure 5. SB membranes contain Rab7 and acquire SYP22 during natural senescence. (*A*) Immunogold detection of anti-GFP in *pLB::GFP-Rab7A2*-expressing nodules. The 10-nm gold particles are present over the SB membranes. (*B*) Double immunolabeling using anti-GFP (detected by 15-nm gold; black arrowhead) and anti-MtRab7 (10-nm gold; white arrowhead) confirm the presence of Rab7 on the SB membranes. (*C*) Immunogold detection of anti-GFP in 5-week-old *pLB::GFP-SYP22*-expressing nodule. The 15-nm gold signal (arrow) is found over the SB membrane in several cells at the base of the nodule. (*D*) Close-up of boxed area in (*C*). (Scale bar, 500 nm in *A*, 200 nm in *B-D*.)

min after addition of the dye (Fig. S5*B*). This suggests that *Medicago* SYP41 indeed marks an early endosomal compartment. GFP-SYP41 also marked numerous dot-like structures in infected nodule cells. However, no association with SBs was observed at any stage of development, whereas dot-like structures were labeled in these cells (Fig. S5*C*). The absence of both SYP41 and Rab5 on SBs makes it unlikely that they acquire Rab7 by sequential interaction with the different compartments of the endocytic pathway.

Functional analyses of Rab7 in symbiosome development. Since Rab7 proteins occur on SBs, we examined whether manipulation of Rab7 activity would interfere with SB development. Therefore, first a dominant-negative construct [T22N] was made locking the protein in the GDP-bound state. Analogous constructs in mammalian cells impair late endosome traffic to lysosomes (Bucci et al., 2000). Expression of *p35S::GFP-Rab7A2[T22N]* in roots resulted in a loss of GFP fluorescence from the endosomes and tonoplast, and instead only cytoplasmic fluorescence was observed (Fig. 6A). This indicates that the GFP construct is indeed in a GDP-locked state as such Rab proteins are kept in the cytoplasm
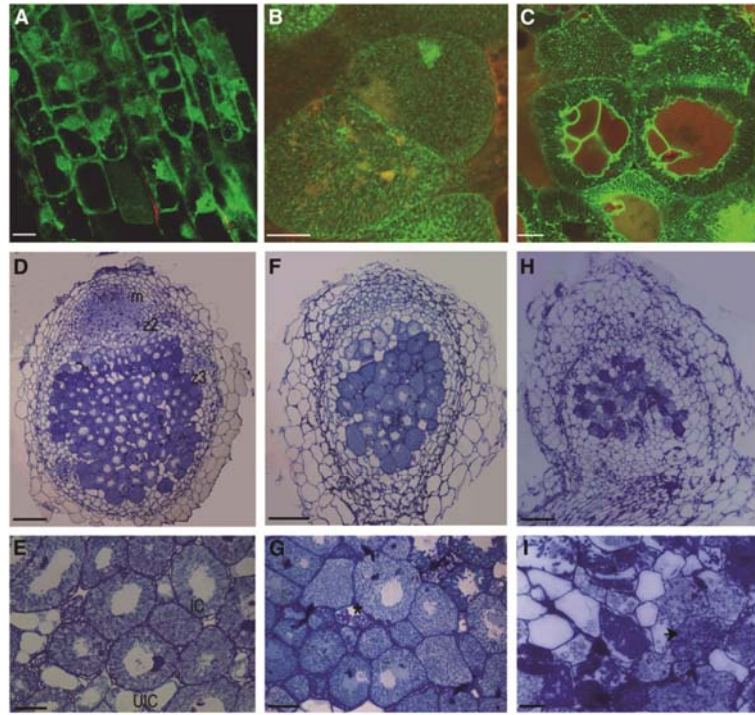
Figure 6. Rab7 is required for SB development and maintenance. (*A*) Confocal image of dominant-negative *p35S::GFP-Rab7A2[T22N]*-expressing root, showing GFP-Rab7A2[T22N] fluorescence in the cytoplasm. (*B*) *pLB::GFP-Rab7A2[T22N]* expression in the nodule also shows fluorescence in the cytoplasm. (*C*) Confocal image of constitutively active *pLB::GFP-Rab7A2[Q67L]*-expressing infected cells in a 14-day-old nodule. Stronger labeling of the tonoplast compared to labeling of the SBs can be observed (cf. Fig. 6C and 4E). The always-active construct does not induce fusion SBs or their transformation into lytic compartments. (*D*) Longitudinal section of a control (empty vector) 14-day-old nodule. Zones: m, meristem; z2, infection zone; z3, fixation zone. (E) Magnification of z3 in (*D*) showing developed (stage 4) nitrogen-fixing SBs. UIC, uninfected cell; IC, infected cell. (*F*) Longitudinal section of a 14-day-old Rab7A1-RNAi nodule. (*G*) Magnification of z3 in (*F*), showing long rod-type (stage 3) SBs present in z3; note intense accumulation of starch grains in uninfected cells (star). (*H*) Longitudinal section of a 21-day-old Rab7A1-RNAi nodule showing signs of early senescence; note most of the tissue is degraded. (*I*) Magnification of (*H*) showing degraded SBs and dead cells recolonized by saprophytic bacteria (arrow). (Scale bars, 10 μm in *A-C*, 100 μm in *D*, 50 μm in *E*.)

through the binding of Rab-GDI factors (Nielsen *et al.*, 2008). However, vacuole formation and root growth were not affected. Similarly, expression of this construct under the control of the nodule-specific *ENOD12* or *LB* promoters did not impair SB development. Also here, GFP fluorescence was only observed in the cytoplasm (Fig. 6B). It seems likely that expression of the Rab7[T22N] protein was not sufficient to act in a dominant-negative manner as vacuole formation was also not affected.

32

It is possible that Rab7 activation on the SB membrane is impaired to avoid fusion and formation of lytic compartments. To investigate this possibility, we tested the effect of a constitutively active Rab7 [Q67L] form on SB maintenance. Expression of *p35S::GFP-Rab7A2[Q67L]* in roots did not affect root growth, and GFP fluorescence occurred on the tonoplast as well as on dot-like endosomes (data not shown). In the nodule, we observed a much stronger labeling of the main vacuole compared to SBs in the *pLB::GFP-Rab7A2[Q67L]* infected cells. By contrast, the tonoplast and SBs are labeled to a similar level in nodules expressing wild-type GFP-Rab7A2. However, SB formation and maintenance as individual units was not affected (Fig. 6*C*). Since active Rab7 is not sufficient to trigger their fusion and formation of lytic compartments, it is probable that components in addition to Rab7 are lacking in the SB membrane.

To further investigate the role of Rab7 in SB development, we knocked down the expression of Rab7A1 using *A. rhizogenes*-mediated RNA interference (RNAi). Rab7A1 RNAi knocked down the expression of both Rab7A1 and A2 as determined by quantitative RT-PCR analysis (Fig. S9). No effect on root development was observed. Approximately 65% of the nodules ($n = 42$) that formed on transgenic Rab7A1 RNAi roots (21 days after inoculation [dai]) showed an early senescence phenotype (Fig. 6*D* and *E*), in contrast with 10% of nodules on roots transformed with an empty vector control ($n = 24$). Since premature senescence is most likely a secondary effect, we studied younger Rab7A1 RNAi nodules (9 and 14 dai). This showed that SB development in these nodules did not proceed further than stage 3 (elongated rods) (Vasse *et al*., 1990) and SBs did not reach the mature stage 4 as in control nodules (Fig. 6*D* to *I*), at which they are able to fix atmospheric nitrogen according to Vasse *et al*. (1990). Instead, premature senescence is induced causing the disintegration of SBs and recolonization of the cells by saprophytic bacteria (Fig. 6*C* and *I*). This shows that SB development becomes arrested at a stage slightly after they normally would acquire Rab7, suggesting that Rab7 is required for the further maturation of the SB.

Syntaxins SYP22, VTI11 and tonoplast intrinsic protein during symbiosome evelopment. The presence of Rab7 on the SB membrane suggests that the SB either has the identity of a Rab7-marked MVB or of a young vacuole. To determine whether SBs acquire a vacuolar identity, we analyzed whether other vacuolar identity markers are associated with the SB during its development. A complex of SNAREs SYP22, VTI11 and SYP51 has been suggested to operate at the *Arabidopsis* tonoplast and to control PVC-to-vacuole trafficking (Sanderfoot *et al*., 2001; Surpin *et al*., 2003; Yano *et al*., 2003; Carter *et al*., 2004; Uemura *et al*., 2004; Ebine *et al*., 2008). Therefore, we studied whether the *Medicago* homologs of the vacuolar SNARE proteins, SYP22 and VTI11, occur on SBs.

A *Medicago* SYP22 homolog (TC100656) and VTI11 homolog (TC95338) were fused to GFP and first expressed in transgenic roots under the control of the *Ubiquitin3* promoter. Both GFP-SYP22 (Fig. 7*A* and *B*) and GFP-VTI11 (Fig. 7*G*) located to the tonoplast of young and mature vacuoles and dot-like structures were labeled. The latter might be PVC or even the TGN, as in *Arabidopsis* SYP22 and VTI11 occur on the tonoplast and on PVCs and VTI11 additionally localized to the TGN (Sato *et al*., 1997; Sanderfoot *et al*., 1999; Bassham *et al*., 2000; Uemura *et al*., 2002, 2004; Carter *et al*., 2004; Samaj *et al*., 2005; Sanmartin *et al*., 2007; Ebine *et al*., 2008). To confirm the localization of the endogenous proteins, we used anti-*Medicago* VTI11 antibody. Immunolocalization of VTI11
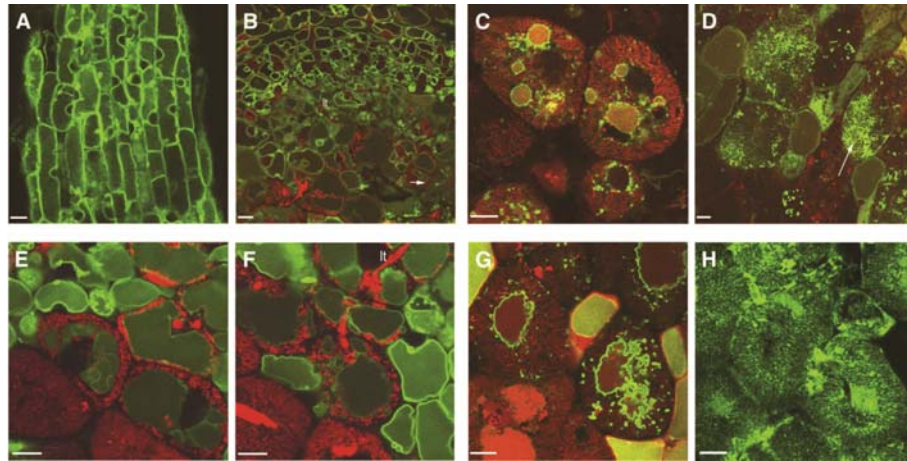
Figure 7. SBs do not have vacuolar identity until the onset of senescence. (*A*) Confocal image of *pUBQ3::GFP-MtSYP22*-expressing root, showing mainly tonoplast labeling. (*B*) Confocal image of *pUBQ3::GFP-MtSYP22*-expressing 14 dai nodule, showing tonoplast labeling. No signal is observed on the SBs (arrow). (*C*) *pLB::GFP-MtSYP22* expression in the infected cells of the fixation zone of 14 dai nodules. GFP-MtSYP22 appears on the tonoplast and dot-like structures, but not on the SBs. (*D*) In 5-week-old *pLB:GFP-MtSYP22*-expressing nodules, GFP-MtSYP22 can be observed over the senescent SB membrane (arrow) in the basal part of the nodule. (*E*) Confocal image of *pUBQ3::At-γ-TIP-GFP*-expressing 14-day-old nodule, showing labeling of the tonoplast, but not of the young differentiating SBs. (*F*) *pUBQ3::At-δ-TIP-GFP*-expressing 14-d-old nodule, showing also tonoplast but not SB labeling. (*G*) Confocal image of *pLB::GFP-MtVTI11* expression in the infected cells of the fixation zone of 14 day nodules. In contrast with tonoplast labeling, SBs are not labeled. (*H*) Immunolocalization of MtVTI11 on 8-week-old wild-type nodule tissue showing the labeling of SB membranes in senescent nodules. Rhizobia in (*B*) to (*F*) are expressing mRFP (red). It, infection thread. (Scale bars, 500 nm in *A* and 200 nm in *B-D*.)

on GFP-SYP22-expressing roots showed a high level of co-localization (Fig. S6), and the VTI11 antibody marked both the tonoplast and dot-like structures. Therefore, we concluded that the GFP fusion constructs can be used to determine the localization of the endogenous proteins.

As SYP22 (and VTI11) in addition to tonoplast localization is thought to reside at MVBs en route to the vacuole, we examined its localization with respect to Rab7 MVBs. Immunolocalization of RAB7 on GFP-SYP22-expressing roots showed co-localization at the tonoplast as well as a partial co-localization in the dot-like structures (Fig. S7). This further suggests that Rab7 MVBs are involved in PVC-to-vacuole traffic.

We analyzed the localization of GFP-SYP22 and GFP-VTI11 in relation to SB development in 14-day-old transgenic nodules, expressed either under the control of the *Ubiquitin3* or *LB* promoter. The pattern of localization was similar for both proteins; they occurred on the tonoplast in both infected and noninfected cells (Fig. 7*A* and *B*). However, developing and mature N$_2$-fixing SBs were not labeled by GFP-SYP22 or GFP-VTI11 in 14-day-old nodules (Fig. 7*C* and *G*). So SBs do not have a vacuolar or PVC identity.

In addition to vacuolar SNARE proteins, we also examined the localization of two tonoplast intrinsic protein (TIP) isoforms from *Arabidopsis*: δ-TIP and γ-TIP. γ-TIP was shown to mark the lytic vacuole in plants, while δ-TIP was shown to additionally mark storage-type vacuoles in vegetative cells (Jauh *et al.*, 1999). GFP-γ-TIP and GFP-δ-TIP expressed under control of the *Ubiquitin3* promoter both labeled the main vacuole in root and nodule cells (Fig. 7*E* and *F*). However, they both do not occur on the SB membrane in young infected cells, supporting the conclusion that SBs do not have a vacuolar identity.

When nodules become older (from 4 weeks after inoculation) they start to senesce, which starts with the fusion and formation of lytic SB compartments in the most proximal (oldest) infected cells (Vasse *et al.*, 1990; Van de Velde *et al.*, 2006). This fusion of SBs to form lytic compartments resembles vacuole formation. Therefore, we wondered whether the SBs at this stage acquire vacuolar identity. Indeed, in 5-week-old nodules, GFP-SYP22 and GFP-VTI11 do occur on the SB membrane in cells in the proximal part of the nodule closest to the root (Fig. 7*D*). In certain cells, actually part of the SBs show labeling of the SB membrane, while other SBs in the same cell have not yet acquired the vacuolar markers (Fig. 7*D*). This likely represents a very early stage of senescence. The association of endogenous VTI11 with SBs during senescence was confirmed using the VTI11 antibody on 8-week-old wild-type nodules (Fig. 7*H*). Rab7 is also still associated with SBs during senescence (data not shown). Immuno-EM analysis of GFP-SYP22 senescent transgenic nodules confirmed that GFP-SYP22 now marks the SB membrane (Fig. 5*C* and *D*).

In Rab7 RNAi roots, neither vacuole formation nor SB senescence is blocked. Therefore, we assumed that the vacuolar syntaxins are still targeted to their membranes despite the reduced levels of Rab7. Immunolocalization of anti-VTI11 in Rab7A1 RNAi roots showed that VTI11 indeed occurs on the tonoplast and endosomes, like in wild-type plants (Fig. S8*A*). Furthermore, in the Rab7A1 RNAi nodules, senescing SBs do contain VTI11 (Fig. S8*B*), indicating the senescence-related acquisition of vacuolar identity.

These observations suggest that the survival and maintenance of the bacteria in individual SB compartments during the N$_2$-fixing stage is achieved by delaying the acquisition of vacuolar identity (e.g., vacuolar SNAREs).

The plasma membrane SNARE SYP132 occurs on symbiosomes throughout their development. A proteomics approach has previously identified a *Medicago* plasma membrane syntaxin SYP132 (TC86779), which immunolocalized to the infection thread membrane as well as to the SB membrane, although it was not reported from which developmental stage (Catalano *et al.*, 2007). Therefore, we wondered whether early SBs (directly after release from the infection threads) contain this syntaxin and whether they retain this marker during further development. We created a GFP fusion construct and studied its localization in roots and nodules. In roots, GFP-SYP132 marks the plasma membrane and occasionally accumulates in spots in the plasma membrane (Fig. 8*A*). In nodules, GFP-SYP132 marks the plasma membrane as well as the infection thread membrane (Fig. 8*B*) and labels the SB membrane as soon as the rhizobia are taken up into the cells (Fig. 8*B* and *C*). GFP-SYP132 strikingly labels the SB membrane throughout all developmental stages up to stage 4 in the fixation zone (Fig. 8*D*) as well as during senescent stages. Therefore, mature SBs appear to have a unique mosaic identity, containing both SYP132 and Rab7.
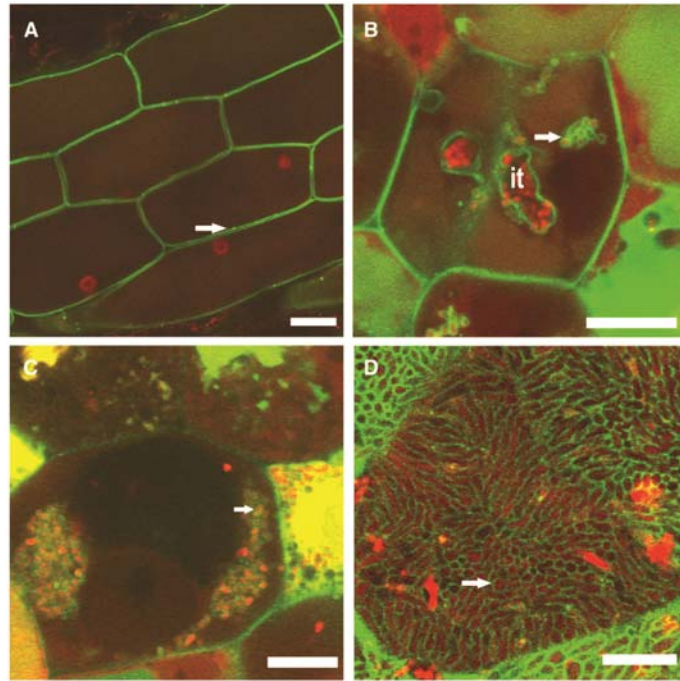
Figure 8. SBs retain plasma membrane identity throughout their development. (*A*) Confocal image of *pUBQ::GFP-SYP132*-expressing root. GFP-SYP132 marks the plasma membrane and occasionally accumulates in spot in the plasma membrane (arrow). (*B*) and (*C*) *pE12::GFP-SYP132*-expressing nodules show GFP-SYP132 on the plasma membrane and infection thread (*it*) membrane as well as just formed SBs ([*B*]; arrow) and early stage SBs ([*C*]; arrow). (*D*) *pLB::GFP-SYP132*-expressing nodule showing GFP-SYP132 marking the SB membrane (arrow) in fully infected cells of the fixation zone. Rhizobia in (*B*) to (*D*) are expressing mRFP (red). (Scale bars, 20 μm in *A* and 10 μm in *B-D*.)

Discussion

We showed that the *Medicago* Rab5s and Rab7A1/A2 are late endosomal membrane identity markers. The latter mark a unique endomembrane compartment in plants that might be positioned in between Rab5 MVBs and the vacuole. SBs do not contain Rab5s at any stage of their development and the TGN marker SYP4, thought to be an early endosome marker, did not occur on SBs. By contrast, Rab7 is acquired by SBs when they have stopped dividing and start to elongate, and it is maintained up to the senescence stage. However, the SBs do not acquire a (lytic) vacuole identity (vacuolar SNAREs) until the onset of senescence. Instead, SBs acquire the plasma membrane SNARE SYP132 from the start of SB formation throughout their development. Therefore, SBs appear to be locked in a unique SYP132 and Rab7 positive stage, and the delay in acquiring vacuolar identity most likely facilitates their maintenance as individual membrane compartments.

The membrane identity markers used in this study were selected based on homology to well-studied *Arabidopsis* counterparts as well as on their expression in infected cells of the nodule, which was confirmed by microarray analysis on RNA from infected cells isolated by laser microdissection. Specific antibodies for Rab5, Rab7 and VTI11 confirm that the corresponding genes are indeed active in the infected as well as uninfected cells of *Medicago* nodules and that the GFP fusion constructs correctly mark the localization of the endogenous proteins.

Medicago has three Rab5 homologs, similar to *Arabidopsis*. These Rab5 proteins mark multivesicular endosomes (100 to 300 nm) in *Medicago* root and nodule cells. The high level of co-localization of these Rab5 endosomes with the (lytic) vacuolar sorting receptor BP-80 identifies them as PVCs, similar as in *Arabidopsis* (Paris and Neuhaus, 2002; Sohn *et al*., 2003; Foresti *et al*., 2006; Lam *et al*., 2007). Labeling by the endosomal tracer FM4-64 shows that the Rab5 MVBs are involved in endocytosis. Therefore, it is very probable that like in *Arabidopsis* (and yeast), the endocytic and vacuolar transport pathways merge at these Rab5-labeled MVBs (Gerrard *et al*., 2000; Pelham, 2002; Tse *et al*., 2004; Lam *et al*., 2007; Jaillais *et al*., 2008; Robinson *et al*., 2008). *Medicago* Rab7A1/A2 is located at 300 to 500 nm MVBs that become labeled with the endocytic tracer FM4-64 as well as the tonoplast. The latter has also been observed in rice and *Arabidopsis* (Saito *et al*., 2002; Nahm *et al*., 2003). Interestingly, the involvement of Rab7-labeled MVBs in endocytosis in plants raises the possibility that, like in mammalian cells, Rab5-labeled MVBs mature into Rab7 MVBs that subsequently fuse with a lytic compartment (Rink *et al*., 2005; Vonderheit and Helenius, 2005). In this case, the Rab7 MVBs function as a transitory compartment between Rab5 late endosomes and the vacuole, like in yeast (Pelham, 2002). Consistent with this hypothesis is the observed co-localization of Rab5 and Rab7 in 30% of the endosomes and the markedly bigger size of Rab7-labeled MVBs compared to Rab5 MVBs, as in animals (Meresse et al., 1995). Co-localization of BP-80 with Rab7 showed markedly less co-localization than BP-80 with Rab5 and Rab7. This might suggest that vacuolar sorting receptors are recycled from the Rab5 MVBs, as these mature to Rab7 MVBs. However, *in vivo* studies on maturating endosomes remain to be done in *Medicago* to prove that Rab5 MVBs mature via Rab7 MVBs. With the current knowledge, it cannot be excluded that Rab7-labeled endosomes are involved in a Rab5-independent endocytic pathway.

SBs do not acquire Rab5s at any stage of their development into mature N_2-fixing organelles. Also, BP-80, which co-localizes with Rab5 on endosomes, does not occur on SB membranes. Even at the stage where Rab7 does not yet occur at the SB membrane, Rab5 and BP-80 are not present. At this stage, SBs also do not show any association of the early endosome marker SYP4. Therefore, it is unlikely that SB formation involves fusion with the TGN or Rab5 endosomes, although these are present in the infected nodule cells.

By contrast, the SB membrane acquires the endosomal/vacuolar marker Rab7A1/A2 when SBs have stopped dividing. This suggests that SBs either have vacuolar identity or Rab7-MVB identity. The absence of the vacuolar syntaxins SYP22 and VTI11 up to the senescence stage suggests that a Rab7-MVB identity is more probable. So although our studies suggest that the Rab5- and Rab7-labeled endosomes can be part of the same endocytic pathway, Rab7 is recruited to the SB membrane in a Rab5-independent manner. In this case, early steps of SB formation are not related to the Rab5-dependent endocytic pathway. It appears that early steps of SB formation do not require any endocytic machin-

ery, and Rab7 might be recruited directly from the cytoplasm to facilitate SB development. An endocytosis-independent process would be consistent with the presence of the plasma membrane-type syntaxin, SYP132, on the SB membrane throughout its development. The combined presence of SYP132 and Rab7 suggests a unique mosaic identity of the SB membrane, which could allow the bacteria to intercept both specific secretory traffic to the plasma membrane and specific endocytic/biosynthetic traffic towards the vacuole. Generally during endocytosis, plasma membrane identity markers are recycled/removed as endocytic vesicles are sorted along the endocytic pathway. Therefore, retaining SYP132 on the SB membrane suggests either an endocytosis-independent process or a block of recycling of SYP132 during endocytosis. We are currently investigating the role of the plasma membrane-directed secretory pathway in SB formation and development.

On the other hand, it is possible that Rab7-labeled endosomes are involved in a yet uncharacterized Rab5-independent endocytic pathway, suggesting the existence of additional not yet characterized endosome compartments in plants. Theoretically, developing SBs might interact with these endosomes before acquiring Rab7. In animal cells, non-Rab5-labeled early endosomes have been identified that are associated with lipid raft/nonclathrin-mediated endocytosis in a pathway that does not lead to fusion with lysosomes (Conrad *et al*., 1995; Shin and Abraham, 2001; Mayor and Pagano, 2007).

Several pathogenic bacteria that are able to survive in vacuole-like compartments in animal cells, such as *Legionella pneumophila* and *Escherichia coli*, have also been shown to acquire the late endosomal marker Rab7 in a Rab5-independent manner (Clemens *et al*., 2000a, 2000b; Shin *et al*., 2000; Passey *et al*., 2008). Like SBs, both are maintained as individual compartments that do not fuse with lysosomes, indicating that Rab7 is not sufficient to induce fusion with a lytic compartment. Even association of constitutively active GTP-locked GFP-Rab7A2[Q67L] with the SB membranes did not induce their fusion and formation of lytic compartments. By contrast, stronger labeling of the tonoplast was observed in the infected cells expressing GFP-Rab7A2[Q67L] compared to SB labeling. This might indicate that there is enhanced trafficking from Rab7 endosomes to the vacuole similar as in animal cells where always-active forms of Rab7 indeed enhance endocytic traffic to lysosomes (Meresse *et al*., 1995). Similarly, in *Legionella* or *Salmonella*-infected animal cells, the presence of an always active Rab7 on the bacteria-containing membrane compartments is not sufficient to promote their fusion with lysosomes (Clemens *et al*., 2000a; Harrison *et al*., 2004). Therefore, components required in addition to Rab7 to facilitate fusion and the transition into a lytic compartment are missing in the SB membrane (Vieira *et al*., 2003).

Vacuolar SNARE proteins play a role in vacuole biogenesis and do occur in plant PVCs and tonoplast (Sato *et al*., 1997; Sanderfoot *et al*., 1999, 2001; Rojo *et al*., 2003; Carter *et al*., 2004; Samaj *et al*., 2005; Bassham and Blatt, 2008; Ebine *et al*., 2008). Therefore, we studied the vacuolar SNAREs SYP22 and VTI11 and showed that they occur on the tonoplast (and likely PVCs) of root cells as well as of infected and uninfected nodule cells. However, they do not occur on young SBs and only appear on the SB membrane as senescence starts, when SBs fuse and form lytic compartments (Van de Velde *et al*., 2006). This process resembles lytic vacuole formation, which fits with the observation that the vacuolar identity markers SYP22 and VTI11 now mark the SB membrane. Therefore, we propose that the delay in acquiring lytic vacuolar identity (e.g., vacuolar SNARE proteins)

by the SBs is facilitating maintenance of SBs as individual N_2-fixing organelles. How this
delay is established remains to be solved.

It has previously been suggested that SBs represent vacuole-like compartments in
analogy to protein storage vacuoles (PSVs) (Mellor, 1989). Lytic vacuoles and storage-type
vacuoles can be distinguished by the respective presence of the vacuolar-targeted TIP pro-
teins γ-TIP and δ-TIP (Jauh *et al*., 1999). The absence of both γ-TIP and δ-TIP on func-
tional SBs suggests that SBs do not have lytic or storage vacuole identity; although we did
not study whether these TIP proteins indeed distinguish PSVs from lytic vacuoles in *Medi-
cago*. During seed germination, PSVs are thought to acquire lytic activity through the de-
livery of newly formed proteases via MVBs (Wang *et al*., 2007). Comparably, the observed
acquisition of vacuolar identity by SBs upon senescence likely allows the delivery of newly
formed proteases to facilitate the switch to lytic compartments.

Our data indicate that Rab7 is not essential for proper localization of vacuolar
SNAREs, as VTI11 localization was not affected in Rab7A1 RNAi roots or in nodule cells
that show an early senescence phenotype. However, redundant roles of additional members
of the Rab7 family cannot be ruled out, as in *Arabidopsis* double, triple, and quadruple
Rab7 mutants did not show obvious phenotypes (T. Ueda, unpublished data in Nielsen *et
al*., 2008). A study in soybean had previously shown that antisense expression of a Rab7
homolog resulted in a more frequent degradation of SBs in vacuole-like compartments
(Cheon *et al*., 1993). However, in this study, the leghemoglobin promoter was used to drive
the antisense construct by which it is first expressed at a late stage of development. Here,
we show that knockdown of Rab7A1/A2 expression actually blocked SB development at a
stage where SBs had started elongation (differentiation) but were not yet fixing nitrogen.
This suggests that Rab7 is essential for proper development into a nitrogen-fixing organelle.
How Rab7 regulates SB development and maintenance remains unclear. It is possible that
unknown components required for SB development/maintenance require Rab7 for proper
targeting to the SBs.

The Rab7 endosomal nature of SBs might explain the reported presence of several
vacuolar enzymes in the SB space (Mellor, 1989; Jones *et al*., 2007), as these are likely
transported to the vacuole via late endosomes. This is further supported by the observation
that a Cys protease, which localizes to the SB space, is indeed detected in both vacuoles
and ~500-nm cytoplasmic vesicles in pea roots and nodules (Vincent and Brewin, 2000).
Although the nature of these ~500-nm cytoplasmic vesicles was not studied, their ultra-
structure seems strikingly similar to the Rab7-MVB.

In conclusion, SB development appears to involve only part of the known/default
endocytic machinery, and this is first used when SBs stop dividing. Which endomembrane
processes have been adapted to support the endocytotic uptake of rhizobia in nodule cells
and the subsequent proliferation of SBs remains to be revealed. The continued presence of
SYP132 during SB development suggests a major role for the secretory pathway. Further-
more, Rab7-containing SBs are maintained as individual N_2-fixing compartments by delay-
ing the acquisition of (lytic) vacuolar identity. Therefore, it will be important to determine
the molecular mechanism by which this is achieved.

Materials and Methods

Plant transformation and rhizobial strains. The *Medicago truncatula* accession Jemalong A17 was used. *Agrobacterium rhizogenes* strain MSU440 (Sonti et al., 1995) was used for hairy root transformations according to Limpens *et al.* (2004). For nodulation, *Sinorhizobium meliloti* strain 2011 or *S. meliloti* 2011-mRFP (Smit et al., 2005) expressing the red fluorescent mRFP protein were used. Nodulation was done according to Limpens *et al.* (2004) using 2 mL (OD600 0.1) rhizobial suspension per plant.

Constructs. *Medicago* Rab5A1, A2, and B and Rab7A1, A2, SYP22, VTI11, SYP132, and SYP4 open reading frames were PCR amplified from 10-day-old nodule cDNA using Phusion high fidelity Taq polymerase (New England Biolabs) and directionally cloned into pENTR-D-TOPO (Invitrogen). *Medicago* SYP22 and VTI11 were directionally cloned with HindIII-KpnI and BamHI-EcoRI, respectively, into a modified pENTR vector (pENTR2) containing a multiple cloning site. *Arabidopsis thaliana* δ-TIP (NM_112495) and γ-TIP (NM_129238) were amplified from *Arabidopsis* Columbia root cDNA and cloned BamHI-EcoRI into pENTR2. pENTR clones Rab5A1, Rab5A2, Rab7A1, Rab7A2, SYP22, VTI11, SYP132, and SYP4 were recombined into either of the following Gateway-compatible binary vectors using LR Clonase (Invitrogen): *p35S*-pK7WGF2-R (containing the *35S* promoter) (Smit et al., 2005), *pUBQ3*-pK7WGF2-R, *pE12*-pK7WGF2-R, and *pLBp*-K7WGF2-R, creating N-terminal GFP-X fusions. pENTR clone Rab5B was recombined into *p35S*-pK7FWG2 (Karimi et al., 2002), *pE12*-pK7FWG2, and *pLB*-pK7FWG2; pENTR clones δ-TIP and γ-TIP were recombined into *UBQ3*-pK7FWG2, creating C-terminal X-GFP fusions. For RNAi, pENTR-Rab7A1 was recombined into pK7GWIWG2(II)-*pUBQ10*:DsRED (Limpens et al., 2005). All constructs were verified by sequencing and restriction digestion. The constructs were transformed to *A. rhizogenes* MSU440 and used for hairy root transformations.

Constitutive-active [Q67L] and dominant-negative [T22N] Rab7A2 constructs were generated via two subsequent PCR reactions using Rab7A2-F x Rab7A2[Q67L]-2/Rab7A2[T22N]-2 and Rab7A2-R x Rab7A2 [Q67L]-1/Rab7A2[T22N]-1 in a first PCR reaction using Phusion high fidelity Taq polymerase (New England Biolobs). PCR primers are presented in Supplemental Table 1 online. The obtained fragments were diluted 1:1000 and used in a second PCR reaction using Rab7A2-F and Rab7A2-R. The resulting fragment was directionally cloned into pENTR-D-TOPO (Invitrogen), verified by sequencing, and subsequently recombined into *p35S*-pK7WGF2-R, *pE12*-pK7WGF2-R, and *pLB*-pK7WGF2-R.

The Gateway-compatible binary vectors containing the *Ubiquitin3* (*UBQ3*), *ENOD12* (*E12*), and pea (*Pisum sativum*) *LB* promoters were created by digesting pK7FWG2 (Karimi et al., 2002) or pK7WGF2-R (Smit et al., 2005) with HindIII-SpeI (removing the 35S promoter) and ligating the corresponding promoter fragments.

Quantitative PCR analysis. Quantitative RT-PCR was conducted on RNA isolated form nitrogen-starved, uninoculated roots, 10-day-old nodules, and 3-week-old nodules as well as on RNA from nodulated Rab7A1 RNAi and control roots. Total RNA was isolated and DNAse treated using the Plant RNeasy kit (Qiagen; according to the manufacturer's in-

structions). cDNA was synthesized from 1 mg total RNA using the Taqman Gold RT-PCR kit (Perkin-Elmer Applied Biosystems) in a total volume of 50 mL using random hexamer primers (10 min 25ºC, 30 min 48ºC, and 5 min 95ºC). Quantitative PCR reactions were performed in triplicate on 1 mL cDNA using the Quantitative PCR Core kit for SYBR Green I (Eurogentec), and real-time detection was performed on a MyiQ (Bio-Rad) (40 cycles of 95ºC for 10s and 60ºC for 1 min) followed by a heat dissociation step (from 65 to 95ºC). Primers were used at a final concentration of 300 nM. GAPDH was used as reference.

Fluorescent microscopy. Transgenic roots and nodules were selected based on GFP or DsRED1 expression using a Leica MZFLIII binocular fitted with HQ470/40, HQ525/50, HQ553/30, and HQ620/60 optical filters (Leica Microsystems). Transgenic nodules were hand-sectioned using double-edged razorblades and mounted on microscope slides in 0.1 M phosphate buffer, pH 7.4, containing 25 mg/mL sucrose. Transgenic roots and sectioned nodules were further analyzed on a Zeiss LSM 510 confocal laser scanning microscope (Carl-Zeiss Axiovert 100 M equipped with a LSM510, an argon laser with a 488-nm laser line, a helium-neon laser with a 543-nm laser line); excitation at 488 nm (GFP; Sytox-Green/Alexa 488) and 543 nm (DsRED1/mRFP/CY3); GFP/Sytox Green/Alexa 588 emission was selectively detected using a 505- to 530-nm band-pass filter; DsRED1/mRFP/CY3 emission was detected in another channel using a 560- to 615-nm band-pass filter.

Immunolocalization. Nodules were hand-sectioned using a double-edged razorblade. Nodule sections or roots were fixed in 1% of freshly depolymerized paraformaldehyde in 1×PBS, pH 7.4, for 30 min at 48ºC. Nodule sections were blocked in normal goat serum or 3% BSA and further incubated with the primary antibody overnight at 48ºC in 1×PBS containing 0.3% Triton X-100. The secondary antibodies anti-Rabbit Alexa 488, anti-mouse Alexa 488, anti-Mouse CY3 (Molecular Probes) were used according to the supplier's instructions. Controls were carried out in the absence of primary antibodies. Nodule sections containing wild-type Sm2011 rhizobia were counterstained with Sytox Green (Molecular Probes) or propidium iodide and examined by confocal microscopy. Primary antibody dilutions were as follows: anti-GFP rabbit (Molecular Probes), 1:200; anti-GFP mouse (Molecular Probes), 1:50; anti-Ara7 (T. Ueda), 1:200; anti-Ara6 (T. Ueda), 1:100; anti-Rab7 mouse (GenScript), 1:50 and 1:100; anti-VTI11 (rabbit) (GenScript), 1:100 and 1:200; anti-BP-80 (N. Paris), 1:100. Affinity-purified polyclonal mouse anti-Rab7 and polyclonal rabbit anti-VTI11 were generated by GenScript against the peptides FLIQANPSDPENFPC (Rab7) and RKMDLEARSLQPNIC (VTI11).

FM4-64 staining. Transgenic roots were selected using the Leica MZFLIII fluorescence stereomacroscope, cut from the plant, and directly placed into a solution of FM4-64 (30 mg/mL) in phosphate buffer (0.1 M, containing 25 mg/mL sucrose) on ice for a minimum period of 30 min. The roots were washed two times in phosphate buffer (0.1 M, containing 25 mg/mL sucrose) to remove the excess FM4-64 and incubated at room temperature for the indicated times.

EM sample preparation by high-pressure freezing and freeze substitution. For tissue processing, a modified method of Thijssen et al. (1997) was used. Nodules and roots were

cryofixed with a Balzers HPM 010 high pressure freezing device and specimens were further placed in heptane. Freeze substitution was performed with a FreasySub unit (Cryotech Benelux, Schagen-NL), from –90 to 0ºC for 68 h. The substitution medium contained 0.3% glutaraldehyde + 0.2% uranyl acetate in acetone. Samples were embedded in LR White resin with 0.5% benzoin methyl ether as a catalyst and polymerized under UV light at –20ºC. Some samples were fixed by a conventional method in 4% paraformaldehyde mixed with 0.3% glutaraldehyde in 50 mM phosphate buffer, pH 7.4, embedded in LR white resin prepared as above and polymerizedwith UV light at –20ºC.

For the analysis of the structure of Rab7A1 RNAi nodules, the tissue was fixed by the conventional method in 4% paraformaldehyde with 3% glutaraldehyde in 50 mM phosphate buffer, pH 7.4, postfixed with 1% OsO4, embedded in LR white resin according to the supplier's recommendations and polymerized at 60ºC.

EM immunodetection. Thin sections (60 nm) were cut using a Leica Ultracut microtome. Nickel grids with the sections were blocked in normal goat serum or 2% BSA in PBS. Grids were incubated overnight at 4ºC with the primary antibody according to dilutions given above. Goat anti-rabbit coupled with 15-nm gold (BioCell) (1:50 dilution), donkey anti-rabbit (15 nm) (1:50), or donkey anti-mouse coupled with 10-nmgold (1:30) (Aurion) was used as secondary antibody. The sections were contrasted with 2% aqueous uranyl acetate and lead citrate and examined using a JEOL JEM 2100 transmission electron microscope equipped with a Gatan US4000 4K×4K camera.

Phylogenetic analyses. Phylogenetic analyses were conducted using MEGA version 4 (Tamura, Dudley, Nei, and Kumar 2007). A multiple protein alignment was made using default parameters: gap opening, 10.00; gap extension, 0.20; residue-specific penalties, on; hydrophilic penalties, on; gap separation distance, 4; end gap separation, off; negative matrix, off; delay divergent sequences, 30%; protein weight matrix, Gonnet Series. From this alignment a midpoint-rooted neighbor-joining tree with bootstraps values (1000 replicates) was drawn.

Accession Numbers. Sequence data from this article can be found in the GenBank/EMBL data libraries or TIGR Gene Indices under the following accession numbers: Rab5A1, TC106962; Rab5A2, TC106963; Rab5B, TC93994; Rab7A1, TC101145; Rab7A2, TC94423; SYP4, TC96961; VTI11, TC95338; SYP22, TC100656; SYP132, TC86779; GAPDH, BT052418.1; *Arabidopsis* δ-TIP, NM_112495; *Arabidopsis* γ-TIP, NM_129238.

References

Alonso A, Garcia-del Portillo F (2004). Hijacking of eukaryotic functions by intracellular bacterial pathogens. *Int. Microbiol* **7**:181-191.

Auriac M-C, Timmers ACJ (2007). Nodulation studies in the model legume *Medicago truncatula*: advantages of using the constitutive EF1α promoter and limitations in detecting fluorescent reporter proteins in nodule tissues. *Mol Plant Microbe Interact* **20**:1040–1047.

Bassham DC, Blatt MR (2008). SNAREs: Cogs and coordinators in signaling and development. *Plant Physiol* **147**:1504–1515.

Bassham DC, Raikhel RV (2000). Unique features of the plant vacuolar sorting machinery. *Curr Opin Cell Biol* **12**:491–495.

Behnia R, Munro S (2005). Organelle identity and the signposts for membrane traffic. *Nature* **438**:597-604.

Bolte S, Brown S, Satiat-Jeunemaitre B (2004). The N-myristoylated Rab-GTPase m-Rabmc is involved in post-Golgi trafficking events to the lytic vacuole in plant cells. *J Cell Sci* **117**:943-954.

Bruckert F, Laurent O, Satre M. (2000). Rab7, a multifaceted GTP-binding protein regulating access to degradative compartments in eukaryotic cells. Protoplasma **210**: 108-116.

Brumell JH, Grinstein S (2004). *Salmonella* redirects phagosomal maturation. *Curr Opin Microbiol* **7**:78-84.

Bucci C, Thomsen P, Nicoziani P, McCarthy J, van Deurs B (2000). Rab7: a key to lysosome biogenesis. *Mol Biol Cell* **11:** 467-480.

Carter C, Pan S, Zouhar J, Avila EL, Girke T, Raikhel NV (2004). The vegetative vacuole proteome of *Arabidopsis thaliana* reveals predicted and unexpected proteins. *Plant Cell* **16**:3285–3303.

Catalano CM, Czymmek KJ, Gann JG, Sherrier DJ (2006). *Medicago truncatula* syntaxin SYP132 defines the symbiosome membrane and infection droplet membrane in root nodules. *Planta* **225**:541-550.

Cheon C-I, Lee N-G, Siddique A-BM, Bal AK, Verma DPS (1993). Roles of plant homologs of Rab1p and Rab7p in the biogenesis of the peribacteroid membrane, a subcellular compartment formed de novo during root nodule symbiosis. *EMBO J* **12:**4125-4135.

Chow CM, Neto H, Foucart C, Moore I (2008). Rab-A2 and Rab-A3 GTPases define a trans-golgi endosomal membrane domain in *Arabidopsis* that contributes substantially to the cell plate. *Plant Cell* **20**:101–123.

Clemens DL, Lee BY, Horwitz MA (2000a). *Mycobacterium tuberculosis* and *Legionella pneumophila* phagosomes exhibit arrested maturation despite acquisition of Rab7. *Infect Immun* **68:**5154-5166.

Clemens DL, Lee BY, Horwitz MA (2000b). Deviant expression of Rab5 on phagosomes containing the intracellular pathogens *Mycobacterium tuberculosis* and *Legionella pneumophila* is associated with altered phagosomal fate. *Infect Immun* **68:**2671-2684.

Conrad PA, Smart EJ, Ying YS, Anderson RG, Bloom GS (1995). Caveolin cycles between plasma membrane caveolae and the Golgi complex by microtubule-dependent and microtubule-independent steps. *J Cell Biol.* **131:**1421-1433.

Dettmer J, Hong-Hermesdorf A, Stierhof Y-D, Schumacher K. (2006). Vacuolar H$^+$-ATPase activity is required for endocytic and secretory trafficking in *Arabidopsis*. *Plant Cell* **18**:715-730.

Ebine K, Okatani Y, Uemura T, Goh T, Shoda K, Niihama M, Terao Morita M, Spitzer C, Otegui MS, Nakano A, Ueda T (2008). A SNARE complex unique to seed plants is required for protein storage vacuole biogenesis and seed development of *Arabidopsis thaliana*. *Plant Cell* **20**:3006-3021.

Ebine K, Ueda T. (2009). Unique mechanism of plant endocytic/vacuolar transport pathways. *J Plant Res* **122**:21-30.

Foresti O, daSilva LLP, Denecke J (2006). Overexpression of the *Arabidopsis* Syntaxin PEP12/SYP21 inhibits transport from the prevacuolar compartment to the lytic vacuole *in vivo*. *Plant Cell* **18**:2275–2293.

Geldner N, Jürgens G (2006). Endocytosis in signalling and development. *Curr Opin Plant Biol* **9**:589-594.

Gerrard SR, Levi BP, Stevens TH (2000). Pep12p is a multifunctional yeast syntaxin that controls entry of biosynthetic, endocytic and retrograde traffic into the prevacuolar compartment. *Traffic* **1**:259-269.

Haas TJ, Sliwinski MK, Martinez DE, Preuss M, Ebine K, Ueda T, Nielsen E, Odorizzi G, Oteguia MS (2007). The *Arabidopsis* AAA ATPase SKD1 is involved in multivesicular endosome function and interacts with its positive regulator LYST-INTERACTING PROTEIN5. *Plant Cell* **19:**1295-1312.

Harrison RE, Brumell JH, Khandani A, Bucci C, Scott CC, Jiang X, Finlay BB, Grinstein S (2004). Salmonella impairs RILP recruitment to Rab7 during maturation of invasion vacuoles. *Mol Biol Cell* **15:**3146-3154.

Jaillais Y, Fobis-Loisy I, Miège C, Gaude T. (2008). Evidence for a sorting endosome in *Arabidopsis* root cells. *Plant J* **53:**237-247.

Jauh GY, Phillips TE, Rogers JC (1999). Tonoplast intrinsic protein isoforms as markers for vacuolar functions. *Plant Cell* **11:**1867-1882.

Jones KM, Kobayashi H, Davies BW, Taga ME, Walker GC (2007). How rhizobial symbionts invade plants: the *Sinorhizobium-Medicago* model. *Nat Rev Microbiol* **5:**619-633.

Jürgens G (2004). Membrane trafficking in plants. *Annu Rev Cell Dev Biol* **20:**481-504

Karimi M, Inze D, Depicker A (2002). GATEWAY vectors for *Agrobacterium*-mediated plant transformation. *Trends Plant Sci* **7:**193-195.

Knodler LA, Celli J, Finlay BB (2001). Pathogenesis trickery: deception of host cell processes. *Nat Rev Mol Cell Biol* **2:**578-588.

Kotzer AM, Brandizzi F, Neumann U, Paris N, Moore I, Hawes C (2004). AtRabF2b (Ara7) acts on the vacuolar trafficking pathway in tobacco leaf epidermal cells. *J Cell Sci* **117:**6377-6389.

Lam SK, Siu CL, Hillmer S, Jang S, An G, Robinson DG, Jiang L (2007a). Rice SCAMP1 defines clathrin-coated, trans-golgi-located tubular-vesicular structures as an early endosome in tobacco BY-2 cells. *Plant Cell* **19**:296-319.

Lam SK, Tse YC, Robinson DG, Jiang L (2007). Tracking down the elusive early endosome. *Trends Plant Sci* **12:**497-505.

Li YB, Rogers SW, Tse YC, Lo SW, Sun SS, Jauh GY Jiang L (2002). BP-80 and homologs are concentrated on post-Golgi, probable lytic prevacuolar compartments. *Plant Cell Physiol* **43:**726-742.

Limpens E, Mirabella R, Fedorova E, Franken C, Franssen H, Bisseling T, Geurts R (2005). Formation of organelle-like N$_2$-fixing symbiosomes in legume root nodules is controlled by DMI2. *Proc Natl Acad Sci U S A* **102:**10375-10380.

Limpens E, Ramos J, Franken C, Raz V, Compaan B, Franssen H, Bisseling T, Geurts R (2004). RNA interference in *Agrobacterium rhizogenes*-transformed roots of *Arabidopsis* and *Medicago truncatula*. *J Exp Bot* **55:** 983-992.

Lipka V, Kwon C, Panstruga R. (2007). SNARE-Ware: The Role of SNARE-Domain Proteins in Plant Biology. *Annu Rev Cell Dev Biol* **23:**147–74.

Mayor S, Pagano RE (2007). Pathways of clathrin-independent endocytosis. *Nat Rev Mol Cell Biol* **8:**603-612.

Mellor RB (1989). Bacteroids in the *Rhizobium*-legume symbiosis inhabit a plant internal lytic compartment: implications for other microbial endosymbioses. *J Exp Bot* **40:**831-839.

Méresse S, Gorvel JP, Chavrier PJ (1995). The rab7 GTPase resides on a vesicular compartment connected to lysosomes. *J Cell Sci* **108:**3349-3358.

Mo B, Tse YC, Jiang L (2006). Plant Prevacuolar/Endosomal Compartments. *Int Rev Cytol* **253:**95-129.

Nahm MY, Kim SW, Yun D, Lee SY, Cho MJ, Bahk JD (2003). Molecular and biochemical analyses of Os-Rab7, a rice Rab7 homolog. *Plant Cell Physiol* **44:**1341-1349.

Nielsen E, Cheung AY, Ueda T (2008). The regulatory RAB and ARF GTPases for vesicular trafficking. *Plant Physiol* **147:**1516-1526.

Otegui MS, Herder R, Schulze J, Jung R, Staehelin LA (2006). The proteolytic processing of seed storage proteins in *Arabidopsis* embryo cells starts in the multivesicular bodies. *Plant Cell* **18:**2567-2581.

Paris N, Neuhaus JM (2002). BP-80 as a vacuolar sorting receptor. *Plant Mol Biol* **50:**903-914.

Passey S, Bradley A, Mellor H. (2008). *Escherichia coli* isolated from bovine mastitis invade mammary cells by a modified endocytic pathway. *Vet Microbiol* **130:**151-164.

Pelham HR (2002). Insights from yeast endosomes. *Curr Opin Cell Biol* **14:**454-462.

Perret E, Lakkaraju A, Deborde S, Schreiner R, Rodriguez-Boulan E (2005). Evolving endosomes: how many varieties and why? *Curr Opin Cell Biol* **17:**423–434.

Pfeffer S, Aivazian D. (2004). Targeting Rab GTPases to distinct membrane compartments. *Nat Rev Mol Cell Biol* **5:**886-896.

Pfeffer SR (2007). Unsolved Mysteries in Membrane Traffic. *Ann Rev Biochem* **76**:629-645.

Rink J, Ghigo E, Kalaidzidis Y, Zerial M (2005). Rab Conversion as a mechanism of progression from early to late endosomes. Cell **122**: 735–749.

Robert S, Chary SN, Drakakaki G, Li S, Yang Z, Raikhel NV Hicks GR (2008). Endosidin1 defines a compartment involved in endocytosis of the brassinosteroid receptor BRI1 and the auxin transporters PIN2 and AUX1. *Proc Natl Acad Sci U S A* **105**:8464–8469.

Robinson DG, Jiang L, Schumacher K. (2008). The endosomal system of plants: charting new and familiar territories. *Plant Physiol* **147**:1482-1492.

Rojo E, Zouhar J, Kovaleva V, Hong S, Raikhel NV (2003). The AtC-VPS protein complex is localized to the tonoplast and the prevacuolar compartment in *Arabidopsis*. *Mol Biol Cell* **14:**361–369.

Roth LE, Stacey G (1989). Bacterium release into host cells of nitrogen-fixing soybean nodules: The symbiosome membrane comes from three sources. *Eur J Cell Biol* **49:**13-23.

Rutherford S, Moore I. (2002). The *Arabidopsis* Rab GTPase family: another enigma variation. *Curr Opin Plant Biol* **5:**518-528.

Saito C, Ueda T, Abe H, Wada Y, Kuroiwa T, Hisada A, Furuya M, Nakano AA (2002). Complex and mobile structure form a distinct subregion within the continuous vacuolar membrane in young cotyledons of *Arabidopsis*. *Plant J* **29**:245-255.

Samaj J, Read ND, Volkmann D, Menzel D, Baluska F (2005). The endocytic network in plants. *Trends Cell Biol* **15:**424-433.

Sanderfoot A (2007). Increases in the number of SNARE genes parallels the rise of multicellularity among the green plants. *Plant Physiol* **144:**6–17.

Sanderfoot A, Kovaleva V, Zheng H, Raikhel N (1999). The t-SNARE AtVAM3p resides on the prevacuolar compartment in *Arabidopsis* root cells. *Plant Physiol* **121:**929–938.

Sanderfoot AA, Assaad FF, Raikhel NV (2000). The *Arabidopsis* genome. An abundance of soluble N-ethylmaleimide-sensitive factor adaptor protein receptors. *Plant Physiol* **124:**1558-1569.

Sanderfoot AA, Kovaleva V, Bassham DC, Raikhel NV (2001). Interactions between syntaxins identify at least five SNARE complexes within the Golgi/prevacuolar system of the *Arabidopsis* cell. *Mol Biol Cell* **12**:3733-3743.

Sato MH, Nakamura N, Ohsumi Y, Kouchi H, Kondo M, Hara-Nishimura I, Nishimura M, Wada Y (1997). The AtVAM3 encodes a syntaxin-related molecule implicated in the vacuolar assembly in *Arabidopsis thaliana*. *J Biol Chem* **272**:24530-24535.

Sanmartín M, Ordóñez A, Sohn EJ, Robert S, Sánchez-Serrano JJ, Surpin MA, Raikhel NV, Rojo E (2007). Divergent functions of VTI12 and VTI11 in trafficking to storage and lytic vacuoles in *Arabidopsis*. *Proc Natl Acad Sci U S A* **104:**3645-3650.

Schimmöller F, Riezman H (1993). Involvement of Ypt7p, a small GTPase, in traffic from late endosome to the vacuole in yeast. *J Cell Sci* **106:**823-830.

Seabra MC, Wasmeier C (2004). Controlling the location and activation of Rab GTPases. *Curr Opin Cell Biol* **16:**451-457.

Shin JS, Abraham SN (2001). Co-option of endocytic functions of cellular caveolae by pathogens. *Immunology* **102**:2-7.

Shin JS, Gao Z, Abraham SN (2000). Involvement of cellular caveolae in bacterial entry into mast cells. *Science* **289**:785-788.

Smit P, Raedts J, Portyanko V, Debellé F, Gough C, Bisseling T, Geurts R. (2005). NSP1 of the GRAS protein family is essential for rhizobial Nod factor-induced transcription. *Science* **308**:1789-1791.

Sohn EJ, Kim ES, Zhao M, Kim SJ, Kim H, Kim Y-W, Lee YJ, Hillmer S, Sohn U, Jiang L, Hwang I (2003). Rha1, an *Arabidopsis* Rab5 homolog, plays a critical role in the vacuolar trafficking of soluble cargo proteins. *Plant Cell* **15:**1057–1070.

Son O, Yang H-S, Lee H-J, Lee M-Y, Shin K-H, Jeon S-L, Lee M-Y, Choi S-Y, Chunb J-Y, Kim H, An C-S, Hong S-K., Kim N-S, Koh S-K, Cho MJ, Kim S, Verma DPS, Cheon C-I (2003). Expression of *srab7* and *SCaM* genes required for endocytosis of *Rhizobium* in root nodules. *Plant Sci* **165:**1239–1244.

Sonti RV, Chiurazzi M, Wong D, Davies CS, Harlow GR, Mount DW, Signer ER (1995). *Arabidopsis* mutants deficient in T-DNA integration. *Proc Natl Acad Sci U S A* **92**:11786-11790.

Surpin M, Raikhel N. (2004). Traffic jams affect plant development and signal transduction. *Nat Rev Mol Cell Biol* **5:**100-109.

Surpin MH, Zheng MT, Morita C, Saito E Avila JJ, Blakeslee A, Bandyopadhyay V, Kovaleva D, Carter A, Murphy M, Tasaka M, Raikhel N (2003). The VTI Family of SNARE Proteins Is Necessary for Plant Viability and Mediates Different Protein Transport Pathways. *Plant Cell* **15:**2885–2899.

Tamura K, Dudley J, Nei M, Kumar S (2007). MEGA4: Molecular Evolutionary Genetics Analysis (MEGA) software version 4.0. *Mol Biol Evol* **24:**1596–1599.

Thijssen MH, Mittempergher F, Van Aelst AC, Van Went JL (1997). Improved ultrastructural preservation of Petunia and Brassica ovules and embryo sacs by high pressure freesing and freeze substitution. *Protoplasma* **197:**199-209.

Tse YC, Mo B, Hillmer S, Zhao M, Lo SW, Robinson DG, Jianga L. (2004). Identification of multivesicular bodies as prevacuolar compartments in *Nicotiana tabacum* BY-2 cells. *Plant Cell* **16:** 672-693.

Ueda T, Uemura T, Sato MH, Nakano A (2004). Functional differentiation of endosomes in *Arabidopsis* cells. *Plant J* **40:**783-789.

Ueda T, Yamaguchi M, Uchimiyia H, Nakano A (2001). Ara6, a plant unique novel type Rab GTPase, functions in the endocytic pathway of *Arabidopsis thaliana. EMBO J* **17:**4730–4741.

Uemura T, Ueda T, Ohniwa RL, Nakano A, Takeyasu K, Sato MH (2004). Systematic analysis of SNARE molecules in *Arabidopsis*: dissection of the post-Golgi network in plant cells. *Cell Struct Func* **29:**49-65.

Uemura T, Yoshimura SH, Takeyasu K, Sato MH (2002). Vacuolar membrane dynamics revealed by GFP–AtVam3 fusion protein. *Genes Cells* **7:**743–753.

Van de Velde W, Pérez Guerra JC, De Keyser A, De Rycke R, Rombauts S, Maunoury N, Mergaert P, Kondorosi E, Holsters M, Goormachtig S (2006). Aging in legume symbiosis. A molecular view on nodule senescence in *Medicago truncatula. Plant Physiol* **141:**711-720.

Vasse J, de Billy F, Camut S, Truchet G. (1990). Correlation between ultrastructural differentiation of bacteroids and nitrogen fixation in alfalfa nodules. *J Bacteriol* **172:**4295-4306.

Via LE, Deretic D, Ulmer RJ, Hibler NS, Huber LA, Deretic V. (1997). Arrest of mycobacterial phagosome maturation is caused by a block in vesicle fusion between stages controlled by rab5 and rab7. *J Biol Chem* **272**:13326-13331.

Vieira OV, Botelho RJ, Grinstein S (2002). Phagosome maturation: aging gracefully. *Biochem J* **366:**689-704.

Vieira OV, Bucci C, Harrison RE, Trimble WS, Lanzetti L, Gruenberg J, Schreiber AD, Stahl PD, Grinstein S (2003). Modulation of Rab5 and Rab7 recruitment to phagosomes by phosphatidylinositol 3-kinase. *Mol Cell Biol* **23:**2501-2514.

Vincent JL, Brewin NJ (2000). Immunolocalization of a cysteine protease in vacuoles, vesicles, and symbiosomes of pea nodule cells. *Plant Physiol* **123:**521-530.

Vonderheit A, Helenius A (2005). Rab7 associates with early endosomes to mediate sorting and transport of Semliki forest virus to late endosomes. *PLoS Biol* **3**:e233.

Wang J, Li Y, Lo SW, Hillmer S, Sun SS, Robinson DG, Jiang L (2007). Protein mobilization in germinating mung bean seeds involves vacuolar sorting receptors and multivesicular bodies. *Plant Physiol* **143:**1628–1639.

Wienkoop S, Saalbach G (2003). Proteome analysis. Novel proteins identified at the peribacteroid membrane from *Lotus japonicus* root nodules. *Plant Physiol* **131:**1080–1090.

Yano D, Sato M, Saito C, Sato MH, Morita MT, Tasaka M. (2003). A SNARE complex containing SGR3/AtVAM3 and ZIG/VTI11 in gravity-sensing cells is important for *Arabidopsis* shoot gravitropism. *Proc Natl Acad Sci U S A* **100:**8589–8594.
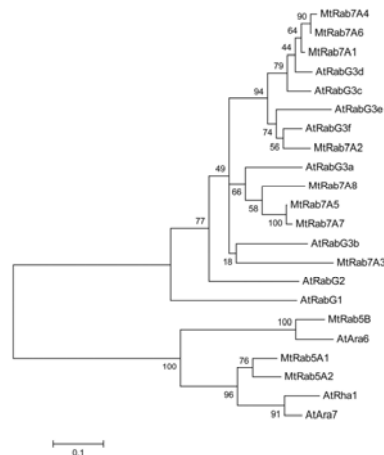
Supporting Information

Figure S1. Phylogenetic comparison of Rab5 and Rab7 proteins from *Medicago* and *Arabidopsis*. The *Medicago* protein names correspond to the following TIGR Gene Indices (Tentative Contig) TC numbers: MtRab5A1 (TC106962), MtRAB5A2 (TC106963), MtRab5B (TC93994), MtRab7A1 (TC101145), MtRab7A2 (TC94423), MtRab7A3 (TC122186), MtRab7A4 (TC140295), MtRab7A5 (TC115133), MtRab7A6 (TC118382, partial gene), MtRab7A7 (TC136113, partial gene), MtRab7A8 (TC135033, partial gene). Classification and naming of *Arabidopsis* Rab5/RabF and Rab7/RabG members as in Rutherford and Moore (2002). The midpoint rooted phylogenetic tree (bootstrap values of 1000 replicates) was constructed with MEGA version 4 using default parameters (see Methods).
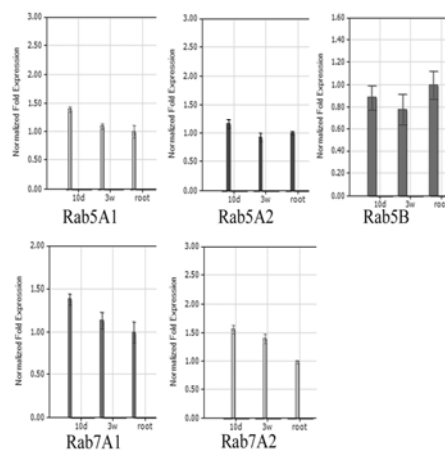

Figure S2. Quantification of Rab5A1, A2 B and Rab7A1, A2 expression levels in roots, 10-day-old nodules and 3-week-old nodules. Relative expression levels were determined by qPCR and normalized using GAPDH as reference.
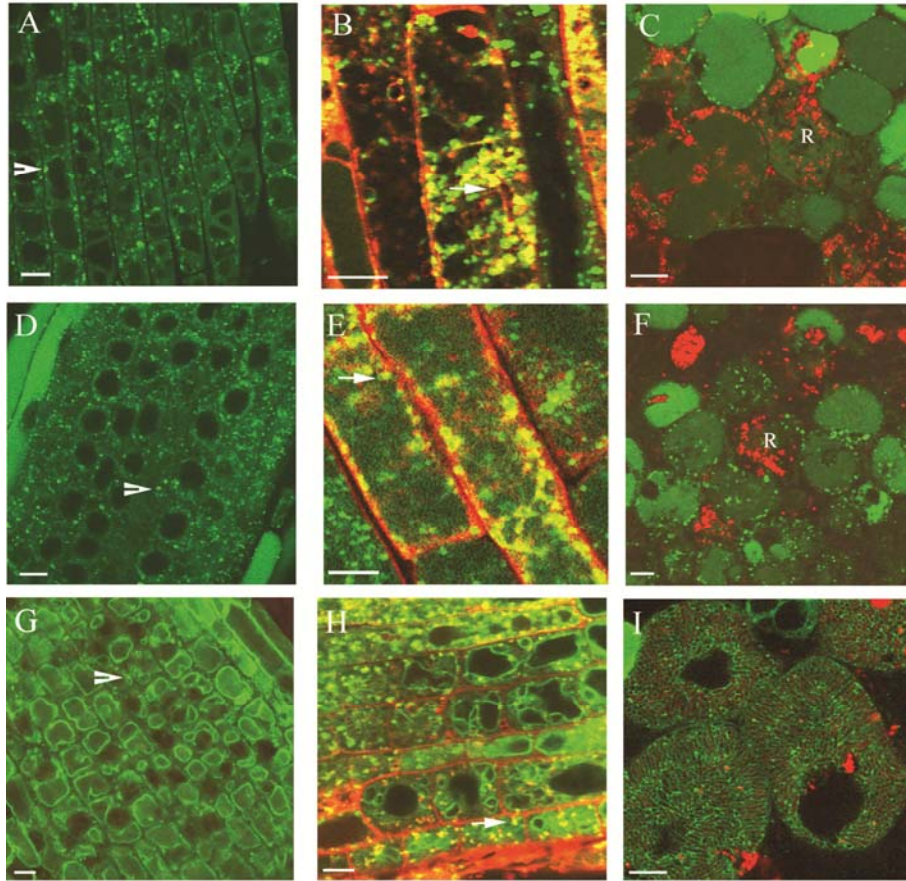
Figure S3. Confocal images of GFP-Rab5A1, GFP-Rab5B and GFP-Rab7A1 in roots and nodules. (*A*) Confocal image of a *p35S::GFP-Rab5A1* expressing root. GFP-Rab5A1 marks dot-like structures, occasionally forming larger dots (arrowhead), likely representing clusters of endosomes. (*B*) Pulse-chase (45 min.) with the fluorescent endosomal tracer FM4-64 in a *p35S::GFP-Rab5A1* expressing root. Yellow signal (arrow represents co-localization of GFP and red-fluorescent FM4-64 signal, showing that the structures are endosomes. (*C*) Distal infection zone of a *pE12::GFP-Rab5A1* expressing nodule. GFP-Rab5A1 labeled endosomes (green dots) are present in the infected cells but no GFP signal is present on SBs after release (R) from the infection thread. The Rhizobia are expressing mRFP (red). The fluorescence in the vacuoles of the nodules cells (also in *F*) is mostly due to autofluorescence, which is often observed in nodule cells compared to vacuoles in roots, although impaired processing of GFP in the nodule vacuoles cannot be ruled out. (*D*) Confocal image of *p35S::GFP-Rab5B* expressing nodule, showing that GFP-Rab5B does not associate with SBs. The rhizobia are expressing mRFP (red). (*G*) Confocal images of a *p35S::GFP-Rab7A1* expressing root. GFP-Rab7A marks dot-like structures (arrowhead) as well as the tonoplast. (*H*) Pulse-chase (45 min.) with the fluorescent endosomal tracer FM4-64 in a *p35S::GFP-Rab7A1* expressing root. O-localization (yellow signal, arrow) in the dot-like structures identifies them as endosomes. (*I*) Confocal image of *pLB::GFP-Rab7A* in the infection zone of the nodule. GFP signal is present on the SBs and in dot-like structures. The rhizobia are expressing mRFP (red). (Scale bars, 10 μm.)
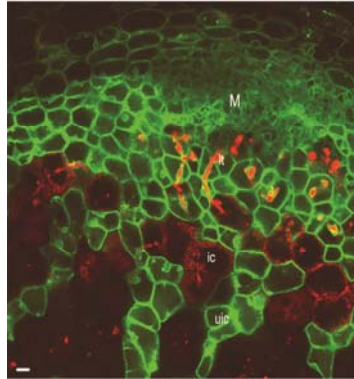
Figure S4. Confocal image of a *Medicago* nodule expressing *p35S::GFP-Rab7A[Q67L]*. GFP signal can be seen in the meristem (M), most distal part of the infection zone and in uninfected nodule cells, showing that the 35s promoter is active in these cells. In cells where SBs can be observed, GFP signal cannot be observed, indicating that the 35S is not or very weak active in cells containing SBs. Rhizobia are expressing mRFP (red). M, meristem; It, infection thread; uic, uninfected cell; ic, infected cell containing SBs. (Scale bars, 10 μm.)
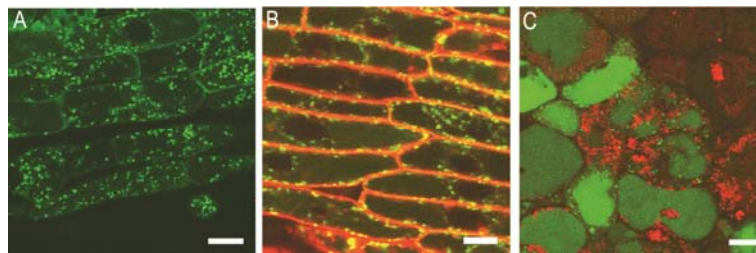

Figure S5. Localization of GFP-MtSYP41 in roots and nodules. (*A*) The pattern of GFP-MtSYP41 in root cells. (*B*) Pulse-chase (25 min.) with fluorescent tracer FM4-64, co-localization of GFP-labeled structures with red FM4-64 (yellow). (*C*) Pattern of GFP-MtSYP41 in nodules. Note the absence of SB labeling. Rhizobia are expressing mRFP (red). (Scale bars, 10 μm.)
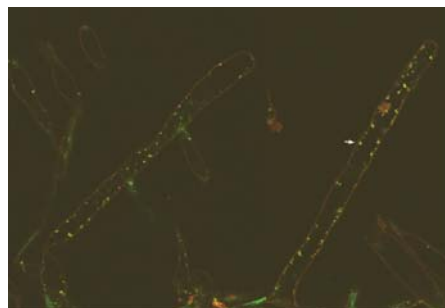

Figure S6. Immunolocalization of VTI11 (red) on GFP-MtSYP22 root (green). Arrow, co-localization.
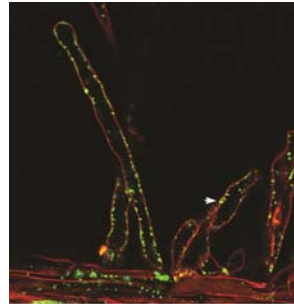
Figure S7. Immunolocalization of Rab7 (red) on GFP-MtSYP22 root (green). Arrow, co-localization.
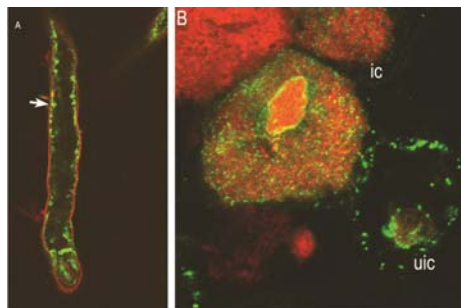

Figure S8. Immunolocalization of VTI11 on Rab7A1 RNAi roots and nodules. (*A*) Root hair. (*B*) Nodule cells. Arrow, endosome; ic, infected cells; uic, uninfected cell.
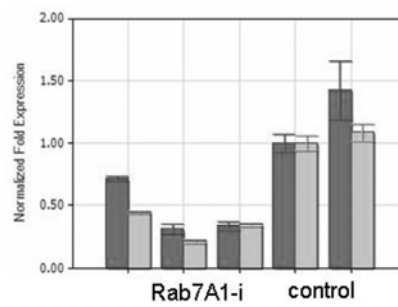

Figure S9. Quantification of Rab7A1 and Rab7A2 knock-down levels in Rab7A1-RNAi nodulated roots. Relative expression levels were determined by qPCR and normalized using GAPDH as reference. Thee independent Rab7A1-RNAi and two empty vector control nodulated roots are depicted. Left bar (dark green), Rab7A1; right bar (blue), Rab7A2.
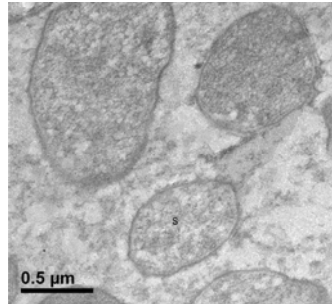
Figure S10. Pre-imune control (mouse pre-immune serum for anti-Rab7A antibodies) in nodule cells. S, SB.
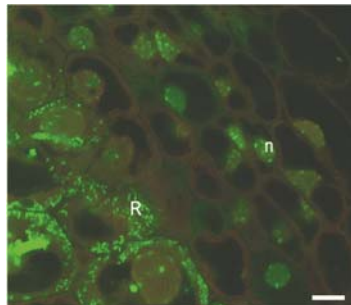

Figure S11. Secondary antibody (anti-mouse CY3) control on wild-type nodules. The rhizobia (R) are counter-stained with SYTOX Green, which also stains nuclei (n). (Scale bar, 10 μm.)

Chapter 3

Rhizobium-legume symbiosis shares an exocytotic pathway required for arbuscule formation

Sergey Ivanov[1], Elena Fedorova[1], Erik Limpens[1], Stephane De Mita[1]§, Andrea Genre[2], Paola Bonfante[2], and Ton Bisseling[1,3]

[1]*Laboratory of Molecular Biology, Graduate School Experimental Plant Science, Wageningen University, Droevendaalsesteeg 1, 6708 PB Wageningen, Netherlands;* [2]*Dipartimento di Biologia Vegetale, Universita di Torino, Viale P.A. Mattioli 25, 10125 Torino, Italy;* [3]*College of Science, King Saud University, Post Office Box 2455, Riyadh 11451, Saudi Arabia. § Present address: Institut de Recherche pour le Développement Montpellier, 911 Avenue, Agropolis BP 64501, 34394 Montpellier, cedex 5, France.*

Endosymbiotic interactions are characterized by the formation of specialized membrane compartments by the host in which the microbes are hosted in an intracellular manner. Two well studied examples, which are of major agricultural and ecological importance, are the widespread arbuscular mycorrhizal symbiosis and the *Rhizobium*-legume symbiosis. In both symbioses, the specialized host membrane that surrounds the microbes forms a symbiotic interface, which facilitates the exchange of, for example, nutrients in a controlled manner and therefore forms the heart of endosymbiosis. Despite their key importance, the molecular and cellular mechanisms underlying the formation of these membrane interfaces are largely unknown. Recent studies strongly suggest that the *Rhizobium*-legume symbiosis co-opted a signaling pathway, including receptor, from the more ancient arbuscular mycorrhizal symbiosis to form a symbiotic interface. Here, we show that two highly homologous exocytotic vesicle-associated membrane proteins (VAMPs) are required for formation of the symbiotic membrane interface in both interactions. Silencing of these *Medicago VAMP72* genes has a minor effect on non-symbiotic plant development and nodule formation. However, it blocks symbiosome as well as arbuscule formation, whereas root colonization by the microbes is not affected. Identification of these VAMP72s as common symbiotic regulators in exocytotic vesicle trafficking suggests that the ancient exocytotic pathway forming the periarbuscular membrane compartment has also been co-opted in the *Rhizobium*-legume symbiosis.

Introduction

During the symbiosis of plants and arbuscular mycorrhizal (AM) fungi as well as in the symbiosis between *Rhizobium* bacteria and legumes the microbes are hosted intracellularly inside specialized membrane compartments of the host (Parniske, 2000). These membrane compartments, although morphologically different, create a symbiotic interface that controls efficient exchange of nutrients and signals and therefore their formation is at the heart of endosymbiosis. Although, these symbiotic interfaces have a pivotal role in endosymbiosis, the molecular and cellular mechanisms by which they are formed are still largely obscure.

In the *Rhizobium*-legume symbiosis, the *Rhizobium* bacteria are hosted inside a novel organ, the root nodule. The formation of this organ, through the reprogramming of root cortical cells, is set in motion by specific lipochito-oligosaccharides, called Nod factors that are secreted by rhizobia (Oldroyd *et al*., 2011). At the same time, Nod factors control the formation of tubular, trans-cellular, cell-wall bound infection structures, called infection threads. In most of the advanced legumes infection threads originate in root hairs and guide the bacteria to nodule primordium cells that are formed from reprogrammed root cortical cells (Oldroyd *et al*., 2011). There, the bacteria are released from the infection threads into the developing nodule cells (Fig. 2*A* and *B*). In the model legume *Medicago truncatula* (*Medicago*) this process continuously occurs due to the activity of an apical nodule meristem, where invasion by infection threads and release of bacteria from these threads occur in a few cell layers just below this meristem (Fig. 2*A* and *B*). Release of bacteria starts with the formation of a local invagination of the infection thread membrane, that is devoid of a structured cell wall, by which an unwalled infection droplet is formed (Fig. 3*C* and *D*) (Brewin, 2004; Rae *et al*., 1992). The formation of this unwalled infection droplet is the start of the formation of a symbiotic interface. It allows the bacteria to come into close contact with the host membrane of the droplet and individual bacteria are subsequently "pinched off" by which they become surrounded by a host membrane (the symbiosome membrane) and together are called symbiosomes (SBs) (Parniske, 2000; Roth and Stacey, 1989). Next, SBs divide and differentiate in organelle-like structures where the bacteria are able to fix atmospheric nitrogen (Vasse *et al*, 1990). The SB membrane facilitates the exchange of fixed nitrogen in return for carbohydrates from the plant (Oldroyd *et al*., 2011). In more basal legume species, as well as *Parasponia,* the only non-legume genus able to form a rhizobium symbiosis, nitrogen-fixing rhizobia are retained in highly branched intracellular thread-like structures, called fixation threads that are continuous with the infection thread (Sprent and James, 2007; deFaria *et al*., 1987).

Like in the *Rhizobium*-legume symbiosis also AM fungi enter the root (Smith and Read, 2008). After traversing the epidermis and outer cortical layers, AM fungal hyphae spread mostly intercellularly in the inner cortex. Subsequently, they enter cortical cells via invagination of the plasma membrane and first "trunk" hyphae are formed that are bound by cell wall of the host (Bonfante-Fasolo *et al*., 1990). In this respect they are similar to the infection threads that are formed in the *Rhizobium*-legume symbiosis. Subsequently, the trunk hypha branches repeatedly to develop the specialized structure known as arbuscule. This highly branched hyphal structure is enveloped by a special extension of the host plasma membrane, the periarbuscular membrane (Smith and Read, 2008). Some cell wall

components typical of the primary plant cell wall (e.g. cellulose, pectins, and hemicellulose) have been immunologically detected in the space between arbuscule and periarbuscular membrane. However, electron microscopy studies show that a structured cell wall is not present, indicating a specialized nature of this membrane compartment (Bonfante-Fasolo *et al.*, 1990; Balestrini and Bonfante, 2005; Balestrini *et al.*, 2005). The specialized nature of the periarbuscular membrane is further demonstrated by the observation that certain proteins localize specifically to the periarbuscular membrane, but not to the host cell plasma membrane or the membrane surrounding the trunk hypha (Pumplin and Harrison, 2009). Similar to the SB membrane, the periarbuscular membrane is thought to facilitate the exchange of nutrients/minerals, especially phosphorus (and nitrogen) in return for photosynthates from the plant (Smith and Read, 2008).

While the molecular and cellular mechanisms of symbiotic interface formation are largely unknown, the signaling pathways that initiate these symbiotic interactions are better studied. In recent years it has become clear that several components of the signaling pathway, called the common signaling pathway that is activated by rhizobial Nod factors in the epidermis are also required for AM symbiosis (Kouchi *et al.*, 2010). Furthermore, in nodules, this common signaling pathway is also essential for the release of the rhizobia from infection threads (SB formation), but not for infection thread formation. This has been demonstrated for the receptor like kinase SymRK, the Calcium- and Calmodulin-dependent kinase (CCamK) as well as its interacting partner (IPD3) (Capoen *et al.*, 2005; Limpens *et al.*, 2005; Godfroy *et al.*, 2006; Yano *et al.*, 2008; Horvath *et al.*, 2011; Ovchinnikova *et al.*, 2011). It is currently not known whether this common signaling pathway is activated by Nod factor receptors in legume nodules. However, in the non-legume *Parasponia*, knockdown of a Nod factor receptor (a single copy gene) specifically blocked the formation of the (intracellular) rhizobial symbiotic interface, i.e. fixation threads (Op den Camp *et al.*, 2011). Furthermore, knock-down of this Nod factor receptor also blocked arbuscule formation by AM fungi, whereas intercellular colonization of the root was not affected (Op den Camp *et al.*, 2011). Consistent with this observation, it was recently shown that also AM fungi produce lipochito-oligosaccharides, with a structure very similar to that of Nod factors (Maillet *et al.*, 2011). Taken together, this strongly suggests that *Rhizobium*-legume symbiosis co-opted the complete signaling pathway from the AM symbiosis and in both interactions this signaling pathway induces the formation of the membrane compartment forming a symbiotic interface. Therefore, we hypothesize that this common signaling pathway activates a similar cellular process that in root cortical cells leads to the formation of fungal and in nodule cells to a rhizobial symbiotic interface. This would imply that in current legumes similar or even identical key regulators are required for the formation of periarbuscular and SB membrane compartments, despite their, at first sight, major morphological differences.

A major morphological difference is the fact that in advanced legumes *Rhizobium* bacteria are individually internalized into SB compartments, which suggests an endocytosis-like process. However, studying the localization of membrane identity markers of the various endocytic compartments did not show any association of key regulators of the default endocytosis pathway at the early steps of SB formation (Limpens *et al.*, 2009). Only later in SB development (as the SBs differentiate) a late endosome/vacuolar marker, the small GTPase Rab7, was observed on the SB membrane. In contrast, a plasma membrane t-

SNARE (see below), syntaxin SYP132, has been shown to be associated with the infection thread membrane, unwalled infection droplets and SBs immediately after their release from the infection thread, and throughout SB development (Limpens *et al*., 2009, Catalano *et al*., 2007). This suggests the involvement of an exocytosis derived process in SB formation. This is further supported by the fact that in *Parasponia* and primitive legumes the membrane that surrounds the fixation threads, like the periarbuscular membrane, remains connected to the plasma membrane (Brewin, 2005; Sprent and James, 2007; deFaria *et al*., 1987). Therefore, we hypothesized that the same exocytotic pathway controls the formation of the symbiotic interface in both interactions.

Exocytosis involves focalized fusion of transport vesicles (with a specific cargo) with their target (plasma) membrane. Vesicle fusion is controlled by a group of proteins named SNAREs (*s*oluble *N*-ethylmaleimide sensitive factor *a*ttachment protein *re*ceptor) and it is accomplished by the formation of a stable core complex of four SNARE motifs of the interacting SNAREs (Lang and John, 2008). Generally, one SNARE protein that locates on the transport vesicle (v-SNARE), pairs with three SNARE proteins (including syntaxins) which reside on the target membrane (t-SNARE) (Lang and John, 2008). In plants, exocytotic processes are mediated by v-SNAREs belonging to the VAMP72 (*v*esicle-*a*ssociated *m*embrane *p*rotein) family (Sanderfoot, 2007, Kwon *et al*., 2008). Previously it has been shown that specific *VAMP72* genes have been recruited in the *Arabidopsis* interaction with biotrophic fungi (Kwon *et al*., 2008). Therefore, we focused on the role of the *MtVAM72* family in the formation of a symbiotic interface in the interaction of *Medicago* with *Sinorhizobium meliloti* and *Glomus intraradices*, respectively. Here, we show that two highly homologous *Medicago* VAMP72s are required for SB as well as arbuscule formation.

Results and Discussion

Identification of *VAMP72* genes in *Medicago*. We identified the *Medicago MtVAMP72* family based on homology with *Arabidopsis* members (Sanderfoot, 2007). Mining of *Medicago* EST and genome sequence (Young *et al*., 2011) data identified seven *MtVAMP72* genes (Table S1 and S2). Phylogenetic analysis using several genome sequences that represent major eudicot clades (Soltis et al., 1999) showed that the VAMP72s can be divided into three groups, namely *VAMP721, VAMP724* and *VAMP727* (Fig. 1; Table S2). The VAMP721 group can be further divided into two subgroups. One includes all *Arabidopsis VAMP721* genes and *Medicago VAMP721a,b,c*, whereas the second ("symbiotic") subgroup includes *MtVAMP721d,e*, but no *Arabidopsis* homologs (Fig. 1). *Arabidopsis* has lost the ability to interact with AM fungi and this is correlated with the loss of several genes involved in the common signaling pathway (Zhu *et al*., 2006). Further, other eudicots with a sequenced genome that can interact with AM fungi do have at least one *VAMP721* member that belongs to the "symbiotic" subgroup. Along this line *MtVAMP721d* and *MtVAMP721e* are the best candidates to be involved in the formation of periarbuscular and SB membrane compartments. Further, these two genes are expressed at relatively high levels in roots, nodules and mycorrhized roots (Fig. S1*A-D*). For these reasons we have analyzed the function of *MtVAMP721d* and *MtVAMP721e* in both interactions.
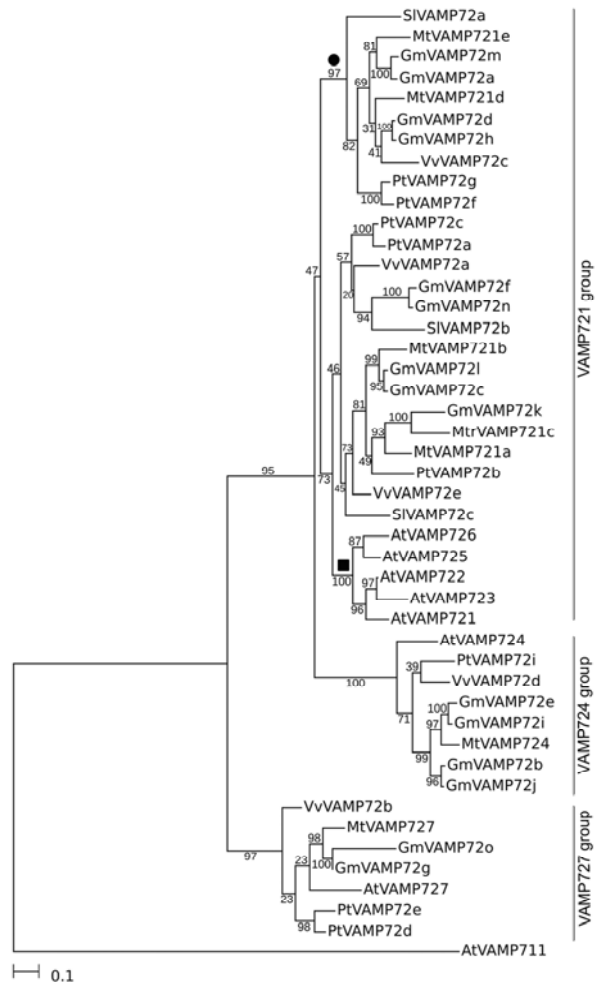
Figure 1. Phylogenetic analysis of *MtVAMP72s*. Unrooted phylogenetic neighbor-joining maximum-likelihood tree of *M. truncatula* (Mt) and *A. thaliana* (At) *Populus thrichocarpa* (Pt), *Glycine max* (Gm), *Solanum lycopersicum* (Sl), *Vitis vinifera* (Vv) VAMP72s. The sequences were identified using BLASTN searches in genome/EST databases and aligned at the protein level using MUSCLE version 3.8.31. The phylogenetic tree was built using PHYML version 3.0 using protein-coding nucleotide sequences aligned using the protein alignment as a template. We used the GTR (general time-reversible) model with gamma-distributed rates of evolution with 6 categories. AtVAMP711 was used as outgroup, 100 bootstrap repetitions were performed to assess robustness of nodes. Note that *MtVAMP721d* and *MtVAMP721e* form a separate "symbiotic" subgroup (●, bootstrap 97%) inside VAMP721 group, whereas other *MtVAMP721a, MtVAMP721b* and MtVAMP721c form other subgroup which also includes all *Arabidopsis* VAMP721 genes (■, bootstrap 73%). The latter are crucial in defense against fungal pathogens.
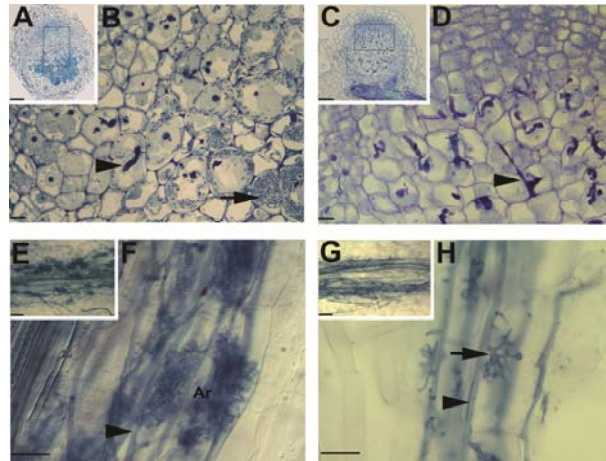
Figure 2. MtVAMP721d and MtVAMP721e are required for symbiosome and arbuscule formation. Light microscopic images of Medicago root nodules on control (*A* and *B*) and *35S::RNAi_{VAMP721d:VAMP721e}* transgenic roots (*C* and *D*). Longitudinal section of a control nodule 14 days post inoculation (*A*) and magnification (*B*) of the region indicated in (*A*), shows cells penetrated by an infection thread (arrowhead), cells containing released and developing symbiosomes (containing *S. meliloti* bacteria) that are filling the host cell (arrow). Section of a *35S::RNAi_{VAMP721d:VAMP721e}* nodule (*C*) and the indicated magnification (*D*) showing cells that are penetrated by an infection thread, but symbiosomes are not formed. Light microscopic images of Medicago control (*E* and *F*) and *35S::RNAi_{VAMP721d:VAMP721e}* transgenic roots (*G* and *H*) infected by *G. intraradices*. Control root (*E*) and its magnification (*F*) show that the fungus forms intraradical hyphae (arrowhead) and mature fine-branched arbuscules (ar) inside inner root cortical cells. *35S::RNAi_{VAMP721d:VAMP721e}* root (*G*) and its magnification (*H*) show that AM fungal hyphae grow intraradically (arrowhead) and form trunk hyphae (arrow) that have entered inner cortical cells. A few major branches are made, but fine-branched arbuscules are not formed. (Scale bar, 100 μm in *A* and *C*, 10 μm in *B* and *D*, 50 μm in *E* and *G*, 25 μm in *F* and *H*.)

Silencing of *MtVAMP721d* and *MtVAMP721e* blocks symbiosome and arbuscule formation. To study the function of *MtVAMP721d* and *MtVAMP721e* we used gene-specific RNAi. Based on quantitative RT-PCR analyses of *Medicago* roots and nodules we also selected *MtVAMP721a* and *MtVAMP724*, since they are expressed at moderate levels in both organs (Fig. S1*A* and *B*). As both *MtVAMP721d* and *MtVAMP721e* are highly homologous, we also created a construct (*35SCaMV::RNAi_{VAMP721d:VAMP721e}*) by which both are knocked down. We obtained composite *Medicago* plants with transgenic roots, using *Agrobacterium rhizogenes* mediated transformation, that were selected through the use of a red fluorescent reporter (Limpens *et al*., 2005, Limpens *et al*., 2004). The gene-specific RNAi constructs reduced the level of their corresponding target RNA to 10-40%, compared to control roots transformed with the empty vector, whereas the expression level of the other *MtVAMP72* genes was not reduced (Fig. S2*A-D*). The composite plants were inoculated with *S. meliloti* and root nodules were analyzed after 14 days. Microscopic sections of nodules (*n*=20 for each construct from independently transformed roots) formed on roots expressing one of the four single gene-specific RNAi constructs showed that they all had a cytology similar to nodules formed on control roots transformed with the empty vector. Transgenic *RNA-*

$i_{VAMP721d:VAMP721e}$ roots had markedly reduced levels of both mRNAs (down to 10-40%) (Fig. S2E). The growth of these transgenic roots and the number of nodules that are formed were only slightly affected (Fig. S3A and B). Light microscopic analysis of nodules collected from $RNAi_{VAMP721d:VAMP721e}$ transgenic roots (n_{roots}=15) revealed the presence of numerous infection threads in the central tissue of these nodules (Fig. 2C and D), however, SBs were absent or present at very low numbers in 18 out of 37 analyzed nodules (48%). Such nodules were not observed on control roots ($n_{nodules}$=0 out of 27, n_{roots}=15; Fig. 2A and B). So knock-down of both *MtVAMP721d* and *MtVAMP721e* specifically blocks SB formation.

To test whether *MtVAMP721d* and *MtVAMP721e* are also required for arbuscule formation, $RNAi_{VAMP721d}$, $RNAi_{VAMP721e}$, $RNAi_{VAMP721d:VAMP721e}$ and $RNAi_{VAMP721a}$ composite plants were inoculated with *G. intraradices*. Plants were analyzed 4 weeks after inoculation. In control and all RNAi roots fungal hyphae successfully colonized the root cortical layers and spread longitudinally along the root axis (Fig 2E and G; Fig. S4). Fully developed arbuscules were efficiently formed in control roots expressing an empty vector (arbuscule presence [a] = 61%; Fig. 2F; Fig. S6), as well as in $RNAi_{VAMP721d}$, $RNAi_{VAMP721e}$ and $RNAi_{VAMP721a}$ roots. However, silencing of both *MtVAMP721d* and *MtVAMP721e* ($RNAi_{VAMP721d:VAMP721e}$) resulted in marked decrease of mature arbuscules (arbuscule presence [a]=6%). Small trunk-like hyphae abundantly occur in root inner cortical cells, but mature arbuscules were only rarely formed (Fig. 2H; Fig. S4). These small trunk-like hyphae are likely the result of an early arrest of arbuscules formation and not the collapse of mature arbuscules. In some plant mutants arbuscules can, at a late stage of development, be absent due to premature collapse (Javot *et al.*, 2007). This collapse of arbuscules is associated with the formation of dense clumps (Smith and Read, 2008; Javot *et al.*, 2007). These dense clumps of collapsed hyphae did not occur in $RNAi_{VAMP721d:VAMP721e}$ roots. Thus, the knock-down of both *MtVAMP721d* and *MtVAMP721e* affects the formation of arbuscules as well as SBs. Arbuscule formation is even more efficiently blocked than SB formation. This might imply that higher levels of *MtVAMP721d* and *MtVAMP721e* are required for arbuscule formation.

Silencing of *MtVAMP721d* and *MtVAMP721e* affects unwalled droplet formation and bacterial release from the infection thread. The lack of SBs in $RNAi_{VAMP721d:VAMP721e}$ nodules allowed us to predict that the formation of an unwalled droplet and subsequent release of bacteria, which marks the start of SB formation, is affected. To address this we compared, by electron microscopy (EM), $RNAi_{VAMP721d:VAMP721e}$ nodules where SBs were absent or present at very low numbers (Fig. 3A and B) to nodules formed on control roots (Fig. 3C and D). In the latter, unwalled infection droplets are formed at infection threads in the cell layer directly adjacent to the meristem (Fig. 2A and B). The unwalled infection droplets are bound by a membrane of the host, but a cell wall is completely lacking (Fig. 3C and D). In the $RNAi_{VAMP721d:VAMP721e}$ nodules infection threads contain a structure that resembles an infection droplet. However, these droplet-like structures still show the presence of a thin layer of cell wall next to the surrounding host membrane (Fig. 3A and B). To confirm that "walled" infection droplets are formed we also used EM computer tomography and made 3-D reconstructions of 360 nm thick section (Fig. 3E-H). This shows that droplet-like structures have been formed and these are bound by a membrane and a cell
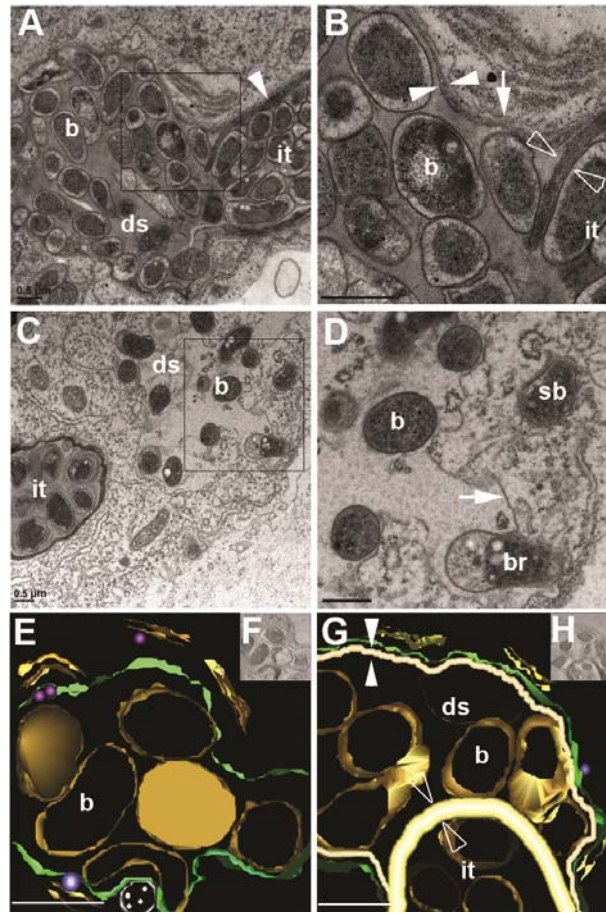
Figure 3. MtVAMP721d and MtVAMP721e are essential for the formation of unwalled infection droplets at infection threads. (*A* and *B*) Electron microscopic images of an infection thread in a *p35S::RNAi$_{VAMP721d:VAMP721e}$* nodule (*A*) and magnification of the designated area (*B*). The infection thread (*it*) is filled with bacteria and bound by a cell wall (arrowhead). At the tip of the thread a droplet-like structure (*ds*) filled with bacteria (*b*) is formed. The droplet-like structure is surrounded by a membrane (*B*, arrow) extending from the infection thread plasma membrane and bound by a cell wall (*B*, white opposed arrowheads) that is markedly thinner than the wall around the infection thread (*B*, open opposed arrowheads). (*C* and *D*) Electron microscopic images of an infection thread in a control nodule (*C*) and magnification of the designated area (*D*). The unwalled droplet (*ds*) is bound by a membrane (arrow), but a cell wall is absent. Bacteria (*b*) are being released (*br*) and form symbiosomes (*sb*). (*E-H*) Electron microscopy computed tomography and 3-D reconstruction of an infection thread in a control (*E* and *F*) and *p35S::RNAi$_{VAMP721d:VAMP721e}$* (*G* and *H*) nodule. Analyses were performed on 360 nm thick sections. In the droplet structure (*ds*) of *RNAi$_{VAMP721d:VAMP721e}$* nodules (*G* and *H*) the bacteria are separated from the host membrane (green) by a cell wall (white, opposed arrowhead). This cell wall is markedly (~3x) thinner (white opposed arrowheads) than the cell wall of the infection thread (*it*) at which a droplet structure is formed (open opposed arrowheads). The unwalled droplets in nodules on control roots (*E* and *F*) are bound only by the host membrane (green) which allows the bacteria (*b*, gold) to come into close contact with it. (Scale bars, 0.5μm in *A-G*.)

wall with a thickness of about 1/3 (0,03nm±0.01; $n_{\text{infection threads}}$=10, n_{nodules}=3) of the infection thread wall (0.10nm±0.03; $n_{\text{infection threads}}$=10, n_{nodules}=3). The presence of a cell wall in the infection droplets prevents a close contact between the bacteria and the host membrane and thereby likely hampers the pinching off of SBs. This can explain why numerous infection threads have such a "walled" infection droplet. The formation of droplet-like structures in the $RNAi_{VAMP721d:VAMP721e}$ nodules suggests that the switch to a specific MtVAMP721d/e controlled exocytosis pathway is impaired that in wild-type nodules is responsible for the formation of an unwalled infection droplet. Our explanation for "walled" droplet formation in $RNAi_{VAMP721d:VAMP721e}$ root nodules is the following; residual levels of MtVAMP721d/e vesicles (due to incomplete silencing) are present in $RNAi_{VAMP721d:VAMP721e}$ root nodules and these are targeted to the infection thread membrane to initiate the formation of an unwalled droplet. Their cargo (possibly cell wall degrading enzymes [Xie *et al.*, 2012], or altered membrane composition) leads to the formation of a cell wall free interface. However, their number is low in comparison to other vesicles involved in growth of the plant cell. The latter may deliver cell wall components and we postulate that they "compete" with the MtVAMP721d/e vesicles by which a thin cell wall is formed instead of a cell wall free interface. Alternatively, the MtVAMP721d/e controlled pathway might be specifically involved in SB formation. In this case, block of SB formation might lead to a droplet that is an intermediate infection thread and unwalled infection droplet. Taken together these data suggest that an exocytotic pathway involving MtVAMP721d/e controls the formation of the symbiotic interface in the *Rhizobium*-legume symbiosis.

MtVAMP721d and MtVAMP721e localize at the site of bacterial release, on symbiosome and periarbuscular membrane. To find further support for a role of MtVAMP721d/e vesicles in symbiotic interface formation, their sub-cellular localization was determined in transgenic roots expressing translational fusions *GFP-MtVAMP721d* or *GFP-MtVAMP721e* under the control of their native promoters. Promoter-GUS analyses showed that these promoters are active in the nodule region where SBs are formed (Fig. 4*C* and *D*). Confocal microscopy of *GFP-MtVAMP721e* expressing nodules (n_{nodules}=5) revealed accumulation of GFP-fluorescence on dot-like structures (Fig. 5*A*). These dot-like structures accumulated at local regions near infection threads where unwalled droplets are formed and SBs start to develop. The subcellular localization of GFP-VAMP721d is very similar to that of GFP-VAMP721e (Fig. S5*A*). The nature of the labeled dot-like structures was investigated using EM immunodetection with an antibody against GFP or an antibody that recognize both MtVAMP721d and MtVAMP721e (Fig. S6*A* and *B*; Fig. S5*C* and *D*). This showed that MtVAMP721d and MtVAMP721e were present on small (~50 nm) vesicles in close association with unwalled infection droplets (Fig. S5*D*) and on/near SB membranes of young SBs (Fig. S5*C*). When we used both antibodies simultaneously we could distinguish the signals using secondary antibodies linked to gold particles with a different size. This showed that the signals coincided (Fig. S5*C*) and indicates the specificity of the anti- MtVAMP721d/e antibodies. Thus, these data are consistent with focal MtVAMP721d/e-mediated delivery of exocytotic vesicles to unwalled droplets and SBs.

Medicago roots expressing *MtVAMP721d::GUS* or *MtVAMP721e::GUS* showed that these promoters are active in the inner cortex, where arbuscules can be formed (Fig. 4*A* and *B*). In *MtVAMP721e::GUS* transgenic roots colonized by *G. intraradices* GUS activity was

slightly higher in cells with arbuscules than in non-infected inner cortical cells (Fig. 4*E*). Roots expressing *GFP-VAMP721e* under the control of its native promoter (n_{roots}=3) were infected by *G. intraradices* and the fusion protein was detected using anti-GFP or anti-MtVAMP721d/e antibodies. This showed that GFP-VAMP721e was abundantly present in root cells containing arbuscules, whereas the level of MtVAMP721e in non-infected inner cortical cells was rather low. In cells containing arbuscules the signal was accumulating over the periarbuscular membrane especially at the fine branches (Fig. 5*C* and *D*; Fig. S5*B*).

So the knock-down studies as well as localization studies show that arbuscule and SB formation are specifically controlled by the MtVAMP721d/e regulated exocytotic pathway. This suggests that SBs, like the periarbuscular endomembrane compartments, represent an apoplastic compartment despite their intracellular nature. At a later stage of development the SB membrane obtains the identity marker Rab7 that also occur at the late endosome/vacuole, whereas vacuolar SNAREs accumulate on SB membrane when senescence is initiated (Limpens *et al.*, 2009). Therefore we conclude that functional SBs do not seem to have a true vacuolar nature but remain as an apoplastic-like compartment. The switch to the MtVAMP721d/e controlled exocytotic pathway allows the targeting of vesicles with a different cargo and this facilitates the formation of a symbiotic interface with specific protein composition (Whitehead and Day, 1997).

In root and nodule meristems we observed MtVAMP721d and MtVAMP721e accumulation at the site of cell plate formation (Fig. 5*B*). The cell plate is a transient membrane compartment created by membrane vesicle fusion in which a cellulose-based cell wall is not yet formed (Jurgens, 2005). Therefore, it is tempting to speculate that part of the machinery that is involved in the formation of a cell plate is co-opted to build the symbiotic interface. MtVAMP721d and MtVAMP721e might not be essential for cell plate formation, because $RNAi_{VAMP721d:VAMP721e}$ has only a slight effect on root growth and nodule formation. However, we can not exclude that the residual levels of *MtVAMP721d* and *MtVAMP721e* in the RNAi roots are sufficient for rather normal root growth. Further, the expression level of
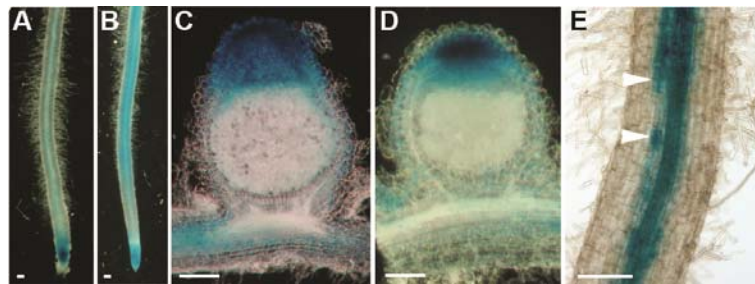

Figure 4. Activity of *MtVAMP721d* and *MtVAMP721e* promoters. The 2.5 kb region upstream of the translational start of *MtVAMP721d* (*A* and *C*) and of *MtVAMP721e* (*B, D* and*E*), respectively were fused to β-glucuronidase (GUS) and transgenic roots expressing these genetic constructs were inoculated by *S. meliloti* 2011 (*C* and *D*) or *G. intraradices* (*E*). Nodules were harvested 14 dpi and were analyzed for GUS activity. Nodules were hand-sectioned. Promoters of *MtVAMP721d* and *MtVAMP721e* are active in the meristem and the infection zone of the nodule where release of bacteria from the infection threads and symbiosome development occurs. Mycorrhized roots were harvested and analyzed for GUS activity 28 days after inoculation. Promoter *MtVAMP721e* shows activity in vascular tissue and arbuscule containing cells (*E*, arrowhead). (Scale bars, 100 μm in *A-E*.)

MtVAMP721a is slightly higher in *MtVAMP721d* and *MtVAMP721e* knock-down lines (Fig. S2*E*) and this might have a compensating effect. This is well in line with studies of Kwon *et al.*, who showed that in *Arabidopsis* two *VAMP721* genes from the "non-symbiotic" subgroup (*AtVAMP721* and *AtVAMP722*) have been recruited in defense against powdery mildew (Fig. S1*E*) and marked reduction of their expression blocked the defense response, but had no effect on plant growth (Kwon *et al.*, 2008). However, a complete loss of function of both *AtVAMP721* and *AtVAMP722* causes severe dwarfism of the plant. Recently, it has been shown that these AtVAMP72s play a crucial role in cell plate formation (Zhang *et al.*, 2011).

The interaction of plants with AM fungi is about 450 million years old (Bonfante and Genre, 2008), whereas the rhizobium symbiosis evolved about 60 million years ago (Sprent, 2008). Recent studies show that AM fungi produce Nod factor-like lipochito-oligosaccharides (Maillet *et al.*, 2011) and that the same *Parasponia* Nod factor receptor is required in both symbiotic interactions (Op den Camp *et al.*, 2011). This strongly suggests that during evolution, rhizobia acquired the ability to make a factor (Nod factor) with a
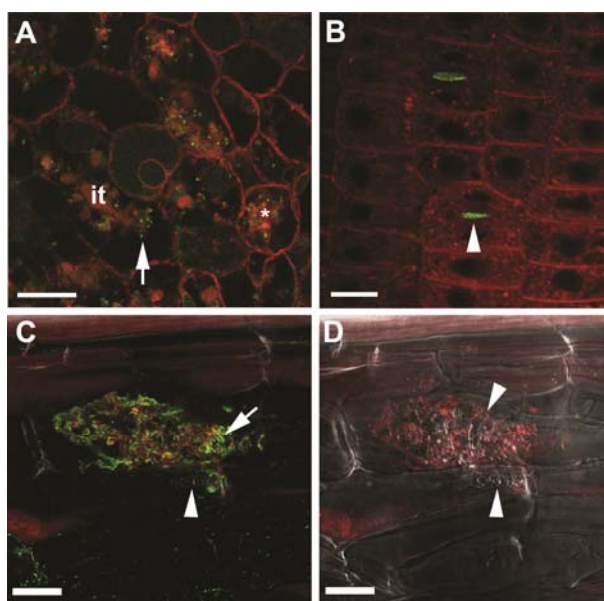

Figure 5. MtVAMP721e marked vesicles accumulate at the site of symbiosome, periarbuscular membrane formation and at cell plates. Confocal microscopy images showing localization of GFP-MtVAMP721e expressed under the control of its native promoter. (*A*) Accumulation of GFP-MtVAMP721e labeled dot-like structures (green) in infected Medicago nodule cells at local regions of infection threads (*it*) where bacteria are released (unwalled droplet, arrow) and around newly formed symbiosomes (asterix). (*B*) Accumulation of GFP-MtVAMP721e at the cell plate (arrowhead) in dividing meristematic cells of a Medicago root. (*C* and *D*) Confocal microscopy picture of immuno-localization of GFP-MtVAMP721e (*C*) and corresponding bright field image (*D*) in a root cortical cell containing an arbuscule. GFP was visualized by anti-GFP antibodies (green fluorescence). The signal is present near fine arbuscule branches (arrow) and absent on intraradical hypha (arrowhead). Samples were contrasted by FM4-64 (red) to visualize membranes. (Scale bar; 20 µm in *A*, *C* and *D*, 10 µm in *B*.)

structure similar to that of more ancient mycorrhizal factors. This is consistent with the idea that rhizobia obtained the genes to make Nod factors by horizontal gene transfer (Sullivan and Ronson, 1998). Here we show that the exocytotic pathway that is required for arbuscule formation is also essential for *Medicago* SB formation. Therefore it is probable that during evolution the acquisition to produce Nod factors provided rhizobia the ability to use the ancient AM machinery to establish an intracellular interface. In this study we focused on the *Medicago* symbiosis. Whether the VAMP721d/VAMP721e controlled exocytosis pathway is also used in other legumes to establish SB formation, or fixation threads, remains to be demonstrated. Our studies on *Medicago* strongly suggest that most plants have genes encoding the core of a mechanism that can support a *Rhizobium* infection process. Nevertheless, while the AM fungal symbiosis is widespread across the plant kingdom, it is perplexing that the *Rhizobium*-legume symbiosis is restricted to legumes and *Parasponia*.

Materials and Methods

Plant transformation and inoculation. *Agrobacterium rhizogenes* MSU440 mediated hairy root transformation was used to obtain transgenic roots (Limpens *et al*., 2004). *M. truncatula* accession Jemalong A17 was grown in perlite saturated with Färhaeus medium without nitrate in a growth chamber at 21ºC and 16/8 h light/darkness. They were inoculated with *S. meliloti* 2011 (OD_{600} 0.1, 2 ml per plant). Root nodules were collected for analysis 10-14 days post inoculation (dpi). *Medicago* plants that were inoculated with *G. intraradices* were co-cultivated with *Allium schoenoprasum* nurse plants in sand/hydrobeads mixture saturated by Hoagland medium. To quantify the infection by the fungus, roots were stained with 0.2% trypan blue and roots were analyzed by light microscopy. In total 75 cm of each transgenic root system was analyzed and the level of infection was quantified as described (Trouvelot *et al.,* 1986).

Cloning. DNA fragments were generated via PCR on *Medicago* genomic DNA or cDNA made from root nodules as a template using Phusion™ High-Fidelity DNA Polymerase (Finnzymes) and gene-specific primers (Table S3). The Gateway® technology (Invitrogen) was used to create genetic constructs for GFP-fusion, promoter-GUS and RNA interference (Karimi *et al*., 2002). TOPO® cloning (Invitrogen) was used to create entry clones. To create RNAi constructs entry clones were recombined into the modified Gateway pK7GWIWG2(II)-*UBQ10*::*DsRED* binary vector (Limpens *et al*., 2005, Limpens *et al*., 2004). To generate GFP-MtVAMP721d and GFP-MtVAMP721e translational fusions, GFP was fused to N-terminal end of MtVAMP721d or MtVAMP721e. Expression of these fusions was driven by 2.5 kb 5' regulatory sequence (*VAMP721d::GFP-VAMP721d* and *VAMP721e::GFP-VAMP721e*).

Gene expression. Total RNA was extracted from roots, root nodules and mycorrhized roots using E.Z.N.A.™ Plant RNA Mini Kit (Omega bio-tek). Equal amounts of total RNA was used to analyze gene expression of *MtVAMP72*s by quantitative real time PCR (qPCR) using iQ™ SYBR® Green Supermix (Bio-Rad) and gene-specific primers (Table S3). Detection of fluorescent signal was performed on a My iQ Real-Time Detection System (Bio-Rad). Gene expression profiles were normalized against the transcription level of reference

gene *MtUBQ10*. Data were compared with *M. truncatula* Gene Expression Atlas data (Benedito *et al*., 2008) (http://mtgea.noble.org/v2/).

Antibodies against MtVAMP721d and MtVAMP721e. Affinity-purified polyclonal rabbit anti-MtVAMP721d antibodies were generated by GenScript against the peptides QKLPSTNNKFTYNC. Protein extraction and immunoprecipitation from transgenic roots expressing GFP-VAMP721a, GFP-VAMP721d or GFP-VAMP721e was performed using GFP Trap®_A Kit (Chromotek) according manufacturer's instructions. To detect GFP fusion protein, proteins were separated on SDS-polyacrylamid gel and probed with anti-GFP antibody (Molecular Probes) in dilution 1:2000 or anti-VAMP721d in dilution 1:100/1:500 and secondary anti-rabbit antibodies conjugated with alkaline phosphatase (Promega).

Confocal laser–scanning microscopy. GFP-fused proteins were visualized on transgenic roots and hand sectioned nodules. Imaging was done on a Zeiss LSM 5 Pascal confocal laser–scanning microscope (Carl Zeiss, GmbH). Immunodetection was performed as described previously (Limpens *et al*., 2009). Goat serum or 3% BSA was used as blocking agent. Polyclonal rabbit anti-GFP antibodies (Molecular Probes) in dilution 1:200 or anti-VAMP721d/VAMP721e in dilution 1:50-100 and secondary anti-rabbit Alexa 488 antibodies (Molecular Probes) in dilution 1:200 were used. Sections were counterstained by FM4-64 (30 µg/mL).

Sample preparation for light and transmission electron microscopy (TEM) and TEM immunodetection. Tissue preparation was performed as described before (Limpens *et al*., 2009). Semi-thin (0.6 µm) for light and thin sections (60 nm) for electron microscopy of the same nodule were cut using a Leica Ultracut microtome (Leica). Nickel grids with the sections were blocked in normal goat serum with 1% milk or 2% BSA in PBS and incubated with the primary antibody according to dilutions given above. Goat anti-rabbit coupled with 15-nm gold (BioCell) (1:50 dilution) were used as secondary antibody. Sections were examined using a JEOL JEM 2100 transmission electron microscope equipped with a Gatan US4000 4K×4K camera.

TEM computer tomography and 3-D reconstruction. The method of Electron Tomographic Analysis adapted for plant tissue was used (Segui-Simarro *et al*., 2004). Sections of 300-360 nm thickness were mounted on 100 nm mesh copper grids coated by Formvar. Tilted images were collected from −55 till 55 degree with a tilt-rotate specimen holder using Serial EM software. Obtained image series were used for 3-D reconstruction using IMOD (Cygwin, Linux) software package. The membrane boundaries were traced manually and 3-D models were computed. Rendering of the obtained images was performed automatically by IMOD mesh command. Four tomograms were reconstructed.

References

Balestrini R, Bonfante P (2005). The interface compartment in arbuscular mycorrhizae: A special type of plant cell wall? *Plant Biosystems* **139**:8-15

Balestrini R, Cosgrove DJ, Bonfante P (2005). Differential location of alpha-expansin proteins during the accommodation of root cells to an arbuscular mycorrhizal fungus. *Planta* **220**:889-899.

Benedito VA, Torres-Jerez I, Murray JD, Andriankaja A, Allen S, Kakar K, Wandrey M, Verdier J, Zuber H, Ott T, Moreau S, Niebel A, Frickey T, Weiller G, He J, Dai X, Zhao PX, Tang Y, Udvardi MK (2008). A gene expression atlas of the model legume *Medicago truncatula. Plant J* **55**:504-513.

Bonfante P, Genre A (2008). Plants and arbuscular mycorrhizal fungi: an evolutionary-developmental perspective. *Trends Plant Sci* **13**:492-498.

Bonfante-Fasolo P, Vian B, Perotto S, Faccio A, Knox LP (1990). Cellulose and pectin localization in root of mycorrhizal Allium porrum: labeling continuity between host cell wall and interfacial material. *Planta* **180**:537-547.

Brewin NJ (2004). Plant Cell Wall Remodelling in the *Rhizobium*-Legume Symbiosis. *Critical Rev Plant Sci* **23**:293-316

Capoen W, Goormachtig S, Rycke RD, Schroeyers K, Holsters M (2005). SrSymRK, a plant receptor essential for symbiosome formation. *Proc Natl Acad Sci USA* **102**:10369-10374.

Catalano CM, Czymmek KJ, Gann JG, Sherrier DJ (2007). *Medicago truncatula* syntaxin SYP132 defines the symbiosome membrane and infection droplet membrane in root nodules. *Planta* **225**:541-550.

de Faria SM, McInroy SG, Sprent JI (1987). The occurrence of infected cells, with persistent infection threads, in legume root nodules. *Can J Bot* **65**:553-558.

Godfroy O, Debellé F, Timmers T, Rosenberg C (2006). A rice calcium- and calmodulin-dependent protein kinase restores nodulation to a legume mutant. *Mol Plant Microbe Interact* **19**:495-501.

Horváth B, Yeun LH, Domonkos A, Halász G, Gobbato E, Ayaydin F, Miró K, Hirsch S, Sun J, Tadege M, Ratet P, Mysore KS, Ané JM, Oldroyd GE, Kaló P (2011). *Medicago* truncatula IPD3 is a member of the common symbiotic signaling pathway required for rhizobial and mycorrhizal symbioses. *Mol Plant Microbe Interact* **24**:1345-1358.

Javot H, Penmetsa RV, Terzaghi N, Cook DR, Harrison MJ (2007). A *Medicago truncatula* phosphate transporter indispensable for the arbuscular mycorrhizal symbiosis. *Proc Natl Acad Sci USA* **104**:1720-1725.

Jürgens G (2005). Plant cytokinesis: fission by fusion. *Trends Cell Biol* **15**:277-283.

Karimi M, Inzé D, Depicker A (2002). GATEWAY vectors for *Agrobacterium*-mediated plant transformation. *Trends Plant Sci* **7**:193-195.

Kouchi H, Imaizumi-Anraku H, Hayashi M, Hakoyama T, Nakagawa T, Umehara Y, Suganuma N, Kawaguchi M (2010). How many peas in a pod? Legume genes responsible for mutualistic symbioses underground. *Plant Cell Physiol* **51**:1381-1397.

Kwon C, Neu C, Pajonk S, Yun HS, Lipka U, Humphry M, Bau S, Straus M, Kwaaitaal M, Rampelt H, El Kasmi F, Jürgens G, Parker J, Panstruga R, Lipka V, Schulze-Lefert P (2008). Co-option of a default secretory pathway for plant immune responses. *Nature* **451**:835-840.

Lang T, Jahn R (2008). Core proteins of the secretory machinery. *Handb Exp Pharmacol*. **184**:107-127.

Limpens E, Ramos J, Franken C, Raz V, Compaan B, Franssen H, Bisseling T, Geurts R (2004). RNA interference in *Agrobacterium rhizogenes*-transformed roots of *Arabidopsis* and *Medicago truncatula*. *J Exp Bot* **55**:983-992.

Limpens E, Mirabella R, Fedorova E, Franken C, Franssen H, Bisseling T, Geurts R (2005). Formation of organelle-like N2-fixing symbiosomes in legume root nodules is controlled by DMI2. *Proc Natl Acad Sci USA* **102**:10375-10380.

Limpens E, Ivanov S, van Esse W, Voets G, Fedorova E, Bisseling T (2009). *Medicago* N2-fixing symbiosomes acquire the endocytic identity marker Rab7 but delay the acquisition of vacuolar identity. *Plant Cell* **21**:2811-2828.

Maillet F, Poinsot V, André O, Puech-Pagès V, Haouy A, Gueunier M, Cromer L, Giraudet D, Formey D, Niebel A, Martinez EA, Driguez H, Bécard G, Dénarié J (2011). Fungal lipochitooligosaccharide symbiotic signals in arbuscular mycorrhiza. *Nature* **469**:58-63.

Oldroyd GE, Murray JD, Poole PS, Downie JA (2011). The rules of engagement in the legume-rhizobial symbiosis. *Annu Rev Genet* **45**:119-144.

Op den Camp R, Streng A, De Mita S, Cao Q, Polone E, Liu W, Ammiraju JS, Kudrna D, Wing R, Untergasser A, Bisseling T, Geurts R (2011). LysM-type mycorrhizal receptor recruited for rhizobium symbiosis in nonlegume *Parasponia*. *Science* **331**:909-912.

Ovchinnikova E, Journet EP, Chabaud M, Cosson V, Ratet P, Duc G, Fedorova E, Liu W, den Camp RO, Zhukov V, Tikhonovich I, Borisov A, Bisseling T, Limpens E (2011). IPD3 controls the formation of nitrogen-fixing symbiosomes in pea and *Medicago* spp. *Mol Plant Microbe Interact* **24**:1333-1344.

Parniske M (2000). Intracellular accommodation of microbes by plants: a common developmental program for symbiosis and disease? *Curr Opin Plant Biol* **3**:320-328.

Pumplin N, Harrison MJ (2009). Live-cell imaging reveals periarbuscular membrane domains and organelle location in *Medicago* truncatula roots during arbuscular mycorrhizal symbiosis. *Plant Physiol* **151**:809-819.

Rae AL, Bonfante-Fasolo P, Brewin NJ (1992). Structure and growth of infection threads in the legume symbiosis with *Rhizobium leguminosarum*. *Plant J* **2**:385-395.

Roth LE, Stacey G (1989) Bacterium release into host cells of nitrogen-fixing soybean nodules: the symbiosome membrane comes from three sources. *Eur J Cell Biol* **49**:13-23.

Sanderfoot A (2007). Increases in the number of SNARE genes parallels the rise of multicellularity among the green plants. *Plant Physiol* **144**:6-17.

Segui-Simarro JM, Austin JR, II, White ER, Staehelin LA (2004). Electron tomographic analysis of somatic cell plate formation in meristematic cells of *Arabidopsis* preserved by high-pressure freezing. *Plant Cell* **16**:836-856.

Smith SE, Read D (2008) in *Mycorrhizal Symbiosis*. (Academic Press, Inc., San Diego).

Soltis PS, Soltis DE, Chase MW (1999). Angiosperm phylogeny inferred from multiple genes as a tool for comparative biology. *Nature* **402**:402-404.

Sprent JI, James EK (2007). Legume evolution: where do nodules and mycorrhizas fit in? *Plant Physiol* **144**:575-581.

Sprent JI. (2008). 60Ma of legume nodulation. What's new? What's changing? *J Exp Bot* **59**:1081-1084.

Sullivan JT, Ronson CW (1998). Evolution of rhizobia by acquisition of a 500-kb symbiosis island that integrates into a phe-tRNA gene. *Proc Natl Acad Sci USA* **95**:5145-5149.

Trouvelot A, Kough J, Gianinazzi-Pearson V (1986) in *Research for estimation methods having a functional significance, Physiological and Genetical Aspects of Mycorrhizae*, eds Gianinazzi-Pearson V, Gianinazzi S (INRA Press, Paris) pp 217–221.

Vasse J, de Billy F, Camut S, Truchet G (1990). Correlation between ultrastructural differentiation of bacteroids and nitrogen fixation in alfalfa nodules. *J Bacteriol* **172**:4295-4306.

Whitehead LF, Day DA (1997). The peribacteroid membrane. *Physiologia Plantarum* **100**:30-44.

Xie F, Murray JD, Kim J, Heckmann AB, Edwards A, Oldroyd GE, Downie JA (2012) Legume pectate lyase required for root infection by rhizobia. *Proc Natl Acad Sci U S A* **109**:633-638.

Yano K, Yoshida S, Müller J, Singh S, Banba M, Vickers K, Markmann K, White C, Schuller B, Sato S, Asamizu E, Tabata S, Murooka Y, Perry J, Wang TL, Kawaguchi M, Imaizumi-Anraku H, Hayashi M, Parniske M (2008). CYCLOPS, a mediator of symbiotic intracellular accommodation. *Proc Natl Acad Sci U S A* **105**:20540-20545.

Young ND, et al. (2011). The *Medicago* genome provides insight into the evolution of rhizobial symbioses. *Nature* doi: 10.1038/nature10625.

Zhang L, Zhang H, Liu P, Hao H, Jin JB, Lin J (2011). *Arabidopsis* R-SNARE proteins VAMP721 and VAMP722 are required for cell plate formation. *PLoS One* 6(10):e26129. Epub 2011 Oct 11.

Zhu H, Riely BK, Burns NJ, Ané JM (2006). Tracing nonlegume orthologs of legume genes required for nodulation and arbuscular mycorrhizal symbioses. *Genetics* **172**:2491-2499.
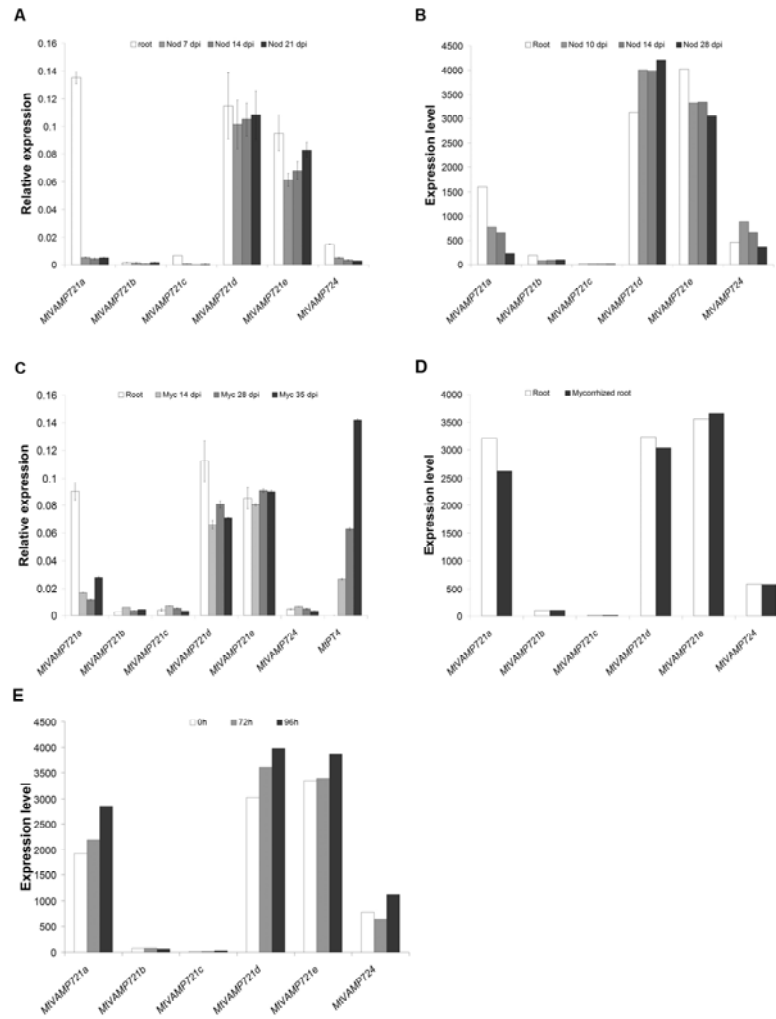
Supporting Information

Figure S1. Expression profile of *MtVAMP72s*. (*A and C*) Quantitative RT-PCR (qPCR) profile of *MtVAMP72*s. qRT-PCR was conducted on RNA isolated from roots and nodules (Nod) 7, 14 and 21 dpi with *S. meliloti* 2011 (*A*) and roots colonized by *G. intraradices* 14, 28 and 35 dpi. *MtVAMP72*s gene expression profiles were normalized against transcription level of reference gene *MtUBQ10*. Values represent means of triplicate runs on two independent biological samples. Error bars indicate standard deviations. This shows that *MtVAMP721d* and *MtVAMP721e* are highly expressed in root nodules. (*B, D* and *E*) Gene expression profile of *MtVAMP72s* based on *M. truncatula* Gene Expression Atlas data (http://mtgea.noble.org/v2/) in nodules 10, 14 and 28 dpi (*B*), mycorrhized roots (*D*) and roots 72 and 96 hours after infection by pathogenic fungus *Phymatotrichopsis omnivore* (Phymatotrichum) (*E*). Note, that none of the MtVAMP721 homologs show a striking transcriptional regulation upon infection by *Phymatotrichopsis omnivore*, although the "non-symbiotic" *MtVAMP721a* appears to be slightly induced.
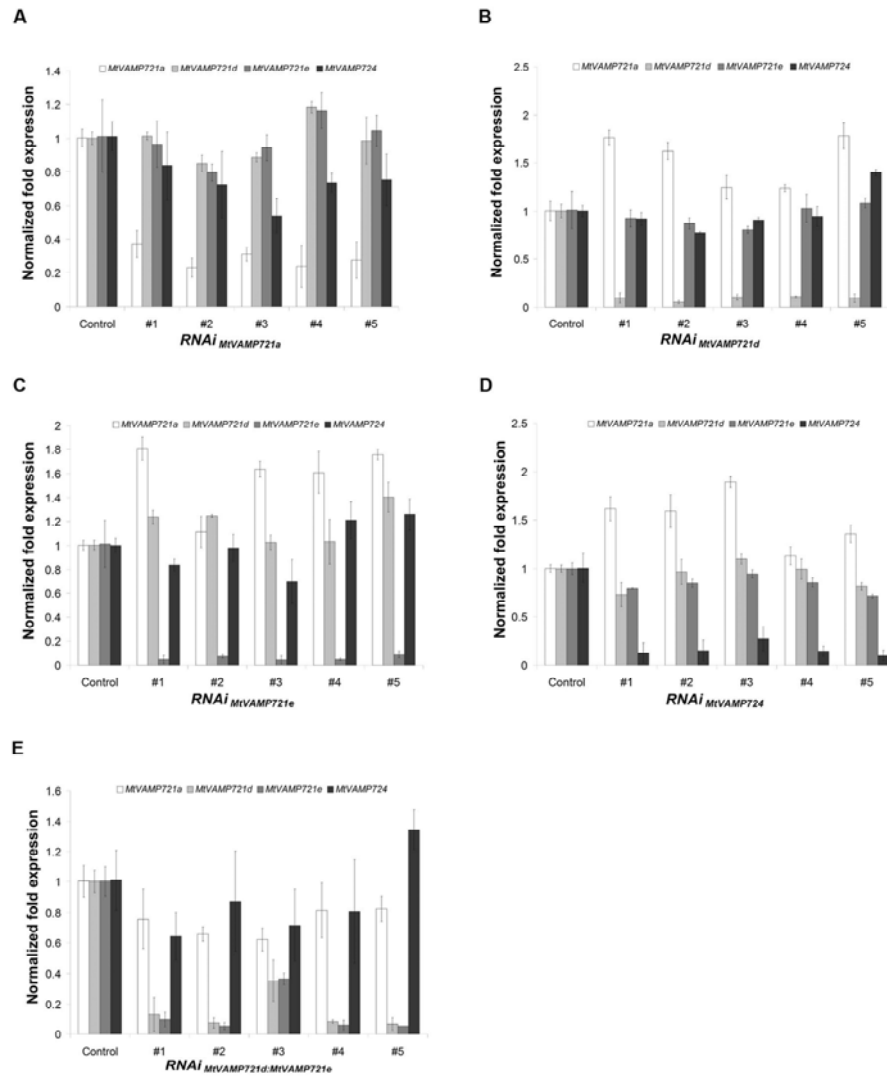
Figure S2. Quantitative RT-PCR (qPCR) of gene-specific RNA interference. Total RNA was extracted independently from five transgenic roots expressing $RNAi_{MtVAMP721a}$ (*A*), $RNAi_{MtVAMP721d}$ (*B*), $RNAi_{MtVAMP721e}$ (*C*), $RNAi_{MtVAMP724}$ (*D*), $RNAi_{VAMP721d:VAMP721e}$ (*E*). Equal amounts of total RNA was subjected to qPCR using gene-specific primers and the expression level of corresponding genes was measured relative to their expression in roots transformed with the empty control vector. *MtUBQ10* transcript level was used as reference. The mean of three independent control roots transformed with an empty vector is shown. Error bars indicate standard deviations.

Figure S3. Effect of *RNAi*_{*VAMP721d:VAMP721e*} on root growth and number of nodules. (*A*) Root elongation of *RNA-i*_{*VAMP721d:VAMP721e*} transgenic roots (*n*=20) was measured in 24 hours intervals during 5 days and compared with root elongation of transgenic roots expressing an empty vector control (*n*=20). Hash sign indicate statist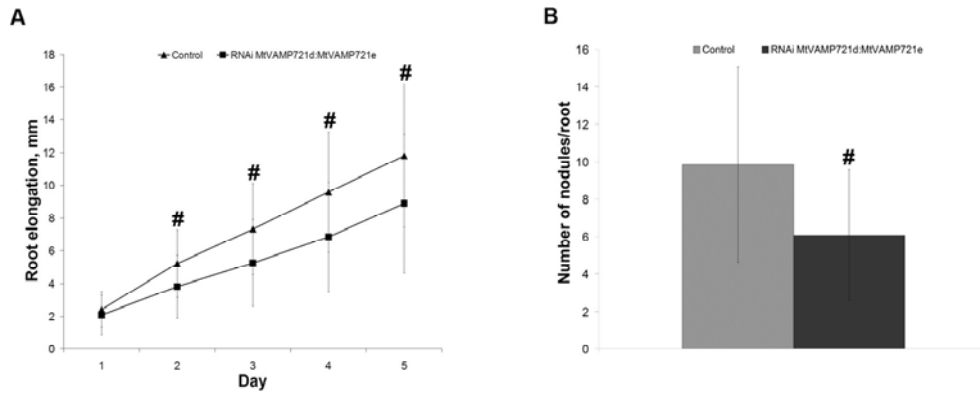ically significant difference (day 1, *P*=0.222; day 2, *P*=0.008; day 3, *P*=0.005; day 4, *P*=0.005; day 5, *P*=0.016). (*B*) Nodule number was counted on each *RNAi*_{*VAMP721d:VAMP721e*} transgenic root (*n*=15) and compared to transgenic control roots (*n*=15). Hash sign indicate statistically significant difference (*P*=0.05). ANOVA test was used for statistical analysis.
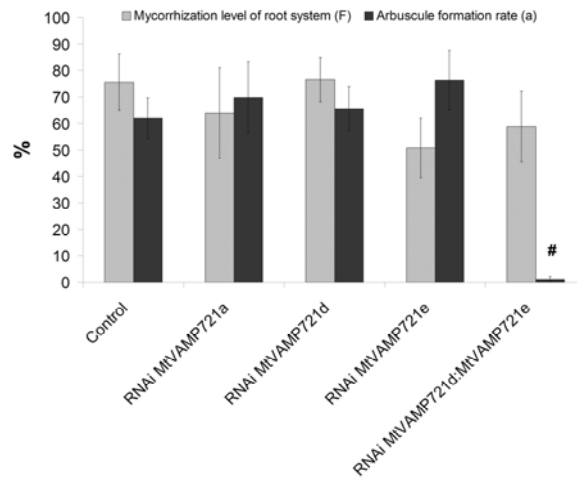
Figure. S4. Arbuscule formation is compromised in *RNAi*_{*MtVAMP721d:MtVAMP721e*} transgenic roots. The *G. intraradices* mycorrhization level of the root system (parameter *M*) is equal in control and *RNAi*_{*MtVAMP721d:MtVAMP721e*} roots (*n*=5, *P*=0.06). However, mature arbuscule abundance (parameter *a*) in *RNAi*_{*MtVAMP721d:MtVAMP721e*} roots is significantly decreased (*n*=5, *P*= <0.001, hash sign indicate statistically significant difference). There was no difference in parameter *a* between control and *RNAi*_{*MtVAMP721a*} (*n*=5, *P*=0.249 and *P*=0.302), *RNAi*_{*MtVAMP721d*} (*n*=5, *P*=0.883 and *P*=0.498) or *RNAi*_{*MtVAMP721e*} (*n*=5, *P*=0.529 and *P*=0.629). Transgenic roots were harvested from composite plants 4 weeks after *G. intraradices* inoculation, stained by trypan blue and analyzed by light microscopy. 75 cm of each transgenic root system was analysed. Error bars indicate standard deviation. ANOVA test was used for statistical analysis.

Figure S5. Localization of MtVAMP721d and MtVAMP721e vesicles at the site of bacterial release and near the SB and periarbuscular membrane. (*A*) MtVAMP721d positive vesicles accumulate at local regions (arrowheads) of infection threads (*it*). Co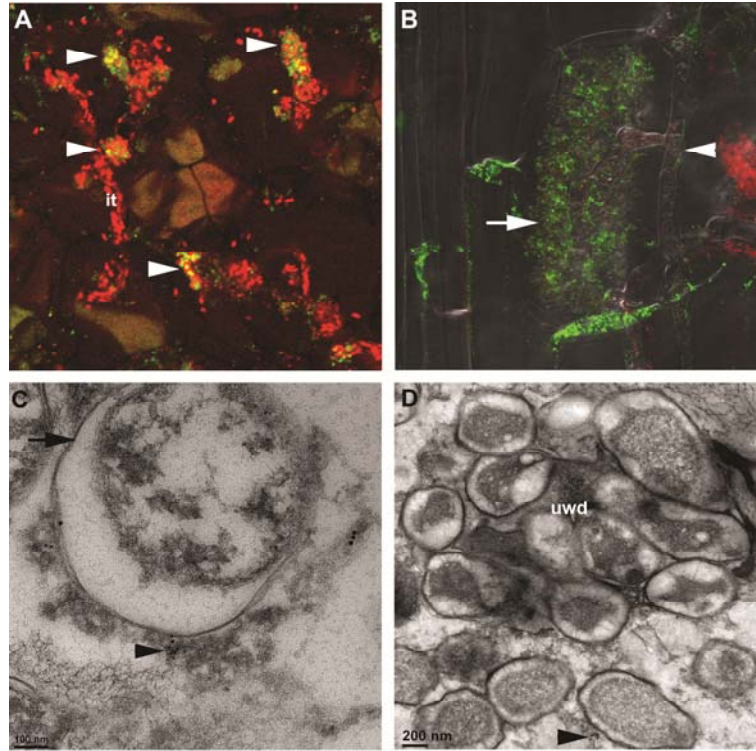mposite plants with transgenic roots expressing *pVAMP721d::GFP-VAMP721d* were inoculated with *S. meliloti* 2011 constitutively expressing RFP. Root nodules were hand-sectioned, exposed to anti-GFP antibodies and secondary antibodies coupled with Alexa488 and analyzed by confocal microscopy. (*B*) Confocal immunolocalization of VAMP721d/e using the anti-VAMP721d/VAMP721e antibody on *Medicago* wild-type root infected by *G. intraradices*. Signal from anti-VAMP721d/VAMP721e antibodies is localized near the fine branches (arrow) of mature arbuscule and absence on intraradical hypha (arrowhead). Root was hand-sectioned and exposed to anti-VAMP721d/VAMP721e antibodies and secondary antibodies coupled with Alexa488. Note the markedly low signal in non-infected cells. (*C* and *D*) GFP-MtVAMP721d and GFP-MtVAMP721e vesicles fuse with the SB membrane (arrow) of young SBs (*C*) and near the site of bacteria release (*D*). GFP-VAMP721e is visualized by electron microscopic immunogold detection on nodules expressing either *pVAMP721e::GFP-VAMP721e* (*C*) or *pVAMP721d::GFP-VAMP721d* (*D*) using anti-GFP antibodies (10 nm) and anti-VAMP721d/VAMP721e antibodies (15 nm). White arrowhead, gold labeled vesicle in contact with the SB membrane. This shows that VAMP721d positive vesicles accumulate at the region of the infection thread where an unwalled droplet (*uwd*) is formed and bacteria are released (*D*). (Scale bars, 10 μm in *A* and *B*, 100 nm in *C*, 200 nm in *D*.)
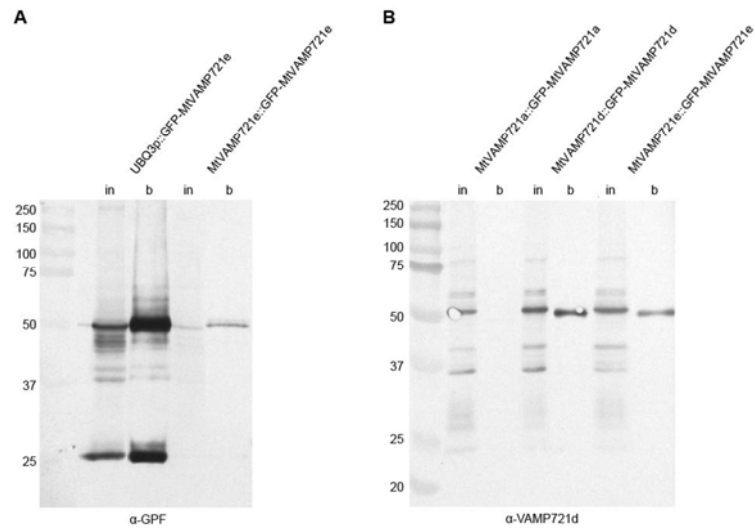
Figure S6. (*A*) MtVAMP721e is present at low level in plant tissue. Total protein fractions were extracted from transgenic roots expressing GFP fusions of *VAMP721e* under control of the constitutive *Arabidopsis UBQ3* or native 2,5 kb promoters and used for immunoprecipitation using anti-GFP coated agarose beads. Equal amount of crude extract (*in*) and bound fraction (*b*) were subjected to immunoblot and detected using anti-GFP antibody. The fusion proteins of the predicted size (53,5 kDa) are detected. Note the presence of free GFP (27 kDa) in *UBQ3::GFP-MtVAMP721e* expressing lines. (*B*) Specific antibodies raised against MtVAMP721d cross-react with VAMP721e. Total protein fractions were extracted from transgenic roots expressing GFP fusions of *VAMP721a*, *VAMP721d* or *VAMP721e* under control of the constitutive *Arabidopsis UBQ3* promoter and used for immunoprecipitation using anti-GFP coated agarose beads. Precipitated proteins were subjected to immunoblot and detected using anti-MtVAMP721d antibody. The antibody against MtVAMP721d cross-reacts with VAMP721e, however, it does not react with VAMP721a.

Table S1. *Medicago VAMP72* genes

Gene name	Corresponding gene locus or TC number
MtVAMP721a	Medtr4g023810*, TC95333
MtVAMP721b	Medtr7g064880
MtVAMP721c	Medtr7g064860, TC171206
MtVAMP721d	Medtr2g034380, TC106930
MtVAMP721e	Medtr4g114750, TC106931
MtVAMP724	TC110430
MtVAMP727	AC233577_38

* Accession numbers are presented according to Phytozome database (http://www.phytozome.net/)

Table S2. Gene sequences used in phylogenetic analysis

Gene name	Corresponding gene locus	Gene name	Corresponding gene locus
GmVAMP72a	Glyma07g34900*	*PtVAMP72a*	POPTR_1s14430
GmVAMP72b	Glyma07g37760	*PtVAMP72b*	POPTR_2s24200
GmVAMP72c	Glyma08g47040	*PtVAMP72c*	POPTR_3s17620
GmVAMP72d	Glyma09g02310	*PtVAMP72d*	POPTR_8s02030
GmVAMP72e	Glyma09g05070	*PtVAMP72e*	POPTR_10s24630
GmVAMP72f	Glyma10g24430	*PtVAMP72f*	POPTR_12s12000
GmVAMP72g	Glyma10g42480	*PtVAMP72g*	POPTR_15s15690
GmVAMP72h	Glyma15g13220	*PtVAMP72i*	POPTR_34s00330
GmVAMP72i	Glyma15g15760	*AtVAMP721*	AT1G04750§
GmVAMP72j	Glyma17g02870	*AtVAMP722*	AT2G33120
GmVAMP72k	Glyma18g37970	*AtVAMP723*	AT2G33110
GmVAMP72l	Glyma18g38010	*AtVAMP724*	AT4G15780
GmVAMP72m	Glyma20g02720	*AtVAMP725*	AT2G32670
GmVAMP72n	Glyma20g18860	*AtVAMP726*	AT1G04760
GmVAMP72o	Glyma20g24540	*AtVAMP727*	AT3G54300
VvVAMP72a	GSVIVG01000524001	*SlVAMP72a*	SGN-U572420†
VvVAMP72b	GSVIVG01010710001	*SlVAMP72b*	SGN-U572423
VvVAMP72c	GSVIVG01012100001	*SlVAMP72c*	SGN-U572424
VvVAMP72d	GSVIVG01017751001		
VvVAMP72e	GSVIVG01028579001		

Accession numbers are presented according to (*) Phytozome database (http://www.phytozome.net/), (§) *Arabidopsis* Information Resource (TAIR, http://www.arabidopsis.org/), (†) Sol Genomics Network (http://solgenomics.net/organism/1/view).

Table S3. Oligonucleotides used in a study

Name	Sequence (5'→3')
For quantitative PCR	
MtVAMP721a-F	CTGTGTGCCATGGCTTCAGTTGTTA
MtVAMP721a-R	GCATCCTACCACACCTTATTCACTTCC
MtVAMP721b-F	CGCTGAATACACCGAGTTCA
MtVAMP721b-R	GTCCAGCAGACTCAACAGCA
MtVAMP721c-F	CGCCCATGATGGATTTACTT
MtVAMP721c-R	CTCCTTCAATTTCGGTCCAA
MtVAMP721d-F	TGTGGCTGCAAAACATGAAGGTAAA
MtVAMP721d-R	TGGAATAACAATAAAGGCCACAGAGAA
MtVAMP721e-F	GATCACCCGGAGGAGGTGAGTAAG
MtVAMP721e-R	GCCACATTTTTCTGCGGATTTTG
MtVAMP724-F	AGATAGATGCAAAACAACAACACGAAGC
MtVAMP724-R	GAGCTGCAATGGCAGGGGAAGTTAC
MtVAMP727-F	GATCGTGGGGAGAAGATTGA
MtVAMP727-R	AACATTTGAAACCCCCACAA
To generate DNA fragments for RNA interference	
MtVAMP721a-F	**CACC**GTGTGCCATGGCTTCAGTTGTTA*
MtVAMP721a-R	ACATTATGCATCCTACCACACCTTATTCA
MtVAMP721d-F	**CACC**GACTCGGGGATAATAAGCACCATTC
MtVAMP721d-R	GAATGGAAACCAAACTTCAAACAGACA
MtVAMP721e-F	**CACC**CCTTAAGAATAAATAAACGCCACTCTCG
MtVAMP721e-R	TAGAAGCATTAGTATATCATCATCACCATCA
MtVAMP724-F	**CACC**TGCGGTGGATTTAACTGTTCAA
MtVAMP724-R	CATCCAATCATACTTTCACCATCTTCA
MtVAMP721d,e -F	AGTTTGGTTTCCATTCCCTTAAGAATAAATA
MtVAMP721d,e -R	TATTTATTCTTAAGGGAATGGAAACCAAACT
To generate DNA fragments of promoter regions	
MtVAMP721a-F	**CACC**AAGCTTTCCAGTGCAAGCTGGTCA*
MtVAMP721a-R	ACTAGTGAATGATCACAATTCACAACTCTC
MtVAMP721d-F	**CACC**AAGCTTTTTATGCCAAACAAGAGCATC
MtVAMP721d-R	ACTAGTTGAAGAAGAGATCTGAGAATGGT
MtVAMP721e-F	**CACC**ATATGATCACAAAGACACAACCACA
MtVAMP721e-R	CTTCTTCTCCACAGATCTATCGAAC
To generate coding sequences of gene of interest	
MtVAMP721a-F	**CACC**ATGGGACAACAATCATTGATCTATAGCTTTG*
MtVAMP721a-R	TCCTACCACACCTTATTCACTTCCCTTCC
MtVAMP721d-F	**CACC**ATGGCGAACAACCAGAATCAGAAG
MtVAMP721d-R	GATAATCACAAGGTTGGAATAACAATAAAG
MtVAMP721e-F	**CACC**ATGGGACAGAACCAAAAATCTCTGA
MtVAMP721e-R	CCTCATCATCATCATCATATAATAATCACA

*-Sequences designated in bold are added to forward primer for TOPO cloning

Chapter 4

Multiple exocytotic markers accumulate at the sites of perifungal membrane biogenesis in arbuscular mycorrhizas

Andrea Genre[1], Sergey Ivanov[2], Mates Fendrych[3], Antonella Faccio[4], Victor Zarsky[5], Ton Bisseling[2] and Paola Bonfante[1]

[1]*Department of Plant Biology, University of Turin, Viale P.A. Mattioli 25, 10125 Torino, Italy;* [2]*Laboratory of Molecular Biology, Graduate School Experimental Plant Science, Wageningen University, Droevendaalsesteeg 1, 6708PB Wageningen, The Netherlands;* [3]*Institute of Experimental Botany, Academy of Sciences of the Czech Republic, Rozvojova´ 263, 165 02 Prague 6, Czech Republic;* [4]*IPP-CNR, Viale P.A. Mattioli 25, 10125 Torino, Italy;* [5]*Department of Experimental Plant Biology, Faculty of Science, Charles University, Vinicna 5, 128 44 Prague 2, Czech Republic*

Arbuscular mycorrhizas (AMs) are symbiotic interactions established within the roots of most plants by soil fungi belonging to the Glomeromycota. The extensive accommodation of the fungus in the root tissues largely takes place intracellularly, within a specialized interface compartment surrounded by the so-called perifungal membrane, an extension of the host plasmalemma. By combining live confocal imaging of green fluorescent protein (GFP)-tagged proteins and transmission electron microscopy (TEM), we have investigated the mechanisms leading to the biogenesis of this membrane. Our results show that pre-penetration responses and symbiotic interface construction are associated with extensive membrane dynamics. They involve the main components of the exocytotic machinery, with a major participation of the Golgi apparatus, as revealed by both TEM and in vivo GFP imaging. The labeling of known exocytosis markers, such as v-SNARE proteins of the VAMP72 family and the EXO84b subunit of the exocyst complex, allowed live imaging of the cell components involved in perifungal membrane construction, clarifying how this takes place ahead of the growing intracellular hypha. Lastly, our novel data are used to illustrate a model of membrane dynamics within the pre-penetration apparatus during AM fungal penetration.

Introduction

Arbuscular mycorrhizas (AMs) are symbiotic associations between Glomeromycota and the majority of plant species (Smith and Read, 2008; Hata *et al.* 2010). These interactions develop in the rhizosphere, where signaling molecules released by both the plant and the fungus keep the respective partner informed of their reciprocal proximity and trigger pre-symbiotic responses ranging from gene regulation to metabolic changes, as well as morphogenetic events such as an increase in hyphal and root branching (Parniske 2008). Following this pre-symbiotic chemical dialog, a pivotal event in the establishment of AM interactions is the adhesion of a fungal hyphopodium to the host root epidermis (Bonfante and Genre, 2008). Direct physical contact, in fact, marks the initiation of the symbiotic phase and represents the first step towards the colonization of inner root tissues. Root colonization is characterized by the development of intracellular fungal structures, including the highly branched arbuscules where the exchange of mineral nutrients for photosynthesis-derived carbohydrates takes place. All intracellular fungal structures are accommodated inside a novel cell compartment, called the symbiotic interface. It is composed of plant cell wall materials and bordered by an extension of the host plasma membrane (Parniske, 2008; Genre and Bonfante 2010).

We have shown that hyphopodium contact causes an impressive reorganization of the epidermal cell cytoplasm, leading to the appearance of a novel structure, the so-called pre-penetration apparatus, or PPA (Genre *et al.*, 2005). This is a broad, columnar aggregation of cytoplasm that predicts the future track of the penetrating hypha through the epidermal cell lumen. A few similarities have been found between the PPA and the infection thread (IT), induced by symbiotic nitrogen-fixing rhizobia (Gage, 2004). Remarkably, the processes of PPA and IT assembly are strictly controlled, in legumes, by the 'common SYM' pathway, a signal transduction pathway that mediates the intracellular accommodation of both AM fungi and rhizobia (Oldroyd and Downie, 2006). Pre-penetration responses are not limited to legumes. The observation of PPA in *Daucus carota* (a plant belonging to the *Asterales*, which are phylogenetically very distant from the *Leguminosae*) suggests that pre-penetration responses are shared among AM hosts (Genre *et al.*, 2008), and have probably been conserved from the common ancestors that first established a symbiotic association with glomeromycetes, at least 400 Mya, in the early Devonian (Redecker *et al.*, 2000).

Furthermore, pre-penetration responses are not restricted to epidermal cells but extend to all root cells that undergo AM colonization. Broad PPAs are organized in cortical cells, associated with arbuscule development (Genre *et al.*, 2008). Such a reoccurrence of the pre-penetration response whenever new intracellular hyphae develop strongly suggests that the PPA has a role in fungal accommodation inside the host cells.

From this perspective, the composition of the PPA, which has been partially elucidated, gives clear indications. Beside the nucleus, whose movements to and from the fungal contact site are associated with the initiation and full development of the PPA, the cytoplasmic aggregate includes thick bundles of cytoskeletal fibers and an extensive proliferation of endoplasmic reticulum (ER). Electron microscopy investigations have also shown an abundance of Golgi apparatus stacks as well as trans-Golgi vesicles and tubules (Genre *et al.*, 2008). Equally, Golgi apparatus stack accumulation has also been observed around

young arbuscules (Pumplin and Harrison, 2009). All of these observations suggest the presence of secretory activity inside the PPA, which has therefore been proposed to have a function in the assembly of the perifungal membrane, the extension of the plant plasma membrane that envelopes each intracellular hypha, maintaining host cell integrity. This has only been postulated so far on the basis of indirect evidence: (i) the PPA anticipates the intracellular fungal route; (ii) PPA dismantling is associated with the appearance of the perifungal membrane; (iii) PPA-like aggregates are also observed in advance of arbuscule branch development; and (iv) plant mutants for SYM pathway genes, where PPA assembly is hampered, are not successfully colonized by AM fungi.

The aim of the reported research is to investigate how the perifungal membrane is built inside the PPA. For this, we have expressed different green fluorescent protein (GFP) constructs in two model plants, the legume *Medicago truncatula* and the non-legume *Daucus carota*, by *Agrobacterium rhizogenes*-mediated root transformation. We have tagged the main elements of the secretory pathway, including the Golgi apparatus and proteins involved in the fusion of secretory vesicles with their target membranes [SNARE (soluble N-ethylmaleimide-sensitive factor attachment protein receptor) proteins of the vesicle associated membrane protein 72 (VAMP72) family and a member of the exocyst complex]. Our results show that such cell components and proteins accumulate inside the PPA aggregate, indicating the onset of a major exocytotic event a short distance from the growing hyphal tip, and strongly suggesting this as the site of perifungal membrane assembly.

Results

GFP:MAN-labeled compartments accumulate inside the PPA. In order to assist the reader in interpreting our images, two pictures of PPAs where the ER is labeled by GFP-HDEL (Genre *et al.*, 2005; Genre *et al.*, 2008) are presented in Fig. S1. Beside being interpreted as a putative marker of exocytotic activity since it was first observed (Parniske, 2008), the intense accumulation of GFP-labeled ER highlights very clearly the PPA outline, making it easier to read the images obtained with the other GFP markers presented in this work.

The expression of GFP-MAN (a fusion of GFP with a-1,2 mannosidase I; Nebenfuhr *et al.*, 1999) in *D. carota* resulted in a bright labeling of spot-like compartments, dispersed in the cytoplasm (Fig. 1*A* and *B*). Such organelles are interpreted as *cis*-Golgi elements according to Nebenfuhr *et al.*, (1999). Occasionally, a weak labeling of the ER and particularly the nuclear envelope was also visible in these lines, probably related to the synthesis of the chimeric proteins in the ER lumen prior to their accumulation in the *cis*-Golgi.

Upon hyphopodium adhesion to an epidermal cell (Fig. 1*C*–*E*), a progressive accumulation of GFP-MAN bodies could be observed in the vicinity of the contact site, corresponding to the PPA area (compare with Fig. S1).

Golgi stacks are extremely motile organelles in the plant cell, where they display rapid movements along the F-actin/ER network (Nebenfuhr et al. 1999). For this reason, visualizing them in still images is not by itself very informative regarding their activity. We therefore acquired several time-lapse movies, recording a frame every 1.6 s over 2 min
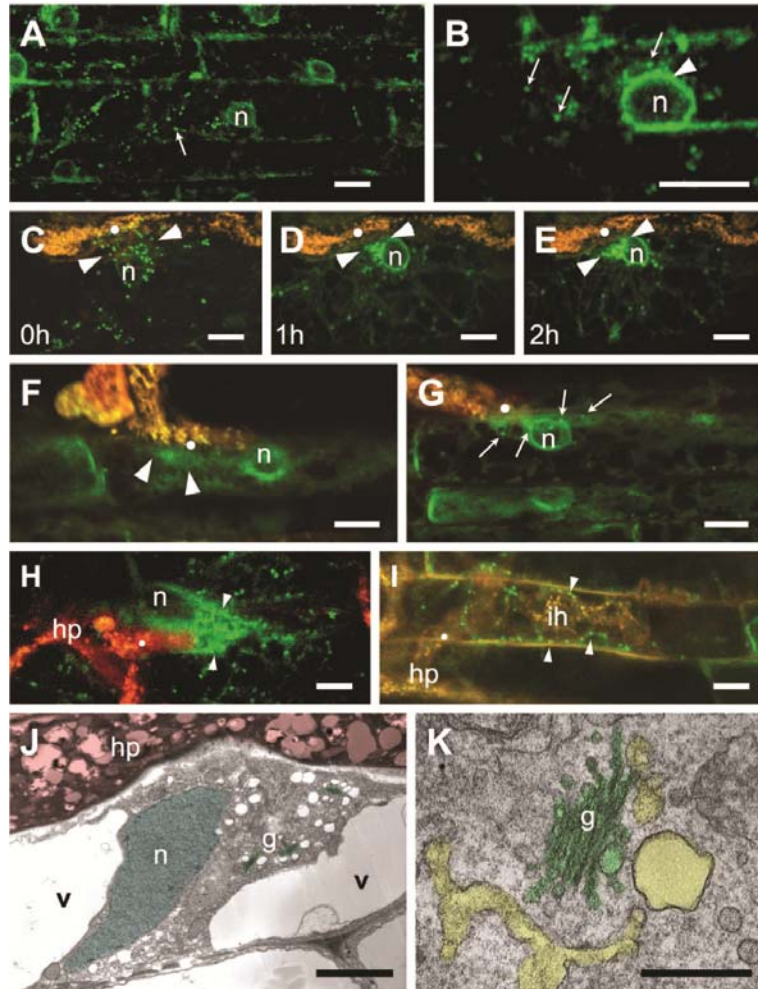
Figure 1. Organization of the Golgi apparatus in *D. carota* during the pre-penetration response. Labeling of the Golgi apparatus by GFP:MAN inside epidermal cells from control roots grown in the absence of the AM fungus is shown in *A* and *B*. Several Golgi stacks (arrows) are visible as bright dots spread across the cytoplasm. The expression of this construct also displays a weak labeling of the nuclear envelope (*B*, arrowhead), marking the position of the nucleus (n). (*C–E*) Time series covering 2 h of observation and showing the progressive accumulation of Golgi stacks in the PPA area (arrowheads) between the nucleus (n) and contact point (•). (*F* and *G*). Golgi stack dynamics upon fungal contact as analyzed through the acquisition of a single focal plane at 1.6 s intervals over 2 min. Image averaging displays green halos in those areas where the GFP:MAN fluorescence has been recorded more often during the observation time. In both images, the brightest areas are associated with the contact point (•) and perinuclear cytoplasm (n). Furthermore, the permanence of a few Golgi stacks within the PPA area is highlighted in G by the presence of isolated green spots (arrows), corresponding to single stacks that have remained still over most of the acquisition time.

intervals. The resulting animations show the rapid dynamics of the Golgi apparatus, both in
control roots and in the presence of the AM fungus. To obtain a global view of the dynam-
ics of the Golgi apparatus, we have then used Leica Confocal Software to prepare averaged
images from each time-lapse movie. Such images show bright areas in those regions where
the GFP-labeled Golgi stacks have passed more often or have stayed for longer, during the
2 min observation. As represented in Fig. 1*F* and *G*, a diffuse fluorescence was observed in
the perinuclear cytoplasm, where Golgi apparatus stacks often pass. Significantly, blurred
areas of green fluorescence could also be clearly seen in the PPA area, in the vicinity of the
hyphopodium contact site. Furthermore, a few bright spots could often be observed in the
PPA area, indicating that a few GFP-MAN compartments have remained still during most
of the observation time. Apart from the perinuclear region, areas and spots of comparable
brightness were not observed in control cells from uninfected roots (Fig. S2). Upon fungal
penetration of the epidermal cell, a dense accumulation of GFP-labeled Golgi stacks can
still be observed in the part of the PPA that is located ahead of the growing hyphal tip (Fig.
1*H*); in contrast, after PPA dismantling, GFP-MAN compartments distribute along the in-
tracellular hypha with a much lower density (Fig. 1*I*). The abundance of Golgi apparatus
stacks in the PPA aggregate was also confirmed by transmission electron microscopy
(TEM) analyses, where several piles of Golgi cisternae were detected (Fig. 1*J*), associated
with an extensive tubular–vesicular *trans*-Golgi network (Fig. 1*K*).

Taken together, these observations indicate that Golgi stacks accumulate inside the
PPA volume, where they also spend a relatively longer time compared with the rest of the
cytoplasm. Such a concentration of the Golgi apparatus activity in the PPA fits in with the
activation of the plant secretory pathway before and during fungal penetration of the epi-
dermal cell.

VAMP72 marks the site of perifungal membrane biogenesis. Membrane fusion in eu-
karyotic cells is regulated by specific proteins known as SNAREs (Brunger, 2006).
SNARE-mediated membrane fusion is achieved by the formation of a highly stable protein
association named the SNARE complex. A typical SNARE complex involves three distinct
types of proteins residing on the target membrane (t-SNARE) and one protein located on
the transport vesicle (v-SNARE) that together contribute to a four-helix bundle of inter-
twined SNARE domains (Brunger, 2006). Since VAMPs of the VAMP72 family are v-
SNAREs known to be involved in secretory processes (Sanderfoot 2007; Kwon *et al.*,
2008a), we chose three constructs where the GFP was fused to VAMP721a, VAMP721d
and VAMP721e. By screening their distribution in the root cells, we observed that all

---

Figure 1. Continued
(H) Persistence of Golgi stacks accumulation during fungal penetration. A penetration hypha developing from
a hyphopodium (hp) has entered the epidermal cell through the initial contact point (•) and is developing
within the PPA area (arrowheads). A large number of Golgi stacks accumulate in the PPA between the pene-
trating hypha and the nucleus (n). (I) Epidermal cell traversed by an intracellular hypha (ih) that has developed
from the hyphopodium (hp) through the contact point (•). Scattered Golgi stacks (arrowheads) are visible in
the cytoplasm surrounding the hypha. (*J* and *K*) Transmission electron micrographs showing Golgi stacks in-
side a PPA. (*J*) The cytoplasmic aggregation, positioned underneath a contacting hyphopodium (hp, red) and
crossing the vacuole (v), includes the nucleus (n, blue) and several Golgi stacks (g, green). (*K*) A higher mag-
nification shows a single Golgi stack (g, green) associated with extensive trans-Golgi membranes (yellow).
(Scale bars. 20 mm in *A–I*. 5 mm in *J*: 0.5 mm in *K*.)

VAMP fusions marked cell division sites inside the meristems of *M. truncatula* (Fig. 2A; Fig. S3*A* and *B*), as well as the tips of growing root hairs (Fig. 2B; Fig. S3*E* and *F*).

    Minor differences could be detected in the distribution pattern of each construct. Cell
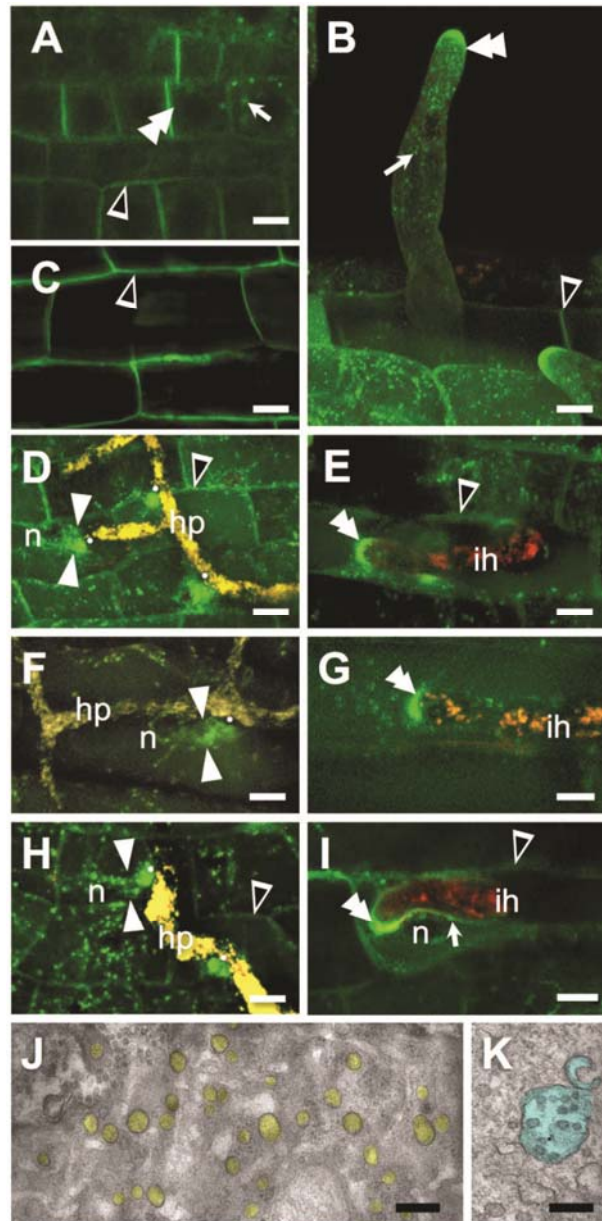

Figure 2. GFP tagging of VAMP72 proteins in *M. truncatula* highlighting vesicle accumulation and perifungal membrane proliferation inside the PPA.

division sites and root hair tips were the only detectable targets of GFP-VAMP721d (Fig. S3*B*, *D* and *F*). In contrast, fluorescence was also detected in the plasma membrane of both meristematic and differentiated cells from the lines expressing GFP-VAMP721a (Fig. S3*A* and *C*) and GFP-VAMP721e (Fig. 2*A–C*), reflecting the retention of the proteins on the target membrane, possibly due to the saturation of the exocytotic pathway by overexpression. Small punctate cytoplasmic bodies were often found also to be labeled by the three VAMP72 constructs (Fig. 2 and Fig. 3).

The VAMP72 constructs therefore proved to be reliable markers of exocytosis in *M. truncatula* root organ cultures (ROCs) as already described in *Arabidopsis* (Kwon *et al*. 2008a, Kwon *et al*. 2008b).

Hyphopodium development on the surface of an epidermal cell induced an accumulation of fluorescence in the vicinity of the contact site, suggesting the local concentration of GFP-tagged secretory vesicles (Fig 2*D*, *F* and *H*). This condition is also supported by electron microscopy images, showing broad clusters of vesicles inside the PPA (Fig. 2*J*).

Later, after fungal penetration, the fluorescence concentrated in the vicinity of the growing hyphal tip (Fig. 2*E*, *G* and *I*) and its position could be deduced based on the cytosolic autofluorescence of *Gigaspora gigantea*. Such a pattern, which can derive from the GFP tagging of VAMP72 proteins in both the secretory vesicles and the membrane where they have just fused, revealed the site of perifungal membrane proliferation.

Also in this condition, the three VAMP72 proteins displayed minor but significant differences in their localization patterns. GFP-VAMP721a (Fig. 2*E*) and GFP-VAMP721d (Fig. 2*G*) were concentrated in the shape of a crescent, just ahead of the growing hyphal tip. In addition to this localization,

GFP-VAMP721e also marked part of the perifungal membrane on the side of the hypha, up to 40–50 mm from the tip (Fig. 2*I*). Both before and after fungal penetration, moving punctuate bodies were constantly labeled in the cytoplasm by the three constructs. Interestingly, TEM images of the PPA aggregate show abundant late endosomes [or multivesicular bodies (MVBs)], as shown in Fig. 2*K*.

Perifungal membrane proliferation involves the exocyst complex. Throughout eukaryotes, vesicle targeting is mediated by a hetero-oligomeric protein complex known as the exo-

Figure 2. Continued

(*A–C*) Pattern of GFP-VAMP721e localization in the root meristem (*A*), atrichoblastic (*B*) and trichoblastic epidermal cells (*C*). In addition, to a number of punctate cytoplasmic bodies (arrows), and a weaker signal along the plasma membrane (black arrowheads), fluorescence mainly accumulated along the newly laid cell walls (double arrow) of meristematic cells (*A*) and in the root hair tip (double arrows) of trichoblasts (*B*), indicating the recruitment of VAMP72 proteins in the root major exocytotic events. (*D–I*) Subcellular localization of GFP-VAMP721a (*D*, *E*), GFP-VAMP721d (*F*, *G*) and GFP-VAMP721e (*H*, *I*) upon hyphopodium (hp) contact (*D*, *F*, *H*) and cell entry (*E*, *G*, *I*). In analogy to uninfected roots, a weak fluorescence was observed along the plasma membrane (black arrow) only for VAMP721a (*D*, *E*) and VAMP721e (*H*, *I*). The three constructs gave rise to an intense fluorescence within the PPA area (arrowheads), generally more focused towards the contact site (●) than the nucleus (n). After cell entry, a crescent-shaped pattern (double arrow) embracing the tip of the intracellular hypha (ih) was observed in the three lines. This distribution of fluorescence is likely to derive from the accumulation of GFP-tagged vesicles and their fusion into the developing perifungal membrane. The latter was more extensively labeled by GFP-VAMP721e (I, arrow). Furthermore, fluorescent punctate bodies were often observed in the PPA area and throughout the cytoplasm (evident in *D*, *G* and *H*). (*J* and *K*) Transmission electron micrographs of the PPA aggregate, showing the abundance of vesicles (*J*, yellow) and MVB (*K*, blue). (Scale bars. 20 mm in *A–I*: 0.5 mm in *J* and *K*.)

cyst, tethering the vesicle to its target membrane prior to SNARE involvement and membrane fusion (Hala *et al.* 2008, Fendrych *et al.* 2010). We therefore chose the EXO84 subunit of the exocyst complex as a further marker of exocytotic activity (Guo *et al.* 1999). GFP-tagged AtEXO84b produced a comparable labeling in both *D. carota* (Fig. 3*A* and *B*) and *M. truncatula* (Fig. 3*C* and *D*), with a moderate but selective labeling of the young root hair tips (Fig. 3 *A* and *B*). In particular, the apical dome was marked by the fluorescent signal only in the root hair tips that were rich in cytoplasm, a hallmark of active tip growth, whereas the GFP fluorescence was absent in vacuolated hairs, where growth is arrested (Fig. 3*C* and *D*).

Significantly, GFP:EXO84b accumulated underneath *G. gigantea* hyphopodia (Fig. 3*E*), highlighting the PPA aggregate with a diffuse signal. During intracellular fungal development, the construct labeled a crescent shape encompassing the growing hyphal tip (Fig. 3*F*).

In conclusion, the constitutive expression of fluorescently labeled AtEXO84b in both *D. carota* and *M. truncatula* selectively marked the growing root hair tips and the area of the developing perifungal membrane, indicating the involvement of the exocyst complex in both processes. In addition, the visualization of GFP:EXO84b around the tip of intracellular hyphae confirmed that the perifungal membrane develops inside the PPA, a short distance ahead of the growing hyphal tip, as already suggested by VAMP constructs.
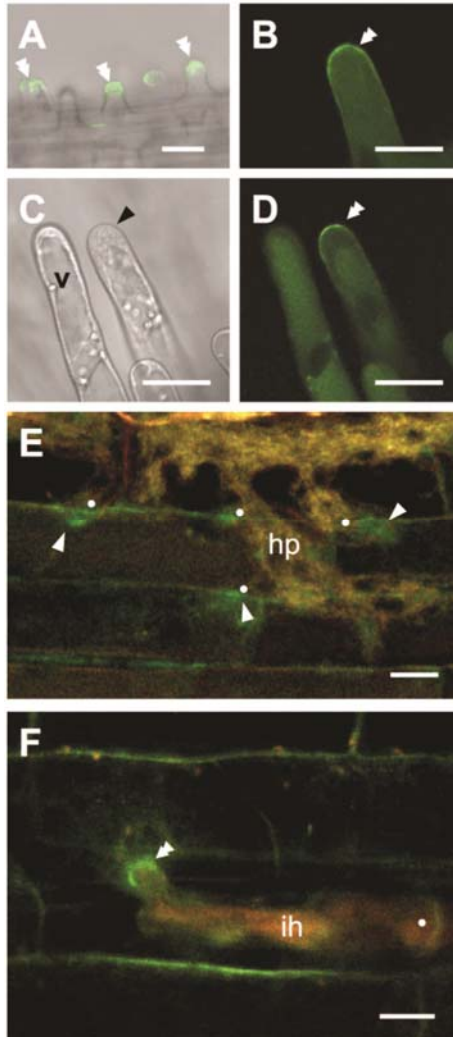

Figure 3. Tagging of exocytotic sites with GFP:EXO84b in *D. carota* and *M. truncatula*. (*A* and *B*) The expression of GFP:EXO84b in control roots of carrot clearly labeled the tips of growing root hairs (double arrows). A superimposition of GFP fluorescence and bright-field is presented in A, whereas a higher magnification of the fluorescence image alone is shown in *B*. (*C* and *D*) An analogous pattern was observed in *M. truncatula*. Comparing the bright-field image in C with the fluorescence in *D* shows that the fluorescent signal (double arrow) is restricted to the growing, cytoplasm-rich hair tip (black arrowhead), whereas a nearby vacuolated root hair (v) is unlabeled, indicating that EXO84b is recruited by the secretory machinery of tip growth. (E) In the presence of a *G. gigantea* hyphopodium (hp) a diffuse fluorescence appears in the PPAs (arrowheads), adjacent to the contact sites (●). (*F*) Upon fungal penetration (●), fluorescence concentrates in a crescent-shaped pattern (double arrow) associated with the tip of the intracellular hypha (ih). (Scale bars, 30 mm in A–D, 20 mm in *E* and *F*.)
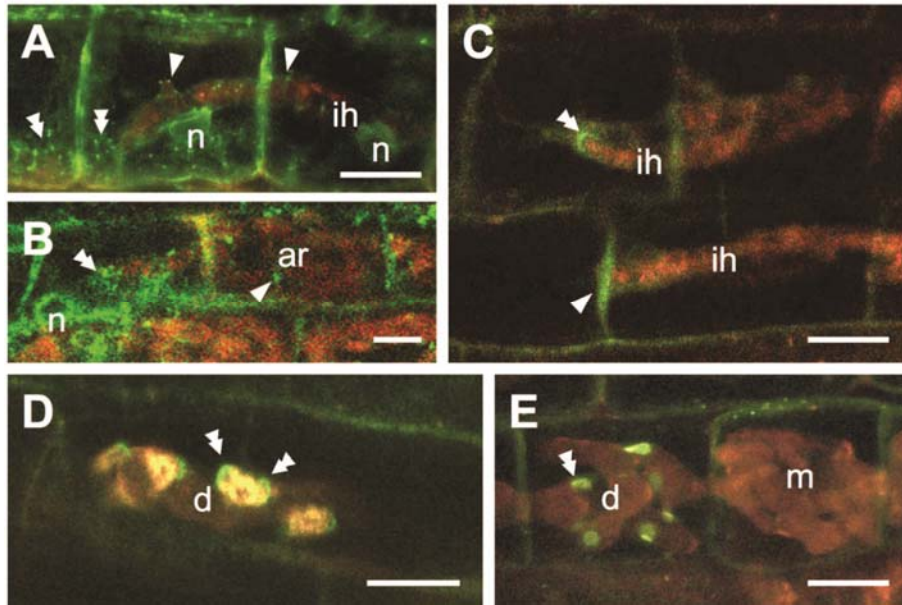
Figure 4. Perifungal membrane biogenesis in the inner cortex of *D. carota* roots. (*A* and *B*) Labeling of the
Golgi apparatus by GFP-MAN. Several Golgi stacks (double arrows) clustered ahead of growing intracellular
hyphae (orange), whereas isolated stacks (arrowheads) distributed along the sides of fully grown intracellular
hyphae (*ih*) and arbuscules (ar). (*C–E*) Similar to what was observed in epidermal cells, GFP-EXO84b labeled
the proliferating perifungal membrane with crescent-shaped patterns (double arrows) associated with the tip of
intracellular hyphae (*C*, *ih*) and developing (*d*) arbuscule branches (*D* and *E*). No signal was associated with
mature arbuscules (*m*), suggesting that the exocyst involvement is limited to the phase of membrane prolifera-
tion. Furthermore, an accumulation of fluorescence was also observed in the sites where hyphae crossed plant
cell walls (*C*, arrowhead), hinting at a possible role for the exocyst complex in the membrane dynamics asso-
ciated with hyphal exit from the host cell. (Scale bars, 20 μm.)

Membrane dynamics in arbuscule development. The small diameter of carrot roots also
allowed the visualization of GFP-MAN and GFP-EXO84b in the root inner tissues. The ac-
cumulation of Golgi stacks that was described during pre-penetration responses in epider-
mal cells was also observed in the inner root cortex of *D. carota*, associated with develop-
ing intracellular hyphae (Fig. 4*A* and *B*). In contrast, cells where an arbusculated coil had
fully developed had a much lower density of labeled Golgi bodies (Fig. 4*B*). A precise la-
beling by GFP-EXO84b was observed only around the tips of developing intracellular hy-
phae (Fig. 4*C*) and branches (Fig. 4*D* and *E*), whereas fully differentiated arbuscules were
not associated with any signal (Fig. 4*E*), indicating the involvement of the exocyst complex
in the proliferation of the periarbuscular membrane. Interestingly, GFP-EXO84b also
marked the sites where a hyphal tip crossed a plant cell wall (Fig. 4*C*), suggesting an addi-
tional role for the exocyst in the fusion between the perifungal membrane and the plas-
malemma upon fungal exit from the cell.

85

Discussion

To investigate the process of perifungal membrane synthesis, we developed ROCs from the legume *M. truncatula* and the non-legume *D. carota*, two established models for the study of AM interactions. The two species give complementary advantages for cell biology investigations: while the large cells of *M. truncatula* can be of help in visualizing the precise subcellular location of the fluorescent constructs, carrot has finer roots which are more amenable to TEM protocols and also allow an easier visualization of the inner root tissues by confocal microscopy.

Although our use of constitutive promoters hampers the direct deduction of a role for the VAMP72 family and exocyst complex in the pre-penetration responses, the fact that all the exocytotic markers that we were able to test were recruited to the fungal penetration site/PPA strongly suggests that this is a major exocytotic event, comparable in intensity with cell plate deposition, apical growth or polarized defense against pathogens.

Furthermore, by labeling functional markers of the exocytotic process such as VAMP72 proteins and the exocyst complex, we were able to visualize indirectly the formation of the perifungal membrane inside the PPA in living root cells. In our observations, in fact, a crescent-shaped structure is constantly observed ahead of the growing intracellular hyphae. This pattern may derive either from the retention of GFP-tagged proteins in the newly formed perifungal membrane (probably due to their overexpression) or from the accumulation of secretory vesicles around the membrane. Combined with fungal autofluorescence, this gave rise to a negative staining for the space comprised between the perifungal membrane and the hypha (interface compartment). We can therefore deduce that the perifungal membrane surrounding the symbiotic interface assembles a short distance ahead of the growing hyphal tip, resembling the development of the IT membrane ahead of the file of rhizobia inside a root hair (Fournier et al., 2008).

Our observations provide direct support for a model of symbiotic interface assembly (Fig. 5), where the required elements of the endomembrane system concentrate at the contact site and along the future route of the intracellular hypha, contributing to the PPA aggregate; vesicle fusion on the plasma membrane facing the penetration site is then proposed to initiate the inward membrane proliferation that associates with fungal penetration and is maintained during the subsequent intracellular hyphal growth.

Perifungal membrane biogenesis in AMs as an exocytotic process. The assembly of an interface compartment, surrounded by a host-derived membrane, is a constant feature in biotrophic interactions. Intracellular extensions of the plasma membrane or large plasmalemma-derived vesicles are found around symbiotic bacteria such as rhizobia (Brewin 2004), endomycorrhizal fungi (Hata *et al.*, 2010) and pathogenic fungi or oomycetes (O'Connell and Panstruga, 2006). Increasing evidence indicates that the *de novo* synthesis of such biotrophic interfaces derives from focal targeting of secretory vesicles (Takemoto *et al.*, 2003, Micali *et al.*, 2010), although this may give rise to membrane protrusions either around the neck (Kankanala *et al.*, 2007) or at the tip of the penetrating hypha (Micali *et al.*, 2011). Generally speaking, biotrophic interfaces are more extended in symbiotic than in pathogenic interactions (An *et al.*, 2006). While the biotrophic growth of filamentous pathogens is often limited to single cells, root infection by nitrogen-fixing bacteria extends
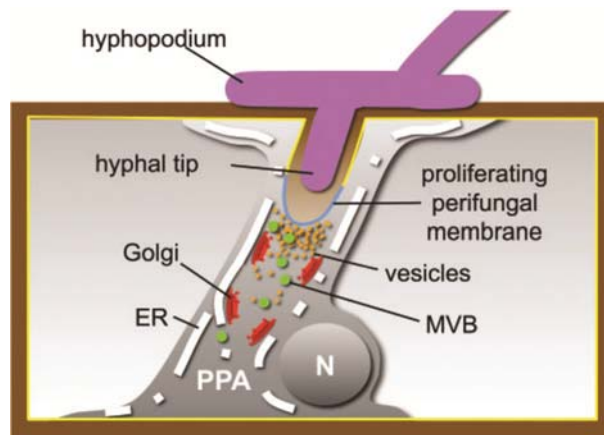
Figure 5. Proposed model of perifungal membrane biogenesis in AMs. The scheme represents intracellular
fungal development in an epidermal cell, reporting the localization of the developing perifungal membrane
and different components of the secretory pathway within the pre-penetration apparatus (PPA). ER, endo-
plasmic reticulum; MVB, multivesicular body; N, nucleus.

throughout the root tissues, with a few similarities to the AM colonization process (Gage,
2004). Rhizobia proceed along the IT, a tubular invagination of the plant plasma membrane
which envelops a filamentous colony of bacteria (Fournier *et al*., 2008). ITs develop from
one cell to the next and can also branch as they cross the root outer and inner cell layers.
Plant cell wall matrix components are found in the IT lumen (Berry *et al*., 2002, Tsyganova
et al., 2009), suggesting that its biogenesis involves exocytosis. Along the same lines, basic
components of the plant cell wall have been localized in the thin space that runs between
the fungal wall and the perifungal membrane (Balestrini and Bonfante, 2005). Taken to-
gether, these features suggest exocytosis to be a central process in interface biogenesis also
for AM interactions.

Our present results provide direct support for this hypothesis indicating an exocyto-
sis-driven proliferation of the perifungal membrane in the vicinity of hyphal tips. We show
that all the elements of the plant secretory pathway accumulate inside the PPA, in strict re-
lation to the process of cell entry by the AM fungus. The ER cisternae expand and Golgi
apparatus activity concentrates in the cytoplasmic aggregate that marks the intracellular
fungal route. Three v-SNARE proteins of the VAMP72 family and a component of the exo-
cyst concentrate in the PPA cytoplasm, indicating this as a site of intense exocytosis, as
previously shown in the case of growing pollen tube tips (Hala *et al*., 2008, Fendrych *et al*.,
2010). Although possibly deriving from the artificial overexpression of the constructs, and
even if we could not discriminate between the direct labeling of the membrane or just the
adjacent secretory vesicles, both VAMP72 and exocyst constructs allowed the visualization
of the perifungal membrane proliferation process in vivo, showing that this takes place
ahead of penetrating and intracellularly growing hyphal tips.

Involvement of the secretory pathway in AM interactions. The reorganization of the Golgi apparatus in arbusculated cells has already been observed by Pumplin and Harrison (2009). Their description of clustered Golgi bodies around the branches of active arbuscules resembles our observations of Golgi stack distribution around intracellular hyphae and young arbuscules, while we did not observe as many Golgi bodies around the mature arbusculated coils of carrot. This suggests that the high dynamicity of the Golgi apparatus may in fact result in different pictures when single snapshots of the organization of a cell are recorded, which was the case for both investigations: while Pumplin and Harrison (2009) have analyzed sectioned samples, we were observing untouched, living roots, but the intensity of the laser radiation required for recording a single z-axis series quickly exhausted the GFP fluorescence, hampering adequate time-lapse acquisitions. Furthermore, it is possible that the terminal arbuscules of *M. truncatula* observed by Pumplin and Harrison (2009) and the intercalary arbusculated coils of carrot that we show in the present study undergo slightly different developmental processes. It has to be noted anyway that the density of Golgi stacks was much higher in the PPA-related cytoplasmic aggregates than in the cytoplasm from any of the colonized cells. This hints at a major role for the Golgi apparatus in the pre-penetration response, with particular reference to the development of the interface matrix and membrane.

Interestingly, frequent passages and relative immobility of the Golgi bodies have been reported in pathogen-induced cytoplasmic aggregations, such as those that *Arabidopsis* epidermal cells develop in response to *Peronospora parasitica* attacks (Takemoto *et al*., 2003). The same authors report the proliferation of ER cisternae in the same area, and we have shown (Genre *et al*., 2009) that ER accumulation in *M. truncatula*, in response to mycorrhizal but also to biotrophic and necrotrophic pathogenic fungi, depends on the functionality of DMI3, a central element of the SYM pathway that also controls *Rhizobium* colonization in legumes. Furthermore, Golgi proliferation (Koh *et al*., 2005) and the involvement of some of the v-SNARE proteins that we have analyzed, such as VAMP721a and VAMP721d (Lipka and Panstruga, 2005; Kwon *et al*., 2008a, Kwon *et al*., 2008b, Frei dit Frey and Robatzek, 2009), have been described in *Arabidopsis* responses to powdery mildews. Similarly, exocyst subunits have been shown to be involved in plant pathogenic interactions (Chong *et al*., 2009, Pecenkova *et al*., 2011).

On the one hand, these results suggest that–at least on a mechanistic basis–some of the plant cell responses to pathogenic and symbiotic microbes can be compared. Both types of interactions activate the secretory pathway and focus it at the contact/penetration site. On the other hand, such comparable secretory mechanisms obviously deliver different combinations of materials to the apoplast. Both responses lead to the deposition of new cell wall components, but at least in the case of incompatible pathogenic interactions, such molecules (which include suberin, lignins and similar resistant polymers) are firstly reinforcing the wall to build a physical barrier against invasion (O'Connell and Panstruga, 2006). In contrast, in the case of symbionts, the soft newly laid cell wall constitutes the niche where the microorganism is going to develop (Genre and Bonfante, 2005). The fact that defense-related compounds are not reported to be released in the presence of AM fungi and rhizobia seems to support this hypothesis, indicating a markedly differential use of the secretory machinery by the plant cell, depending on the nature of the interacting microbe.

The sustained membrane flux required for perifungal membrane proliferation in AMs is not unidirectional. The frequent observation of late endosomes in TEM images of the PPA (as shown in Fig. 2*K*) suggest, on the one hand, that the punctate bodies labeled by the VAMP constructs could indeed be endosomes, probably involved in the recycling of the v-SNAREs back from the plasma membrane. On the other hand, such observations confirm the simultaneous presence of exo- and endocytosis, an acknowledged feature common to all major secretory events.

Besides the recycling of surplus membrane, endosomes can be directly involved in signaling (Geldner and Robatzek, 2008). This possibility is particularly intriguing in AM interactions, where a lot of attention is currently being focused on the signaling molecules (Maillet *et al*., 2011) and signal transduction mechanisms (Chabaud *et al*., 2011) that mediate fungal recognition by the host plant. Although the study of signal exchange within the interface remains at present out of our reach, it will be important to investigate whether pre-symbiotic signaling in the rhizosphere and post-contact interface biogenesis are mediated by the same mechanisms. In this respect, evidence is emerging of a role for AM fungal effector proteins (Kloppholtz *et al*., 2011), similar to what occurs in pathogenic interactions, and important clues about their delivery to the plant cell can come from the comparison of membrane dynamics before and after fungal contact.

Materials and Methods

Construct integration in *A. rhizogenes*. All of the constructs used for this study were GFP fusions expressed in plants under the constitutive promoters *35S* from Cauliflower mosaic virus (*35S*CaMV) or *Arabidopsis Ubiquitin3* (*UBQ*). To visualize the ER (Haseloff *et al*., 1997), the GFP was fused to the signal peptide HDEL, causing the chimeric protein to accumulate inside the ER lumen. Transformed ROCs expressing this construct were already available and had been used for previous studies (Genre et al. 2008). In GFP-MAN the GFP is fused to the a-1,2 mannosidase I gene. Since the encoded protein accumulates in *cis*-Golgi cisternae, this construct was used to visualize Golgi stacks inside the plant cytoplasm (Nebenfuhr et al. 1999). In this case, competent *A. rhizogenes* cells (strain Ar1193) were transfected by electroporation according to Dower *et al*. (1988) with a suspension of pBIN20 vector carrying the GFP:MAN construct (kindly provided by Andreas Nebenfuhr, University of Colorado, USA). The GFP-EXO84b construct is a fusion of GFP with the EXO84b component of the exocyst, a protein complex made up of at least eight subunits, which is involved in tethering secretory vesicles to their target membranes during polar exocytosis (Fendrych *et al*., 2010). The construct, inserted in a pK7FWG2 vector, was introduced into Ar1193 *A. rhizogenes* by electroporation. In GFP-VAMP721a, GFP:VAMP721d and GFP:VAMP721e the GFP is fused to the coding sequences of three different VAMP family members and those were expressed under the *Arabidopsis UBQ3* promoter.

Plant and fungal materials. *Medicago truncatula* genotype Jemalong A17 and the horticultural *D. carota* var. *sativus* were used in this study. *Agrobacterium rhizogenes*-transformed ROCs expressing the different GFP constructs were obtained according to Boisson-Dernier *et al*. (2001) for *M. truncatula* and according to Becard and Fortin (1988)

for carrot. Transformed roots with a high level of fluorescence were selected 21 d after in-oculation, decontaminated and subcultured on M medium at 25ºC in the dark for subsequent use as ROCs. GFP-MAN was only expressed in carrot, the three VAMP72 constructs were expressed in *M. truncatula*, while GFP:EXO84b lines were produced in both plants.

The AM fungus used in this study was *G. gigantea* isolate HC/FE30 (Herbarium Cryptogamicum Fungi, University of Torino, Italy), which is characterized by a strong cytoplasmic autofluorescence (Sejalon-Delmas *et al*. 1998).

To obtain mycorrhizal interactions in vitro, spores were pre-germinated, placed in Petri dishes with fresh root cultures and covered with 25 mm Lumox film (Dutscher SAS), as described in Genre *et al*. (2008). *Medicago* truncatula ROCs were grown in vertically oriented Petri dishes to favor the development of a regular fishbone-shaped root system (Chabaud *et al*., 2002). The non-gravitropic carrot ROCs were initially grown horizontally and then switched to vertical growth following fungal inoculation in order to facilitate hyphal targeting of young lateral roots. Petri dishes were visually screened to detect highly ramifying hyphae and root–fungus contacts, which were then examined by confocal and electron microscopy.

Confocal microscopy. A Leica TCS-SP2 confocal microscope was used for all the experiments described in this work. GFP fluorescence was excited using the 488 nm line of the argon laser and recorded at 500–525 nm. Gigaspora gigantea autofluorescence was excited with the same laser band and acquired at 570–700 nm. A scanning resolution of $1,024 \times 1,024$ pixels was chosen and serial optical sections were acquired with 1 or 2 mm resolution along the z-axis. Bright-field images were acquired simultaneously using the transmission detector of the microscope. For each transformed line, a minimum of 10 independent roots was examined. In all cases the living roots were observed untouched, using the Lumix film as a coverslip, inside the Petri dish into which the roots were grown, taking advantage of a long-distance ×40 water immersion objective (Leica HCX Apo 0.80). In the case of the GFP:MAN lines, Golgi stack movements were recorded by time-lapse acquisitions at 1.6 s intervals for 2 min, using the same imaging conditions.

Electron microscopy. Samples for TEM were processed as described in Genre *et al*. (2008). Briefly, root segments were fixed in 2% glutaraldehyde, post-fixed in 1% OsO4, stained with aqueous 0.5% uranyl acetate and then dehydrated in an ascending series of ethanol to 100% followed by absolute acetone. Samples were then infiltrated in Epon–Araldite (Hoch, 1986) resin and flat-embedded (Howard and O'Donnell, 1987). The resin was polymerized for 24 h at 60ºC. Embedded samples were processed for ultramicrotomy: semi-thin sections (0.5 mm) were stained with 1% toluidine blue, and ultra-thin (70 nm) sections were counter-stained with uranyl acetate and lead citrate (Reynolds, 1963). These were used for TEM analyses under a Philips CM10 transmission electron microscope.

References

An Q, Huckelhoven R, Kogel KH, van Bel AJE (2006). Multivesicular bodies participate in a cell wall-associated defence response in barley leaves attacked by the pathogenic powdery mildew fungus. *Cell Microbiol* **8**:1009–1019.

Balestrini R, Bonfante P (2005). The interface compartment in arbuscular mycorrhizae: a special type of plant cell wall? *Plant Biosyst* **139**:8–15.

Becard G, Fortin JA (1988). Early events of vesicular-arbuscular mycorrhiza formation on Ri T-DNA transformed roots. *New Phytol* **108**:211–218.

Berry AM, Rasmussen U, Bateman K, Huss-Danell K, Lindwalland S, Bergman B (2002). Arabinogalactan proteins are expressed at the symbiotic interface in root nodules of Alnus spp. *New Phytol* **155**:469–479.

Boisson-Dernier A, Chabaud M, Garcia F, Becard G, Rosenberg C, Barker DG (2001). Agrobacterium rhizogenes-transformed roots of *Medicago* truncatula for the study of nitrogen-fixing and endomycorrhizal symbiotic associations. *Mol Plant-Microbe Interact* **14**:695–700.

Bonfante P, Genre A (2008). Plants and arbuscular mycorrhizal fungi: an evolutionary–developmental perspective. *Trends Plant Sci* **13**:492–498.

Brewin NJ (2004). Plant cell wall remodelling in the *Rhizobium*–legume symbiosis. *Crit Rev Plant Sci* **23**:293–316.

Brunger AT (2006). Structure and function of SNARE and SNARE-interacting proteins. Q Rev Biophys **38**:1–47.

Chabaud M, Venard C, Defaux-Petras A, Becard G, Barker D (2002). Targeted inoculation of *Medicago* truncatula in vitro root cultures reveals MtENOD11 expression during early stages of infection by arbuscular mycorrhizal fungi. *New Phytol* **156**:265–273.

Chabaud M, Genre A, Sieberer BJ, Faccio A, Fournier J, Novero M et al. (2011). Arbuscular michorrizal hyphopodia and germinated spore exudates trigger Ca2+ spiking in the legume and nonlegume root epidermis. *New Phytol* **189**:347–355.

Chong YT, Gidda SK, Sanford C, Parkinson J, Mullen RT, Goring DR (2009). Characterization of the *Arabidopsis* thaliana exocyst complex gene families by phylogenetic, expression profiling, and subcellular localization studies. *New Phytol* **185**:401–419.

Dower WJ, Miller JF, Ragsdale CW (1988). High efficiency transformation of *E. coli* by high voltage electroporation. *Nucleic Acids Res* **16**:6127–6145.

Fendrych M, Synek L, Pecenkova T, Toupalova H, Cole R, Drdova E, Nebesárová J, Sedinová M, Hála M, Fowler JE, Zársky V (2010) The *Arabidopsis* exocyst complex is involved in cytokinesis and cell plate maturation. *Plant Cell* **22**:3053–3065.

Fournier J, Timmers AC, Sieberer BJ, Jauneau A, Chabaud M, Barker DG (2008). Mechanism of infection thread elongation in root hairs of *Medicago truncatula* and dynamic interplay with associated rhizobial colonization. *Plant Physiol* **148**:1985–1995.

Frei dit Frey N, Robatzek S (2009). Trafficking vesicles: pro or contra pathogens? *Plant Biol* **12**:437–443.

Gage DJ (2004). Infection and invasion of roots by symbiotic, nitrogen-fixing Rhizobia during nodulation of temperate legumes. *Microbiol Mol Biol Rev* **68**:280–300.

Geldner N, Robatzek S (2008). Plant receptors go endosomal: a moving view on signal transduction. *Plant Physiol* **147**:1565–1574.

Genre A, Bonfante P (2010). The making of symbiotic cells in arbuscular mycorrhizal roots. In Arbuscular Mycorrhizas: Physiology and Function, 2nd edn. Edited by Koltai, H. and Kapulnik, Y. pp. 57–71. Springer, Dordrecht, The Netherlands.

Genre A, Chabaud M, Faccio A, Barker DG, Bonfante P (2008) Prepenetration apparatus assembly precedes and predicts the colonization patterns of arbuscular mycorrhizal fungi within the root cortex of both *Medicago truncatula* and *Daucus carota*. *Plant Cell* **20**:1407–1420.

Genre A, Chabaud M, Timmers T, Bonfante P, Barker DG (2005). Arbuscular mycorrhizal fungi elicit a novel intracellular apparatus in *Medicago truncatula* root epidermal cells before infection. *Plant Cell* **17**:3489–3499.

Genre A, Ortu G, Bertoldo C, Martino E, Bonfante P (2009). Biotic and abiotic stimulation of root epidermal cells revealsncommon and specific responses to arbuscular mycorrhizal fungi. *Plant Physiol* **149**:1424–1434.

Guo W, Grant A, Novick P (1999). Exo84p is an exocyst protein essential for secretion. *J Biol Chem* **274**:23558–23564.

Hala M, Cole R, Synek L, Drdova E, Pecenkova T, Nordheim A, Lamkemeyer T, Madlung J, Hochhold-inger F, Fowler JE, Zársky V (2008). An exocyst complex functions in plant cell growth in arabidopsis and tobacco. *Plant Cell* **20**:1330–1345.

Haseloff J, Siemering KR, Prasher DC, Hodge S (1997). Removal of a cryptic intron and subcellular localization of green fluorescent protein are required to mark transgenic *Arabidopsis* plants brightly. *Proc Natl Acad Sci U S A* **94**:2122–2127.

Hata S, Kobae Y, Banba M (2010). Interactions between plants and arbuscular mycorrhizal fungi. *Int Rev Cell Mol Biol* **281**:1–48.

Hoch HC (1986). Freeze-substitution of fungi. In Ultrastructure Techniques of Microorganisms. Edited by Aldrich, H.C. and Todd, W.J. pp. 183–211. Plenum Press, New York.

Howard RJ, O'Donnell KL (1987). Freeze substitution of fungi for cytological analysis. *Exp Mycol* **11**:250–269.

Kankanala P, Czymmek K, Valent B (2007) Roles for rice membrane dynamics and plasmodesmata during biotrophic invasion by the blast fungus. *Plant Cell* **19**:706–724.

Kloppholz S, Kuhn H, Requena N (2011) A secreted fungal effector of glomus intraradices promotes symbiotic biotrophy. *Curr Biol* **21**:1204–1209.

Koh S, Andre A, Edwards H, Ehrhardt D, Somerville S (2005). *Arabidopsis thaliana* subcellular responses to compatible Erysiphe cichoracearum infections. *Plant J* **44**:516–529.

Kwon C, Bednarek P, Schulze-Lefert P (2008b). Secretory pathways in plant immune responses. *Plant Physiol* **147**:1575–1583.

Kwon C, Neu C, Pajonk S, Yun HS, Lipka U, Humphry M, Bau S, Straus M, Kwaaitaal M, Rampelt H, El Kasmi F, Jürgens G, Parker J, Panstruga R, Lipka V, Schulze-Lefert P (2008). Co-option of a default secretory pathway for plant immune responses. *Nature* **451**:835-840.

Lipka V, Panstruga R (2005). Dynamic cellular responses in plant–microbe interactions. *Curr Opin Plant Biol* **8**:625–631.

Maillet F, Poinsot V, André O, Puech-Pagès V, Haouy A, Gueunier M, Cromer L, Giraudet D, Formey D, Niebel A, Martinez EA, Driguez H, Bécard G, Dénarié J (2011). Fungal lipochitooligosaccharide symbiotic signals in arbuscular mycorrhiza. *Nature* **469**:58-63.

Micali CO, Neumann U, Grunewald D, Panstruga R, O'Connell R (2011). Biogenesis of a specialized plant–fungal interface during host cell internalization of Golovinomyces orontii haustoria. *Cell Microbiol* **13**:210–226.

Nebenfuhr A, Gallagher LA, Dunahay TG, Frohlick JA, Mazurkiewicz AM, Meehl JB, Staehelin LA (1999). Stop-and-go movements of the plant Golgi stacks are mediated by the acto-myosin system. *Plant Physiol* **121**:1127–1141.

O'Connell RJ, Panstruga R. (2006) Teˆte aˋ teˆte inside a plant cell: establishing compatibility between plants and biotrophic fungi and oomycetes. *New Phytol* **171**:699–718.

Oldroyd G, Downie A (2006). Nuclear calcium changes at the core of symbiosis signaling. *Curr Opin Plant Biol* **9**:351–357.

Parniske M (2008). Arbuscular mycorrhiza: the mother of plant root endosymbioses. *Nat Rev Microbiol* **6**:763–775.

Pecenkova T, Hala M, Kulich I, Kocourkova D, Drdova E, Fendrych M, Toupalová H, Zársky V (2011). The role for the exocyst complex subunits Exo70B2 and Exo70H1 in the plant–pathogen interaction. *J Exp Bot* **62**:2107–2016.

Pumplin N, Harrison MJ (2009). Live-cell imaging reveals periarbuscular membrane domains and organelle location in *Medicago truncatula* roots during arbuscular mycorrhizal symbiosis. *Plant Physiol* **151**:809–819.

Redecker D, Kodner R, Graham LE (2000). Glomalean fungi from the Ordovician. *Science* **289**:1920–1921.

Reynolds EW (1963). The use of lead citrate at high pH as an electron opaque stain in electron microscopy. *J Cell Biol* **17**:208–212.

Sanderfoot A (2007) Increases in the number of SNARE genes parallels the rise of multicellularity among the green plants. *Plant Physiol* **144**:6–17.

Sejalon-Delmas N, Magnier A, Douds DD, Becard G (1998). Cytoplasmic autofluorescence of an arbuscular mycorrhizal fungus *Gigaspora gigantea* and nondestructive fungal observations in planta. *Mycologia* **90**:921–926.

Smith SE, Read DJ (2008). Mycorrhizal Symbiosis. Academic Press, New York.

Takemoto D, Jones DA, Hardham AR (2003). GFP-tagging of cell components reveals the dynamics of subcellular re-organization in response to infection of *Arabidopsis* by oomycete pathogens. *Plant J* **33**:775–792.

Tsyganova AV, Tsyganov VE, Findlay KC, Borisov AY, Tikhonovich IA, Brewin NJ (2009). Distribution of legume arabinogalactan protein-extensin (AGPE) glycoproteins in symbiotically defective pea mutants with abnormal infection threads. *Cell Tissue Biol* **3**:93–102.
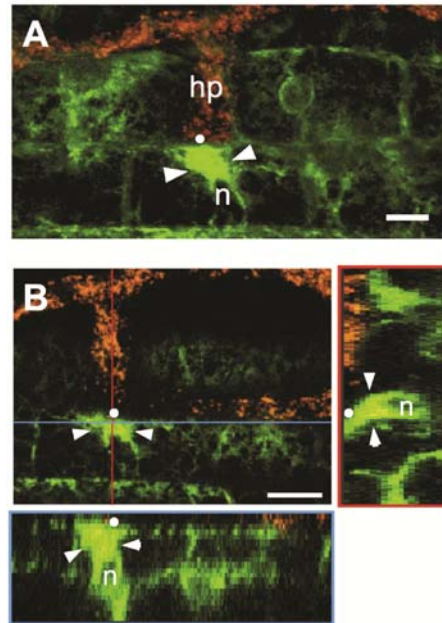
Supporting Information

Figure S1. Orthogonal sectioning of a PPA labeled with GFP-HDEL. The outline of a fully developed PPA (arrowheads) is presented in *A* by labeling the ER with GFP-HDEL. This top view confocal projection shows an epidermal cell of *D. carota* contacted by a hyphopodium (*hp*) of *G. gigantea*. GFP fluorescence (green) highlights the accumulation of ER cisternae in the cytoplasmic aggregation that lays between the nucleus (*n*) and the hyphopodium contact point (•). Fungal cytoplasmic autofluorescence is visualized in orange. (*B*) shows three orthogonal sections cut through a different epidermal cell displaying a fully developed PPA (arrowheads) extending from the nucleus (*n*) to the contact site (•) with the hyphopodium. (Scale bars, 20μm.)
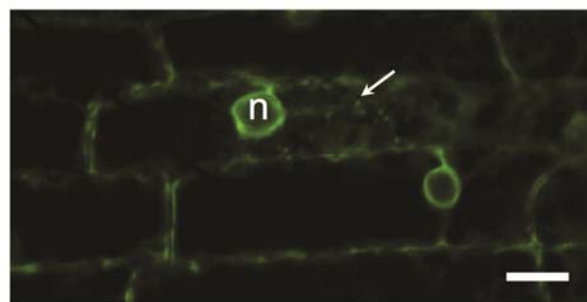
Figure S2. Golgi stack dynamics in epidermal cells from an uninfected carrot root. Image averaging displays green halos where the GFP-MAN fluorescence has been recorded more often during the observation time. The brightest areas correspond to the perinuclear cytoplasm (*n*). Isolated dots can also be seen (arrow), corresponding to single stacks. Their weaker brightness when compared to those observed inside the PPA (see Fig. 1) is related to their shorter permanence in fixed positions. (Scale bar, 20μm.)
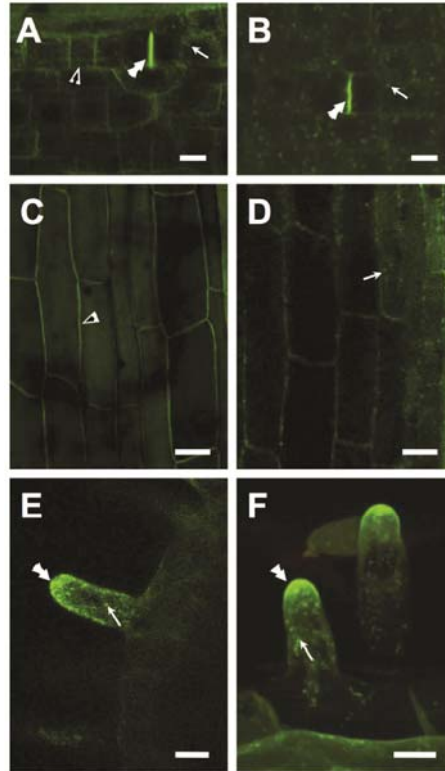
Figure S3. Subcellular localization of GFP-VAMP721a and GFP-VAMP721d constructs in uninfected roots of *D. carota*. (*A,* and *B*) In the meristem, both GFP-VAMP721a (*A*) and GFP-VAMP721d (*B*) labeled the newly laid-down cell walls (double arrows). A weak signal along the plasma membrane was only observed with GFP-VAMP721a (black arrow). (*C* and *D*) The plasma membrane labeling (black arrow) extended to the differentiated epidermis in GFP-VAMP721a lines (*C*) and was absent in roots expressing GFP:VAMP721b (*D*). (*E* and *F*) In trichoblasts, both GFP-VAMP721a (*E*) and GFP:VAMP721d (*F*) labeled the tips of growing root hairs (double arrows). Moving punctate bodies in the cytoplasm (arrows) were often observed with both constructs. (Scale bars, 20μm.)

Chapter 5

Concluding remarks

Sergey Ivanov and Ton Bisseling

Symbiosome development; morphology

In legume root nodule cells rhizobia are hosted in membrane compartments made by the plant. This membrane compartment, containing one or a few rhizobia, is named symbiosome (SB). This is a transient organelle that fixes nitrogen. In this thesis I studied the identity of the SB from the time of its formation, which is release from the infection thread, to development into the functional N_2-fixing organelle. As a final step, I studied SB degradation which occurs when host cells become senescent. These studies have been performed on *Medicago truncatula* (*Medicago*). This model legume plant forms indeterminate root nodules, which, due to the continuous activity of their apical meristem, have a gradient of developmental stages; from the meristem to root attachment point. This forms the basis to divide the nodule in subsequent zones (Fig. 1A) with the meristem at the most distal position. Adjacent to the meristem is the infection zone. In this zone SBs are formed, divide, enlarge and differentiate. In the fixation zone the SBs are fully differentiated and fix nitrogen. Subsequently, they are degraded in the most proximal zone that is named zone of senescence.

SBs are formed by release of bacteria from infection threads (IT) in the first and second cell layer of the infection zone. There unwalled droplets are formed on IT, which are patches that lack a cell wall, and subsequently SBs are pinched of from these droplets (Fig. 1A). The SBs first divide and subsequently differentiate into enlarged SBs (Fig. 1A). The transition from infection zone to fixation zone is characterized by major morphological and developmental changes in SBs and infected cells. This is the place where the rhizobial nitrogenase complex (*nif*) genes are switched on and sudden accumulation of starch indicates a major change in host metabolism (Vasse *et al*., 1990; Yang *et al*., 1991; de Maagd *et al*., 1994). Also changes in permeability of SB and bacteroid membrane reflect major changes in SB physiology (Mergaert *et al*., 2005, Oldroyd *et al*., 2011). In addition, SBs become spatially ordered in comparison to the rather random distribution in the infection zone (Fedorova *et al*., 2007; Whitehead *et al*., 1998).

So at the transition from infection to fixation zone the SBs become N_2-fixing "organelles". During several cell layers in the nitrogen fixation zone the SBs remain functional, but finally, in the zone of senescence the SBs are turned into lytic compartments that fuse with each other and the vacuole. In this way rhizobia are killed and digested and their components are recycled by the host (Fig. 1A). The occurrence of all these developmental zones in a *Medicago* root nodule allows studies on all steps of SB development from bacterial release of infection threads until SB degradation in longitudinal nodule sections (Fig. 1A).

Symbiosome development; identity markers

We have studied the identity of the SB membrane from release of SBs from infection thread till their termination during senescence. To do this we made use of identity markers of endocytotic and exocytotic pathways. These identity markers are proteins involved in vesicle fusion and specific sets of them are present on different membrane compartments (Uemura *et al*., 2004, Bassham and Blatt, 2007). These identity markers are small Rab GTPases and SNARE proteins which prime and execute fusion of membranes, respectively. Rab GTPases act as switches by cycling between a guanosine triphosphate (GTP)- ("switch on") and a guanosine diphosphate (GDP)-bound ("switch off") form (Barnekow *et al*., 2009). SNARE proteins work in a complex where one SNARE protein is located on the transport
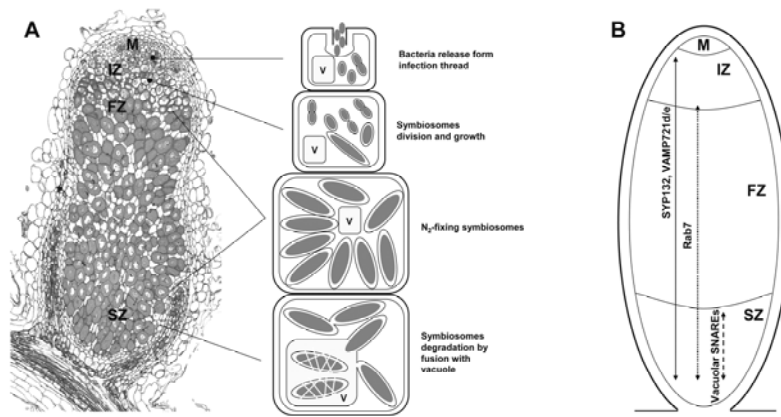
Figure 1. Zonation of *Medicago* root nodules (*A*). Longitudinal section through a *Medicago* nodule. The apical meristem (*M*) constantly provides new cells to the nodule tissues. In the infection zone (*IZ*) bacteria are released from infection threads forming SBs which divide, grow and differentiate into N_2-fixing organelle-like structures. The switch from IZ to fixation zone (*FZ*) occurs when the SBs first express the *nif* genes and their subcellular location becomes highly ordered. After several days of fixation SB undergo degradation by fusing with each other and plant vacuoles (*v*) in senescence zone (*SZ*). (*B*). Schematic representation of the occurrence of membrane identity markers on SB membranes. Plasma membrane localized SNARE proteins SYP132 and VAMP721d/e are present on SBs from release till the senescence. GTPase Rab7 appeared on SB membrane when SB are fully developed and start to fix nitrogen. It is present on SB membranes within the fixation zone and zone of senescence. The vacuolar SNAREs appear on SB membranes at the onset of senescence.

vesicle (v-SNARE), which pairs with three SNARE proteins that reside on the target membrane (t-SNARE). Formation of this complex of four SNARE proteins brings the two membranes close to each other and allows them to fuse (Lang and John, 2008) (Fig. 2; Table 1). We have studied the occurrence of these identity markers on SBs during all steps of development; from the release of bacterial from infection thread, until SB degradation (Fig. 1B).

The release of SBs from infection threads resembles, at a cytological level, an endocytotic process or phagocytosis as occurring in animal cells. The latter is a specific form of endocytosis. Therefore release of SBs has often been described as an endocytotic-like process (Verma, 1992; Brewin, 2004; Parniske 2000). For this reason we studied whether membrane identity markers of endocytic compartments occur on SBs. However, neither unwalled droplets nor young SBs do ever contain t-SNARE MtSYP4 (identity marker of early endosomes) or MtRab5 (identity marker of late endosomes). Therefore it seems highly unlikely that the release of SBs is derived from endocytosis, despite the cytological similarity.

In contrast to the absence of endocytotic identity markers, *Medicago* SYP132 appears to be present on SBs from release up to senescence (Fig. 1B). MtSYP132 is a plasma
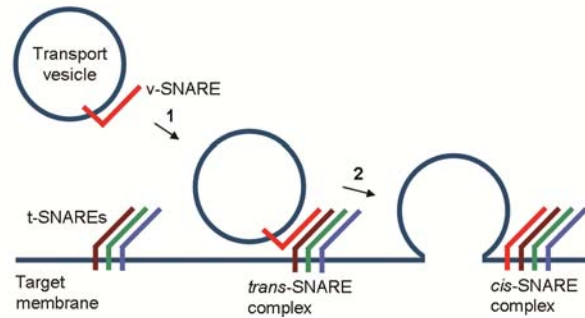
Figure 2. Schematic representation of SNARE protein complex formation. A typical SNARE complex involves three distinct types of SNARE proteins residing on the target membrane (t-SNAREs) and one SNARE protein located on the transport vesicle (v-SNARE). *1*. Transport vesicles in close vicinity to their target membrane bind to it by a tethering complex (not shown). This allows the specific recognition of the v-SNARE by its partners in the target membrane by which a *trans*-SNARE complex is formed. *2*. Conformational changes in the *trans*-SNARE complex bring the two membranes close to each other and provide energy for their fusion. After fusion all parts of SNARE complex are localised on target membrane forming *cis*-SNARE complex. *cis*-SNARE complex is rapidly disassembled by the action of effector proteins and v-SNAREs leave target membrane and are ready for next round of fusion.

membrane located t-SNARE and it is involved in secretory pathways (Sanderfoot, 2007, Kalde *et al*., 2007). The occurrence of this protein during release and further steps of SB development suggested that exocytosis derived mechanisms control release and development of SBs. This conclusion is strongly supported by our studies on v-SNAREs. We showed in chapter three that a specific exocytotic pathway is required for the formation of unwalled droplets, the release of bacteria and probably also further development of SBs. This exocytotic pathway is controlled by two members of the VAMP72 family. This is a family of v-SNAREs involved in exocytosis. We found that two out of five highly homologous MtVAMP721s are specifically required for symbiosis. MtVAMP721d and MtVAMP721e are essential for unwalled droplet formation and bacteria release, whereas RNAi of these two VAMP72s has only a mild effect on root growth and nodule formation. The involvement of a specific exocytotic pathway allows formation of a membrane compartment and a symbiotic interface with new properties that facilitate the N_2-fixing symbiosis.

After their development, SBs are maintained as N_2-fixing organelles. Small GTPase Rab7 which is a molecular marker of late endosomes/vacuoles appears on SBs when they start to fix nitrogen (Fig. 1B). It is present on SB membranes within the fixation zone and zone of senescence. In non-symbiotic cells Rab7 activates the assembly of a vacuolar SNARE complex (Epp *et al*., 2011). This SNARE complex normally assembles on the tonoplast and is involved in the fusion of vesicles with the tonoplast as well as in the homotypic fusion of small vacuoles. However, SBs do not fuse with vacuoles during their maintenance as N_2-fixing organelle. Therefore, we studied the occurrence of vacuolar SNAREs on SBs and showed in chapter two that t-SNAREs (MtSYP22, MtVTI11) are not present on

Table 1. SNARE proteins on different plant membrane compartments

Membrane compartment	t-SNARE	v-SNARE
ER/Golgi	SYP81, SEC20, USE1	SEC22
cis-Golgi	SYP31/32, MEMB1, BET1	SEC22
trans-Golgi	SYP31/32, GOS1, SFT1	SEC22
trans-Golgi network/Early endosome	SYP41/42*, SYP61, VTI12	YKT61, VAMP727
Late Endosome/Vacuole	SYP21/22*, SYP51/52, VTI11*	VAMP711
Storage Vacuole	SYP21/22*, SYP51/52, VTI11*	VAMP727
Plasma Membrane	SYP121/122, SYP131/132*, SNAP33	VAMP721/722, VAMP724*; MtVAMP721a/d/e*
Cell Plate	SYP111/112, NPSN1, SYP71	VAMP721/722; MtVAMP721d/e*

* Medicago SNAREs used in this thesis

functional SBs. They appear on SB membranes only at the onset of senescence (Fig. 1B). As a result it may promote homotypic fusion of SBs and fusion with vacuoles during senescence. Hence, by recruiting Rab7 on the SB membrane, the host cell may obtain very good control over the fate of SBs and prime them for termination by fast assembly of vacuolar SNARE complexes and fusion with vacuole. This is important in case of unfavorable environmental conditions (*e.g.* drought, dark stress, low soil oxygen level, *etc*.) since in this way the host avoids loss of valuable photosynthates. As it is a process that is controlled by the host we prefer to name it controlled termination of symbiosis to distinguish it from senescence which occurs due to aging of cells.

Thus, using plant cell membrane identity markers, we were able to obtain first insight in endomembrane pathways that are involved in SB formation, development, maintenance and senescence.

DNF1 is involved in an exocytotic-like process controlling symbiosome differentiation

The involvement of exocytosis in formation of SB is further underlined by the role of DNF1. *DNF1* (*defective in nitrogen fixation*) encodes a nodule specific variant of a subunit of the signal peptidase complex (Wang *et al.*, 2010). This complex locates in endoplasmic reticulum (ER) and cleaves off ER targeting signal peptides of nascent secreted polypeptides before being transported in vesicles to the plasma membrane. In *dnf1* nodules rhizobia are released from infection thread and the SBs are able to divide, but, in contrast to *wt* nodules, bacteroids are not enlarged. DNF1 appears to be essential for the processing of secreted nodule-specific cysteine-rich (NCR) peptides. Van de Velde and co-authors showed that NCRs are transported to the SBs and regulate differentiation of rhizobia in these enlarged bacteroids (Van de Velde *et al.*, 2010). In *dnf1* NCRs are not targeted to the SBs, but retain in the ER as unprocessed polypeptides. The studies with *dnf1* underline the im-

portance of exocytotic processes in SB development. Since VAMP721s act at the last step of an exocytotic pathway (fusion of transport vesicles with target membrane) it is tempting to speculate that DNF1 and MtVAMP721d/e are active in the same pathway and MtVAMP721d/e vesicles possibly deliver processed NCRs to SB s. Thus, our findings that MtSYP132 and MtVAMP721d/e are essential for SB formation and development as well as the *dnf1* study suggest that SB is an apoplastic compartment.

Symbiosome nature: apoplast versus vacuole

In contrast to our studies that point to an apoplastic nature of the SBs, several rather old studies pointed to a vacuolar identity of the SBs. Such view on SB identity is based on biochemical observation that indicated that the (peribacteroid) space between bacteroid and SB membrane has an acidic nature and contains several proteins typically found in vacuoles, namely; proteases, acid trehalase, alpha-mannosidase isoenzyme II and a protein protease inhibitor (Whitehead and Day, 1997). The vacuolar proteins were identified in SBs isolated from mature soybean nodules. It is probable that in such nodules senescence has already started in some cells. We showed in *Medicago* that these senescing SBs are turned into lytic compartments and vacuolar protein will very likely accumulate in these SBs. We assume that the vacuolar proteins identified in soybean SB isolates are the result of "contaminating" senescing SBs. In these senescing SBs these vacuolar proteins have a clear function while this is not the case in N_2-fixing SBs.

One of the major arguments that SBs have a vacuolar nature is relied on the presumed acidic nature of the peribacteroid space (Udvardi *et al*., 1991). However, direct pH measurements by confocal microscopy using a pH sensitive fluorescent dye (neutral red) shows that the peribacteroid space is non acidic (Alexandr Gavrin, Elena Fedorova, personal communication).

Our studies using membrane identity markers of tonoplast (vacuolar SNAREs) provided a more direct way to show that during its formation, development and functioning as an N-fixing organelle, SBs do not have a vacuolar identity. This conclusion finds additional support in a study using the tonoplast aquaporin (γ-TIP) from *Arabidopsis*. When expressed in *Medicago* nodules, it does not localize on SB membrane (Limpens *et al*., 2009), whereas it is present on tonoplasts of infected cells.

So taken together our studies on membrane identity markers strongly support the conclusion that SBs have an apoplastic rather than vacuole-like nature.

Nod factor signaling and symbiosome formation

The *Rhizobium*-legume symbiosis is initiated by specific lipochito-oligosaccharides (LCOs) that are secreted by *Rhizobium* and are called Nod factors. Perception of Nod factors and the subsequent activation of the signal transduction mechanism have been best studied in Nod factor induced responses in the root epidermis and the formation of nodule primordia in the root cortex. Upon Nod factor perception a signal transduction cascade is activated in the epidermis which initiates several cellular responses such as Ca^{2+} spiking, expression of specific genes, root hair deformation and curling and infection thread formation. Furthermore, Nod factor perception at the epidermis results most likely in cytokinin production that subsequently causes cell division in the cortex leading to the formation of root nodule primordia (Oldroyd and Downie, 2008; op den Camp *et al*., 2011). In short, the Nod factor

signaling cascade involves the following components: Nod factors are recognized by specific LysM domain receptor-like kinases. In *Medicago*, these are NFP and LYK3 that are located in the plasma membrane. NFP (Nod Factor Perception) is a receptor with low requirement towards Nod factor structure and it is responsible for all Nod factor induced responses including calcium spiking and transcriptional responses (Oldroyd and Downie, 2008). In contrast, LYK3 (LysM motif receptor-like kinase 3) has a high-stringency towards Nod factor structure and mediates bacterial infection (Limpens *et al*., 2003; Smit *et al*., 2007). These two receptors most likely form heterodimers (Madsen *et al*., 2011). Therefore it is probable that another LysM receptor is involved, together with NFP, in triggering responses like calcium oscillations. The Nod factor signaling cascade that is activated involves SymRK, a plasma membrane located leucine-rich repeat receptor-like kinase (DMI2 in *Medicago*) and an ion channel located at the nuclear envelope (DMI1). Perception of the calcium oscillations involves CCamK, a nuclear Ca^{2+} and calmodulin (CaM)-dependent kinase (DMI3) and a protein interacting with CCamK (IPD3). Downstream of CCamK and IPD3 there are several transcription factors that regulate Nod factor-induced gene expression (Kouchi *et al*., 2010; Oldroyd *et al*., 2011).

Although the role of the Nod factor signaling pathway in epidermis and cortical responses has been studied most frequently, several components of this signaling pathway are also shown to be important for bacterial release and SB formation in legume root nodules. These are SymRK, CCamK and IPD3 (Capoen *et al*., 2005; Limpens *et al*., 2005; Godfroy *et al*., 2006, Horvath *et al*., 2011; Ovchinnikova *et al*., 2011). Loss-of-function mutations in SymRK and CCamK cause a block of all Nod factor induced responses. However, when SymRK was specifically knocked–down in nodules or when a rice CCamK ortholog was introduced into *Medicago dmi3* mutant, its role in SB formation was revealed. Nodules with many infection threads were formed on such plants. However, bacterial release from these infection threads into nodule cells was blocked (Capoen *et al*., 2005; Limpens *et al*., 2005; Godfroy *et al*., 2006). Further support for a function of Nod factor signaling in SB formation came from studies on *ipd3* mutants. In *Medicago*, knock-out mutations in IPD3 lead to formation of small nodules which contain numerous infection threads. However, release from these infection threads is blocked. These data underline the importance of the signaling module DMI2-DMI3-IPD3 in SB formation.

I hypothesize that this module is activated upon Nod factor perception in the nodule. This hypothesis is consistent with the fact that the rhizobial genes essential for Nod factor production are active in the nodule (Schlaman *et al*., 1991; Walker and Downie, 2000; Den Herder *et al*., 2007) and also the Nod factor receptor genes are active in the apex of the nodule (Limpens *et al*., 2005; Mbenque *et al*., 2010). This hypothesis implies that Nod factor perception and signal transduction can (directly) induce cell biological processes that are essential for intracellular accommodation of rhizobium. Support for this hypothesis has recently been obtained by studies on evolution of Nod factor signaling.

Evolutionary origin of Nod factor signaling

A clue concerning the evolutionary origin of the Nod factor signaling cascade came from studies that showed that the DMI module is also required for establishing the endosymbiosis with arbuscule mycorrizal (AM) fungi. Therefore, they are named common symbiotic genes and the encoded proteins form the common symbiotic signaling pathway. This gave

rise to the hypothesis that *Rhizobium*-legume symbiosis recruited part of the signaling pathway from the far more ancient AM symbiosis (Kouchi *et al*., 2010). However, loss-of-function mutations in Nod factor receptors do not affect mycorrhization in model legumes (Madsen *et al*., 2003; Radutoiu *et al*., 2003). This led to the hypothesis that in legumes different receptors trigger this common signaling pathway in the two symbiotic interactions. However, two recent breakthrough studies strongly suggest that Nod factor receptors evolved from ancestral Myc factor receptors. It was shown that AM fungi produce LCOs very similar in structure to Nod factors and plants treated with these LCOs are better colonized by AM fungi (Maillet *et al*., 2011). Strong support that Nod factor receptors evolved from a Myc factor receptor came from studies on *Parasponia*. This is the only non-legume genus that also is able to establish a *Rhizobium*-nodule symbiosis. It evolved this symbiosis independently from legumes. As it evolved more recently it can provide insight in how the *Rhizobium* symbiosis evolved. In legumes *NFP* is part of a small gene family. However, *Parasponia* only has a single *NFP* like gene. Knock-down of *Parasponia NFP* blocks the intracellular accommodation of both rhizobia and AM fungi. It suggests that during evolution *Rhizobium* acquired the ability to produce LCOs that resemble Myc factors and in this way became able to activate the same signaling cascade as AM fungi. So, it is very intriguing how rhizobia acquired the ability to produce Nod factors. Genes encoding Nod factor synthesis (Nod genes) are located on symbiotic plasmids or gene islands in the genome and have a different evolutionary history in comparison to the rest of the genome (Cough and Cullimore, 2011; Masson-Boivin *et al*., 2009) This strongly suggests that they have been acquired by horizontal transfer. However, their origin remains elusive as genes similar to bacterial Nod genes are not found in transcriptome data of AM fungi (Tisserant *et al*., 2011). So, the mycorrhizal signaling perception mechanism, including LCO receptor, has been co-opted during evolution to facilitate *Rhizobium* Nod factor signaling (op den Camp *et al*., 2011; Streng *et al*., 2011).

Most important for the work described in this thesis is that the formation of the symbiotic interface is blocked when expression of *Parasponia NFP* was knocked down. In *Parasponia* rhizobia enter root nodule cells by cell wall bound infection threads. However, in contrast to *Medicago*, bacteria are not released into nodule cells. Instead, bacteria are able to fix N_2 within highly branched threads, called fixation threads. These fixation threads remain attached to the infection thread. In contrast to SBs fixation threads are bound by a cell wall. This wall is markedly thinner than that of infection thread and so also in this case the formation of a symbiotic interface most likely involves a switch to a different exocytotic pathway. Therefore, fixation thread and SB formation most likely involve similar mechanisms. In *Parasponia* transgenic roots with a reduced level of *NFP* expression, infection threads successfully invade root nodule cells, but fixation threads are not formed. Also arbuscule formation is blocked in these roots. Arbuscules are formed when AM fungal hypha enter a cortical cell. First it forms a cell wall bound trunk. This trunk forms several major branches which subsequently branch in multiple fine branches. These fine branches are surrounded by a host (periarbuscular) membrane but are not bound by a cell wall. Knock down of *Parasponia NFP* resulted in a block of the formation of fine branches but trunk formation, like infection thread formation, is not affected. Therefore I postulate that the rhizobial Nod factors activate the same signaling cascade as LCOs of AM fungi and in both

cases a similar exocytotic process that controls the formation of a symbiotic interface, is activated.

Molecular mechanisms linking LCO signaling and symbiosome (arbuscule) formation

I showed in chapter three that *Rhizobium* and AM fungi symbioses exploit the same host cellular mechanisms to form the symbiotic interface. Similar to knock-down of *Parasponia* NFP the post-transcriptional silencing of *MtVAMP721d* and *MtVAMP721e* blocks not only rhizobial release from infection threads and SB formation, but also the formation of fine arbuscule branches (Chapter 3) supporting the hypothesis that similar cell biological mechanisms are induced in intracellular accommodation of both microsymbionts. Is the LCO signaling pathway able to trigger these cellular mechanisms? In this thesis it is shown that MtVAMP721d and MtVAMP721e especially accumulate in cells where arbuscules or SBs are formed (Chapter 3). However, it is also shown that there are no significant changes in the level of *MtVAMP721d* and *MtVAMP721e* mRNA during symbiotic membrane formation in both symbioses. Therefore, post-translational regulation of *MtVAMP721d* and *MtVAMP721e* appears to play a crucial role. A similar regulation of VAMP72 accumulation seems to occur in the interaction of plants and biotrophic pathogenic fungi. *Arabidopsis* homologs of MtVAMP721d/e (AtVAMP721 and AtVAMP722) focally accumulate beneath the site of fungal penetration into leaf epidermal cells (Kwon *et al*., 2008). Furthermore, the AtSYP121 (PEN1) which is a t-SNARE complex partner of AtVAMP721 and AtVAMP722 (Kwon *et al*., 2008) (Table 1) forms plasma membrane microdomain beneath the penetration site. Such accumulation of both components of a SNARE complex is not controlled at the gene expression level and therefore also seems to involve post transcriptional regulation (Bhat *et al*., 2005; Kwon *et al*., 2008). Therefore, I postulate that LCO signaling regulates targeting of MtVAMP721d and MtVAMP721e at a post-translational level. How such post-translational regulation can be achieved by Nod factor signaling? The SNARE complex activity is regulated either by direct modification of its components (phosphorylation, palmitoylation) or by specific molecular regulators that alter SNARE-SNARE interactions (Snyder *et al*., 2006). Phosphorylation plays an important role in regulation of SNARE complex stability enhancing or repressing interaction between its components. Sites for such modification have been discovered in all members of SNARE complex in animals and plants (Snyder *et al*., 2006, Nuhse *et al*., 2003). One of the Nod factor receptors (in *Medicago* LYK3) as well as DMI2 (SymRK) have a cytoplasmic kinase domain which potentially is able to phosphorylate SNAREs located on the plasma membrane as well as on transport vesicles (VAMP72). In *Arabidopsis* plasma membrane syntaxin SYP122 was reported to be rapidly phosphorylated in response to the bacterial elicitor flagellin (Nuhse *et al*., 2003) and phosphorylation of SYP121 (PEN1) is needed for full disease resistance activity against biotrophic pathogenic fungi (Pajonk *et al*., 2008). Flagellin is recognized by the plasma membrane located leucine rich repeat receptor-like kinase FLS2 which similar to LYK3 and DMI2 has a cytosolic kinase domain. However, SYP122 is phosphorylated by a cytosolic calcium-dependent kinase activity (Nuhse *et al*., 2003). Perception of flagellin triggers the influx of Ca^{2+} that activates calcium dependent protein kinases (Segonzac and Zipfel, 2011) which promote flg22-regulated phosphorylation of SNAREs. Similarly, Nod factors and diffusible AM fungal signals also induce rapid influx

of Ca^{2+} (Felle *et al*., 1998; Navazio *et al*., 2007). Thus, phosphorylation of SNARE complexes in response to LCO signaling is well possible. However, whether this is indeed the case and whether it results in accumulation of MtVAM72d/e vesicles remains to be demonstrated.

In addition to phosphorylation of SNAREs, Nod factor signaling might transcriptionally activate genes encoding specific molecular regulators which alter SNARE-SNARE interactions. This can cause the targeting and accumulation of MtVAMP721d/e at sites where the symbiotic interface is formed. Nod factor signaling activates the nuclear located kinase CCamK that interacts with IPD3. The CCamK-IPD3 complex is thought to activate transcription factors (Oldroyd *et al*., 2011). The importance of transcriptional regulation induced by this complex is demonstrated by studies on an *ipd3* mutant. In *ipd3* nodules several genes that are induced at an early stage of development are not activated (Ovchinnikova *et al*., 2011). Among these is an interesting candidate namely the nodule specific remorin gene *MtSYMREM1* (Ovchinnikova *et al*., 2011). This gene is of specific interest as a loss of function mutation causes a phenotype that is similar to that of *MtVAMP721d/e* knock-down nodules; infection threads are formed but release from these infection threads is blocked. Further MtSYMREM1 is located at sites that could be unwalled droplets (Lefebvre *et al*., 2010), so the target site of the MtVAMP72d/e vesicles. Remorins are exclusively detected in sterol- and sphingolipid-enriched domains of the plasma membrane commonly referred to as lipid rafts (Mongrand et al., 2010). In focal exocytosis, lipid rafts accumulate t-SNAREs (Puri and Roche, 2006; Tsai *et al*., 2007) and such a SNARE-lipid raft association is essential for spatial control of exocytosis and/or regulation of SNARE functioning (Tsai *et al*., 2007). The plasma membrane microdomains of AtSYP121 (see above) can be stained with the fluorescent dye filipin which is used to visualize lipid rafts (Bhat *et al*., 2005). Therefore, it is tempting to speculate that Nod factor signaling triggered expression of *MtSYMREM1* specifically induces accumulation of t-SNARE partners of MtVAMP721d/e, for example MtSYP132, and by this focally targets the MtVAMP72d/e secretory pathway to unwalled droplets to induce bacteria release.

Do MtVAMP721d/e have a function at early stages of the AM fungal symbiosis?

The accumulation and focal targeting of SNAREs in plant-pathogenic fungi interaction is part of a complex process that results in the formation of a so-called cytoplasmic aggregation (CA) This is a cytoskeleton driven accumulation of organelles, including the plant nucleus, ER, Golgi apparatus and membrane vesicles at the penetration site (Hardham *et al*., 2007). Similarly, *Medicago* root epidermal cells respond to AM fungi at the sites where AM fungi form appresoria like structures, hyphopodia, with the formation of a CA-like structure (Genre *et al*., 2005; Genre and Bonfante, 2007). However, in AM symbiosis a column of cytoplasm that completely traverses the host cell is formed. This structure is named the pre-penetration apparatus (PPA) and when the fungus enters the cell at this site a perifungal membrane is formed around it by the host. Subsequently, hyphae colonize *Medicago* roots by intercellular infection, but a PPA is also created in inner cortex cells where arbuscules are formed (Genre *et al*., 2008). In chapter four we showed by over-expression of MtVAMP721d and MtVAMP721e fused to GFP that MtVAMP721d/e accumulate at the contact site with hyphopodia and in the perifungal membrane formation. This suggests that

MtVAMP721d/e are also important for intra-cellular infection at early stages of the interaction. Their targeting might be controlled by LCO signaling as PPA formation is impaired in *dmi2* and *dmi3* mutants (Genre *et al.*, 2005; 2009). However, knock-down of *MtVAMP721d* and *MtVAMP721e* does not block trans-cellular fungal penetration of the root at early stages nor during arbuscular trunk formation in cells where arbuscules are formed (Chapter 3). So these studies do not support a role of the MtVAMP72d/e at early stages of the interaction of AM fungi and plants. This also holds for the *Rhizobium-Medicago* interaction as knock-down of *MtVAMP721d* and *MtVAMP721e* has no effect on infection thread formation. Therefore, we can not exclude that the accumulation of MtVAMP721d/e GFP fusions at perifungal membranes is the result of expression driven by a strong heterologous promoter. Alternatively at early stages other MtVAMP72 members might be functionally redundant with MtVAMP721d/e. The latter is supported by the observation that also MtVAMP721a accumulates at the site of perifungal membrane formation.

Thus, to determine whether and which MtVAMP72 members play a role at early stages of the AM fungal and *Rhizobium* symbiosis additional experiments are required. The use of native promoters and double and triple knock-down of different MtVAMP721 will help to dissect their role in early steps of infection.

Conclusion

The finding that *Rhizobium* symbiosis has co-opted the signaling mechanism as well as cellular mechanism from AM fungi symbiosis to facilitate an intracellular life style, has major implications for strategies to transfer the nodule symbiosis to non-legume crops. This is a "dream" that is already about a century old (Streng *et al.*, 2011). The AM fungal symbiosis is far more ancient than the rhizobial symbiosis. It is also wide spread in the plant kingdom and almost 80% of plant species can establish an AM symbiosis. This implies that plants which are able to interact with AM fungi contain in principle the genes that are necessary for the intracellular accommodation of *Rhizobium*. So the question is no longer why the *Rhizobium*-legume symbiosis is specific for legumes, but why non-legumes are not yet able to establish this symbiosis?

References

Barnekow A, Thyrock A, Kessler D (2009). Rab proteins and their interaction partners. *Int Rev Cell Mol Biol* **274**:235-74.

Bassham DC, Blatt MR (2008). SNAREs: Cogs and coordinators in signaling and Development. *Plant Physiol* **147**:1504–1515.

Bhat RA, Miklis M, Schmelzer E, Schulze-Lefert P, Panstruga R (2005). Recruitment and interaction dynamics of plant penetration resistance components in a plasma membrane microdomain. *Proc Natl Acad Sci U S A* **102**:3135-3140.

Brewin NJ (2004). Plant cell wall remodelling in the *Rhizobium*-legume symbiosis. *Critical Rev Plant Sci* **23**:293-316.

Capoen W, Goormachtig S, Rycke RD, Schroeyers K, Holsters M (2005). SrSymRK, a plant receptor essential for symbiosome formation. *Proc Natl Acad Sci USA* **102**:10369-10374.

de Maagd RA, YangW-C, Goosen-de Roo L, Mulders IHM, Roest HP, Spaink HP, Bisseling T, Lugtenberg BJJ (1994). Down-regulation of expression of the *Rhizobium leguminosarum* outer membrane protein gene *ropA* occurs abruptly in interzone II-III of pea nodules and can be uncoupled from *nif* gene activation. *Mol Plant Microb Interact* **7**:276-281.

Den Herder J, Vanhee C, De Rycke R, Corich V, Holsters M, Goormachtig S (2007). Nod factor perception during infection thread growth fine-tunes nodulation. *Mol Plant Microbe Interact* **20**:129-137.

Epp N, Rethmeier R, Krämer L, Ungermann C (2011). Membrane dynamics and fusion at late endosomes and vacuoles-Rab regulation, multisubunit tethering complexes and SNAREs. *Eur J Cell Biol* 90:779-85.

Fedorova EE, de Felipe MR, Pueyo JJ, Lucas MM (2007). Conformation of cytoskeletal elements during the division of infected *Lupinus albus* L. nodule cells. *J Exp Bot* **58**:2225-2236.

Felle HH, Kondorosi E, Kondorosi A, Schultze M (1998). The role of ion fluxes in Nod factor signaling in *Medicago sativa. Plant J* **13**:455-463.

Fournier J, Timmers AC, Sieberer BJ, Jauneau A, Chabaud M, Barker DG (2008). Mechanism of infection thread elongation in root hairs of *Medicago truncatula* and dynamic interplay with associated rhizobial colonization. *Plant Physiol* **148**:1985-1995.

Genre A, **Bonfante P** (2007). Check-in procedures for plant cell entry by biotrophic microbes. *Mol Plant Microbe Interact* 20:1023-1030.

Genre A, Chabaud M, Faccio A, Barker DG, Bonfante P (2008). Prepenetration apparatus assembly precedes and predicts the colonization patterns of arbuscular mycorrhizal fungi within the root cortex of both *Medicago truncatula* and *Daucus carota. Plant Cell* **20**:1407-1420.

Genre A, Chabaud M, Timmers T, Bonfante P, Barker DG (2005). Arbuscular mycorrhizal fungi elicit a novel intracellular apparatus in *Medicago truncatula* root epidermal cells before infection. *Plant Cell* **17**:3489-3499.

Genre A, Ortu G, Bertoldo C, Martino E, Bonfante P (2009). Biotic and abiotic stimulation of root epidermal cells reveals common and specific responses to arbuscular mycorrhizal fungi. *Plant Physiol* **149**:1424-1434.

Godfroy O, Debellé F, Timmers T, Rosenberg C (2006). A rice calcium- and calmodulin-dependent protein kinase restores nodulation to a legume mutant. *Mol Plant Microbe Interact* **19**:495-501.

Gough C, Cullimore J (2011). Lipo-chitooligosaccharide signaling in endosymbiotic plant-microbe interactions. *Mol Plant Microbe Interact* **24**:867-878.

Hardham AR, Jones DA, Takemoto D (2007). Cytoskeleton and cell wall function in penetration resistance. *Curr Opin Plant Biol* **10**:342-348.

Horváth B, Yeun LH, Domonkos A, Halász G, Gobbato E, Ayaydin F, Miró K, Hirsch S, Sun J, Tadege M, Ratet P, Mysore KS, Ané JM, Oldroyd GE, Kaló P (2011). *Medicago* truncatula IPD3 is a member of the common symbiotic signaling pathway required for rhizobial and mycorrhizal symbioses. *Mol Plant Microbe Interact* **24**:1345-1358.

Kalde M, Nühse TS, Findlay K, Peck SC (2007). The syntaxin SYP132 contributes to plant resistance against bacteria and secretion of pathogenesis-related protein 1. *Proc Natl Acad Sci USA* **104**:11850-11855.

Kouchi H, Imaizumi-Anraku H, Hayashi M, Hakoyama T, Nakagawa T, Umehara Y, Suganuma N, Kawaguchi M (2010). How many peas in a pod? Legume genes responsible for mutualistic symbioses underground. *Plant Cell Physiol* **51**:1381-1397.

Kwon C, Neu C, Pajonk S, Yun HS, Lipka U, Humphry M, Bau S, Straus M, Kwaaitaal M, Rampelt H, El Kasmi F, Jürgens G, Parker J, Panstruga R, Lipka V, Schulze-Lefert P (2008). Co-option of a default secretory pathway for plant immune responses. *Nature* **451**:835-840.

Lang T, **Jahn** R (2008). Core proteins of the secretory machinery. *Handb Exp Pharmacol*. 184:107-127.

Lefebvre B, Timmers T, Mbengue M, Moreau S, Hervé C, Tóth K, Bittencourt-Silvestre J, Klaus D, Deslandes L, Godiard L, Murray JD, Udvardi MK, Raffaele S, Mongrand S, Cullimore J, Gamas P, Niebel A, Ott T (2010). A remorin protein interacts with symbiotic receptors and regulates bacterial infection. *Proc Natl Acad Sci USA* **107**:2343-2348.

Limpens E, Franken C, Smit P, Willemse J, Bisseling T, Geurts R (2003). LysM domain receptor kinases regulating rhizobial Nod factor-induced infection. *Science* **302**:630-633.

Limpens E, Ivanov S, van Esse W, Voets G, Fedorova E, Bisseling T (2009). *Medicago* N2-fixing symbiosomes acquire the endocytic identity marker Rab7 but delay the acquisition of vacuolar identity. *Plant Cell* **21**:2811-2828.

Limpens E, Mirabella R, Fedorova E, Franken C, Franssen H, Bisseling T, Geurts R (2005). Formation of organelle-like N2-fixing symbiosomes in legume root nodules is controlled by DMI2. *Proc Natl Acad Sci USA* **102**:10375-10380.

Madsen EB, **Antolín-Llovera M**, **Grossmann C**, **Ye J**, **Vieweg S**, **Broghammer A**, **Krusell L**, **Radutoiu S**, **Jensen ON**, **Stougaard J**, **Parniske M** (2011). Autophosphorylation is essential for the in vivo function of the *Lotus japonicus* Nod factor receptor 1 and receptor-mediated signalling in cooperation with Nod factor receptor 5. *Plant J* 65:404-417

Madsen EB, Madsen LH, Radutoiu S, Olbryt M, Rakwalska M, Szczyglowski K, Sato S, Kaneko T, Tabata S, Sandal N, Stougaard J (2003). A receptor kinase gene of the LysM type is involved in legume perception of rhizobial signals. *Nature* **425**:637-640.

Maillet F, Poinsot V, André O, Puech-Pagès V, Haouy A, Gueunier M, Cromer L, Giraudet D, Formey D, Niebel A, Martinez EA, Driguez H, Bécard G, Dénarié J (2011). Fungal lipochitooligosaccharide symbiotic signals in arbuscular mycorrhiza. *Nature* **469**:58-63.

Masson-Boivin C, Giraud E, Perret X, Batut J. (2009). Establishing nitrogen-fixing symbiosis with legumes: how many *Rhizobium* recipes? *Trends Microbiol* **17**:458-466.

Mbengue M, Camut S, de Carvalho-Niebel F, Deslandes L, Froidure S, Klaus-Heisen D, Moreau S, Rivas S, Timmers T, Hervé C, Cullimore J, Lefebvre B (2010). The *Medicago truncatula* E3 ubiquitin ligase PUB1 interacts with the LYK3 symbiotic receptor and negatively regulates infection and nodulation. *Plant Cell* 22:3474-3488.

Mergaert P, Uchiumi T, Alunni B, Evanno G, Cheron A, Catrice O, Mausset AE, Barloy-Hubler F, Galibert F, Kondorosi A, Kondorosi E (2006). Eukaryotic control on bacterial cell cycle and differentiation in the *Rhizobium*-legume symbiosis. *Proc Natl Acad Sci U S A* 103:5230-5235.

Mongrand S, Stanislas T, Bayer EM, Lherminier J, Simon-Plas F (2010). Membrane rafts in plant cells. *Trends Plant Sci* **15**:656-63.

Oldroyd GE, Murray JD, Poole PS, Downie JA (2011). The rules of engagement in the legume-rhizobial symbiosis. *Annu Rev Genet* **45**:119-144.

Oldroyd GED, Downie JA (2008). Coordinating nodule morphogenesis with rhizobial infection in legumes. *Annu Rev Plant Biol* **58**:519-546.

Op den Camp R, Streng A, De Mita S, Cao Q, Polone E, Liu W, Ammiraju JS, Kudrna D, Wing R, Untergasser A, Bisseling T, Geurts R (2011). LysM-type mycorrhizal receptor recruited for *Rhizobium* symbiosis in nonlegume *Parasponia*. *Science* **331**:909-912.

Op den Camp R, Streng A, De Mita S, Cao Q, Polone E, Liu W, Ammiraju JS, Kudrna D, Wing R, Untergasser A, Bisseling T, Geurts R (2011). LysM-type mycorrhizal receptor recruited for *Rhizobium* symbiosis in nonlegume *Parasponia*. *Science* **331**:909-912.

Ovchinnikova E, Journet EP, Chabaud M, Cosson V, Ratet P, Duc G, Fedorova E, Liu W, den Camp RO, Zhukov V, Tikhonovich I, Borisov A, Bisseling T, Limpens E (2011). IPD3 controls the formation of nitrogen-fixing symbiosomes in pea and *Medicago* Spp. *Mol Plant Microbe Interact* **24**:1333-1344.

Parniske M (2000). Intracellular accommodation of microbes by plants: a common developmental program for symbiosis and disease? *Curr Opin Plant Biol* **3**:320-328.

Puri N, Roche PA (2006). Ternary SNARE complexes are enriched in lipid rafts during mast cell exocytosis. *Traffic* **7**:1482-94.

Radutoiu S, Madsen LH, Madsen EB, Felle HH, Umehara Y, Grønlund M, Sato S, Nakamura Y, Tabata S, Sandal N, Stougaard J (2003). Plant recognition of symbiotic bacteria requires two LysM receptor-like kinases. *Nature* 425:585-592.

Sanderfoot A (2007). Increases in the number of SNARE genes parallels the rise of multicellularity among the green plants. *Plant Physiol* **144**:6-17.

Schlaman HR, Horvath B, Vijgenboom E, Okker RJ, Lugtenberg BJ (1991). Suppression of nodulation gene expression in bacteroids of *Rhizobium leguminosarum* biovar *viciae*. *J Bacteriol* **173**:4277-4287.

Smit P, Limpens E, Geurts R, Fedorova E, Dolgikh E, Gough C, Bisseling T (2007). *Medicago* LYK3, an entry receptor in rhizobial nodulation factor signaling. *Plant Physiol* 145:183-191.

Streng A, op den Camp R, Bisseling T, Geurts R (2011). Evolutionary origin of *Rhizobium* Nod factor signaling. *Plant Signal Behav* **6**:1510-1514.

Tisserant E, Kohler A, Dozolme-Seddas P, Balestrini R, Benabdellah K, Colard A, Croll D, Da Silva C, Gomez SK, Koul R, Ferrol N, Fiorilli V, Formey D, Franken P, Helber N, Hijri M, Lanfranco L, Lindquist E, Liu Y, Malbreil M, Morin E, Poulain J, Shapiro H, van Tuinen D, Waschke A, Azcón-Aguilar C, Bécard G, Bonfante P, Harrison MJ, Küster H, Lammers P, Paszkowski U, Requena N, Rensing SA, Roux C, Sanders IR, Shachar-Hill Y, Tuskan G, Young JP, Gianinazzi-Pearson V, Martin F (2012). The transcriptome of the arbuscular mycorrhizal fungus Glomus intraradices (DAOM 197198) reveals functional tradeoffs in an obligate symbiont. *New Phytol* **193**:755-769.

Tsai PS, De Vries KJ, De Boer-Brouwer M, Garcia-Gil N, Van Gestel RA, Colenbrander B, Gadella BM, Van Haeften T (2007). Syntaxin and VAMP association with lipid rafts depends on cholesterol depletion in capacitating sperm cells. *Mol Membr Biol* **24**:313-24.

Uemura T, Ueda T, Ohniwa RL, Nakano A, Takeyasu K, Sato MH (2004). Systematic analysis of SNARE molecules in *Arabidopsis*: dissection of the post-Golgi network in plant cells. *Cell Struct Func* **29**:49-65.

Van de Velde W, Zehirov G, Szatmari A, Debreczeny M, Ishihara H, Farkas A, Mikulass K, Nagy A, Tiricz H, Satiat-Jeunemaître B, Alunni B, Bourge M, Kucho K, Abe M, Kereszt A, Maroti G, Uchiumi T, Kondorosi E, Mergaert P (2010). Nodule specific peptides govern terminal differentiation of bacteria in symbiosis. *Science* **327**:1122-1126.

Vasse J, **de Billy F**, **Camut S**, **Truchet G** (1990). Correlation between ultrastructural differentiation of bacteroids and nitrogen fixation in alfalfa nodules. *J Bacteriol* 172:4295-4306.

Verma DPS (1992). Signals in root nodule organogenesis and endocytosis of *Rhizobium*. *Plant Cell* 4: 373-382.

Vincent JL, Brewin NJ (2000). Immunolocalization of a cysteine protease in vacuoles, vesicles, and symbiosomes of pea nodule cells. *Plant Physiol* **123**:521-530.

Walker SA, Downie JA (2000). Entry of *Rhizobium leguminosarum* bv. *viciae* into root hairs requires minimal Nod factor specificity, but subsequent infection thread growth requires nodO or nodE. *Mol Plant Microbe Interact* **13**:754-762.

Wang D, Griffitts L, Starker C, Fedorova E, Limpens E, Ivanov S, Bisseling T, Long S (2010). A nodule specific protein secretory pathway required for nitrogen-fixing symbiosis. *Science*, **327**:1126-1129.

Whitehead LF, Day DA (1997). The peribacteroid membrane. *Physiologia Plantarum* **100**:30-44.

Whitehead LF, Day DA, Hardham AR (1998). Cytoskeleton arrays in the cells of soybean root nodules: the role of actin microfilaments in the organisation of symbiosomes. *Protoplasma* 203:194-205.

Yang W-C, Horvath B, Hontelez L, Van Kammen A, Bisseling T (1991). *In situ* localization of *Rhizobium* mRNAs in pea root nodules: *nifA* and *nifH* localization. *Mol Plant Microb Int* **4**:464-468.

Appendices

Summary

In symbiosis of plants and arbuscular mycorrhizal fungi as well as in *Rhizobium*-legume symbiosis the microbes are hosted intracellularly, inside specialized membrane compartments of the host. These membrane compartments are morphologically different but similar in function, since they control the exchange of compounds between host and its microsymbiont thus forming a highly specialized symbiotic interface. These are the arbuscules, containing highly branched fungal hyphae, and organelle-like symbiosomes containing *Rhizobium* bacteria. Recent studies have markedly extended our insight in the evolution of the signaling mechanism underlying the formation of these symbiotic interfaces. These studies strongly suggest that *Rhizobium* co-opted the complete signaling mechanism (including lipo-oligosaccharides signal molecules) from the more ancient arbuscular mycorrhizal fungi symbiosis. Further, in plant species (*Parasponia*) where rhizobium nodulation evolved rather recent and independent from legumes, the same lipo-oligosaccharide receptor is essential for the formation of the rhizobial symbiotic interface as well as arbuscules. Therefore, it seems likely that *Rhizobium* symbiosis also co-opted the cellular mechanism controlling arbuscule formation to form a rhizobial symbiotic interface. This would imply that even after co-evolution in legumes the key regulators involved in the formation of these interfaces are similar or even identical.

In this thesis I have shown that *Rhizobium*-legume symbiosis shares with arbuscular mycorrhizal symbiosis molecular and cell biological mechanisms that control symbiotic interface formation. I identified a plant exocytotic pathway marked by two highly homologous vesicle associated membrane proteins (VAMP) that control the formation of the symbiotic interface in both symbioses. RNAi of these two *Medicago* VAMP genes did not affect non-symbiotic plant development or nodule formation. However, it hampered the formation of cell wall free regions at infection threads, and therefore blocks symbiosome formation. Further arbuscule formation was blocked, whereas root colonization was not affected. By identifying these VAMPs as common symbiotic regulators in secretory vesicle trafficking, we postulated that during evolution of *Rhizobium* symbiosis pre-existing cellular mechanisms of the arbuscular mycorrhizal fungal symbiosis have been co-opted. These finding also revealed a primary role of exocytosis in symbiosome formation. Using identity markers of endocytotic compartments of plant cell (early endosome and late endosome) such as small GTPases belonging to the Rab family and SNARE (*s*oluble *N*-ethylmaleimide sensitive factor *a*ttachment protein *re*ceptor) proteins, I have shown that they never occur on symbiosome membranes at any stage of symbiosome formation and development. This strongly suggests that symbiosome formation is not derived from the endocytotic pathway. Nevertheless, symbiosomes acquire the vacuolar marker Rab7 when they reach an elongated stage. However, vacuolar SNAREs which execute fusion of membranes are not present on functional symbiosomes, but they do appear on symbiosome membranes at the onset of senescence when symbiosomes are turned into a lytic compartment. Therefore, I postulate that the acquisition of Rab7 primes the symbiosomes for degradation by which the host has full control over its microsymbiont. So my studies make untenable long-standing hypothesis that symbiosomes originate from endocytosis-like process and represent endocytic (vacuolar) compartments and instead they show that symbiosomes have an apoplastic nature.

Samenvatting

In sommige symbioses van planten en micro-organismen worden de microben gehuisvest in gespecialiseerde cellen van de gastheer. De twee best bestudeerde zijn de endosymbioses van planten met *Rhizobium* bacteriën respectievelijk arbuscular mycorrhizae (AM) schimmels. In beide gevallen worden de microben gehuisvest binnen in de plantencel, in membraancompartimenten gemaakt door de plant. De membraancompartimenten die de schimmel en bacteriën omgeven zijn morfologisch erg verschillend. Maar de functie is heel vergelijkbaar omdat deze membraan controleert welke componenten tussen de symbionten kunnen worden uitgewisseld. Deze membraan functioneert als een symbiontisch raakvlak die het mogelijk maakt dat de microben in de cel aanwezig kunnen zijn. Bij afwezigheid hiervan wordt de plantencel simpelweg opgegeten.

De interactie van *Rhizobium* bacteriën en vlinderbloemige planten leidt tot de vorming van een nieuw orgaan, de wortelknol, waarvan een speciaal celtype wordt geïnfecteerd door *Rhizobium*. *Rhizobium* vult deze cellen als een organelachtige structuur die symbiosoom worden genoemd. Deze bestaat uit de bacterie omringd door een plantenmembraan. De AM schimmels infecteren bestaande wortelcellen. Hierin maken ze een zeer fijn vertakte structuur, arbuskel genaamd, die omringd wordt door een membraan van de gastheer. In beide symbioses is de vorming van het symbiontisch raakvlak door de gastheer een zeer belangrijke stap. In dit proefschrift is het moleculaire mechanisme dat ten grondslag ligt aan de vorming van deze symbiontische raakvlakken bestudeerd.

Het onderzoek richtte zich eerst op de vorming van symbiosomen. Het proces waarmee de bacteriën worden opgenomen in de plantencel lijkt sterk op een proces dat endocytose wordt genoemd. In dierlijke systemen wordt endocytose b.v. gebruikt om bacteriën op te nemen en te transporteren naar lysosomen, waar de bacterie gedood wordt. Dat de vorming van symbiosomen van endocytose is afgeleid was een zeer algemeen geaccepteerde hypothese.

Plantencellen bevatten zeer verschillende mebraancompartimenten. Om te zorgen dat de juiste vesikel naar het juiste membraancompartiment worden getransporteerd bevatten vesikels en targetmembranen bepaalde eiwitten die als identiteitsmarker functioneren. Zulke identiteitsmarkers maken het ook mogelijk om te bestuderen of symbiosoomvorming is afgeleid van endocytose. Geen van de identiteitsmarkers die vroege stappen van endcytose karakteriseren werden op symbiosomen aangetoond. Hiermee werd bewezen dat symbiosoomvorming niet is ontstaan uit een endocytotisch proces en daarmee werd een lang geaccepteerde hypothese weerlegd.

Door gebruik te maken van identiteitsmarkers die karakteristiek zijn voor exocytose kon worden aangetoond dat een specifieke exocytose pathway is gerekruteerd voor de vorming van symbiosomen. Deze exocytose pathway is niet essentieel voor plantengroei maar wel essentieel voor de vorming van het symbiontisch raakvlak. Door deze pathway uit te schakelen kon worden vastgesteld dat deze pathway ook essentieel is voor de vorming van arbuskels in de AM schimmel symbiose.

De AM schimmel symbiose komt wijd verspreid in het plantenrijk voor. Deze symbiose is 450 miljoen jaar geleden onstaan. Dus nog voordat planten wortels konden vormen. Het succes van deze endosymbiose wordt onderstreept door het feit dat meer dan tachtig procent van de huidige hogere planten deze symbiose hebben behouden. In tegenstelling

hiermee is de *Rhizobium* symbiose veel recenter (60 miljoen jaar) ontstaan. En is deze na-
genoeg specifiek voor vlinderbloemige planten. Op grond hiervan is het dan ook zeer waar-
schijnlijk dat de *Rhizobium* symbiose het mechanisme om een symbiontisch raakvlak te
vormen heeft overgenomen van de veel oudere AM schimmel symbiose. Deze waarneming
sluit nauw aan bij eerdere studies die lieten zien dat het signaal molecuul en de bijbe-
horende herkenning en signalering die o.a. de vorming van het symbiontische raakvlak in-
duceren in beide symbioses identiek of van elkaar afgeleid zijn.

Deze waarnemingen hebben belangrijke implicaties. Het is zeer waarschijnlijk dat
Rhizobium zowel het signaleringsmechanisme als moleculaire mechanisme dat gebruikt
wordt om het symbiontisch raakvlak te vormen gerekruteerd heeft van de veel oudere AM
schimmel symbiose. Aangezien deze symbiose zeer wijd vespreid voorkomt in het planten-
rijk, komen de genen die nodig zijn voor de *Rhizobium* symbiose niet alleen voor bij vlin-
derbloemigen maar zijn ze (latent) aanwezig bij het merendeel van alle hogere planten.
Deze kennis is van grote betekenis bij het ontwikkelen van strategieën om de *Rhizobium*
knol symbiose over te dragen naar niet-vlinderbloemige gewassen.

Acknowledgements

This thesis could not have been completed without the contribution of many people. I would like to thank all people who supported me throughout all this years:

Prof. dr. Ton Bisseling, Dr. Elena Fedorova and Dr. Erik Limpens.
Maria Augustijn and Marie-Jose van Iersel
Dr. Henk Franssen and Dr. Olga Kulikova
Alessandra Lillo and Wei Liu
Yury Tikunov and Olga Zaitseva
Chunting Lang, Aleksandr Gavrin and Vid Karmarkar
Dr. Rene Geurts
Jan Verver, Marijke Hartog and Jan Hontelez
Ting Ting Xiao, Gerben Bijl, Rik op den Camp, Silvester de Nooijer, Stefan Schilderink
Arend Streng, Natalia Savelyeva, Sjef Moling, Evgenia Ovchinnikova, Adam Folta, Timofey Nemankin, Maryam Seifi Kalhor, Trupti Sharma, Rik Huisman
Dr. Stephane De Mita, Dr. Joan Wellink, Dr. Ludmilla Mlynarova
Prof. Dr. Paola Bonfante and Dr. Andrea Genre

Andrius Zukas, Vaida Urbonaite, Maria Lopez Perron and Sergio Oliveira
Sergey Laptenok
IJCU Recreators Utrecht: Richard Willems, Jaap van Breda, Valentin Kuzar, Bob Joosten, Juraj Fabus, Elger Niemendal, Sjors Janssen, Frank Sarfati, Frank Kenter, Marco Bontan, Andres Blijenberg, Daniel Domanovsky, Peter Gdovjak, Judith Risse, Kees Tempelaars, Veronika Strnadova, Robin Booij.

My mother Tatiana Ivanova

Publications

Ivanov S, Fedorova EE, Limpens E, DeMita S, Genre A, Bonfante P, Bisseling T (2012). *Rhizobium*-legume symbiosis shares an exocytotic pathway required for arbuscule formation. *Proc Natl Acad Sci USA* 2012 **109**:8316-8321.

Genre A, Ivanov S, Fendrych M, Faccio A, Zársky V, Bisseling T, Bonfante P (2012). Multiple exocytotic markers accumulate at the sites of perifungal membrane biogenesis in arbuscular mycorrhizas. *Plant Cell Physiol* **53**:244-55.

Liu W, Kohlen W, Lillo A, Op den Camp R, Ivanov S, Hartog M, Limpens E, Jamil M, Smaczniak C, Kaufmann K, Yang WC, Hooiveld GJ, Charnikhova T, Bouwmeester HJ, Bisseling T, Geurts R (2011). Strigolactone biosynthesis in *Medicago truncatula* and rice requires the symbiotic GRAS-type transcription factors NSP1 and NSP2. *Plant Cell* **23**:3853-65.

Humphry M, Reinstadler A, Ivanov S, Bisseling T, Panstruga R (2011) Durable broad spectrum powdery mildew resistance in pea *er1*plants is conferred by natural loss-of-function mutations in *PsMLO1*. *Mol Plant Pathol* **12**:866-78.

Ivanov S, Fedorova E, Bisseling T (2010). Intracellular plant microbe associations: secretory pathways and the formation of perimicrobial compartments. *Curr Opin Plant Biol* **13**:372-7.

Wang D, Griffitts L, Starker C, Fedorova E, Limpens E, Ivanov S, Bisseling T, Long S (2010). A nodule specific protein secretory pathway required for nitrogen-fixing symbiosis. *Science* **327**:1126-9.

Limpens E, Ivanov S, van Esse W, Voets G, Fedorova E, Bisseling T (2009). *Medicago* N2-fixing symbiosomes acquire the endocytic identity marker Rab7 but delay the acquisition of vacuolar identity. *Plant Cell* **21**:2811-2828.

Ksenzenko VN, Ivashina TV, Dubeĭkovskaia ZA, Ivanov SG, Nanazashvili MB, Druzhinina TN, Kalinchuk NA, Shibaev VN (2007). The *pssA* gene encodes UDP-glucose: polyprenyl phosphate-glucosyl phosphotransferase initiating biosynthesis of *Rhizobium leguminosarum* exopolysaccharide. *Bioorgan Chem* (Moscow) **33**:160-166.

Curriculum Vitae

Sergey Ivanov was born on the 9th of September 1980 in Naberezhnye Chelny, a city in the Republic of Tatarstan, USSR. He finished his high school education in 1997. In 1998 he started his five years education in a Faculty of Biology and Agriculture, Elabuga State University, Russia. During this time genetics and molecular biology became his favorite topics. This motivated him to start his work as a research assistant in the Laboratory of Genetics, Kazan State University, Russia where he worked on molecular mechanisms of adaptive mutagenesis of microorganisms. In 2004 he moved further and started his Msc study at RAS Institute of Biochemistry and Physiology of Microorganisms in Puschino State University, Russia. He completed his thesis in the Laboratory of Molecular Microbiology on the multiprotein complex of exopolysaccharide biosynthesis of nitrogen-fixing bacteria *Rhizobium leguminosarum*, supervised by Dr. Tatiana Ivashina. In June 2006 he obtained his Msc degree. During his Msc studies he met Dr. Elena Fedorova from the laboratory of Nitrogen Fixation at the Institute of Plant Physiology in Moscow, Russia. She gave him an opportunity to study as a PhD student in a joint project with the Laboratory of Molecular Biology at Wageningen University, The Netherlands. He started his PhD study in December 2006 under the supervision of promoter Prof. Ton Bisseling and co-promoters Dr. Elena Fedorova and Dr. Erik Limpens. Within his PhD project he studied molecular mechanism of intracellular accommodation of bacteria during *Rhizobium*-legume symbiosis. This work was presented on several national and international conferences and in the form of publicly available publications. In January 2012 he started his post-doctoral research in a group of Dr. Maria Harrison at Boyce Thompson Institute for Plant Research, Cornell University, USA.

Education Statement of the Graduate School

Experimental Plant Sciences

The Graduate School **EXPERIMENTAL PLANT SCIENCES**

Issued to:　Sergey Ivanov
Date:　　　6 September 2012
Group:　　Molecular Biology, Wageningen University & Research Centre

1) Start-up phase	*date*
▶　First presentation of your project	
Symbiosome membrane identity markers	Sep 28, 2007
▶　Writing or rewriting a project proposal	
▶　Writing a review or book chapter	
Ivanov S., Fedorova E., Bisseling T. (2010) Intracellular plant microbe associations: secretory pathways and the formation of perimicrobial compartments. Curr. Op. Plant Biol. 13:372377.	2010
▶　MSc courses	
▶　Laboratory use of isotopes	
Course 'Safe handling with radioactive materials and sources', level 5B	May 26-28, 2009
Subtotal Start-up Phase	*9.0 credits**

2) Scientific Exposure	*date*
▶　EPS PhD student days	
EPS PhD student day, Wageningen	Sep 13, 2007
EPS PhD student day, Leiden	Feb 26, 2009
▶　EPS theme symposia	
EPS theme 1 Symposium 'Plant Developmental Biology', Wageningen	Oct 11, 2007
EPS theme 1 Symposium 'Plant Developmental Biology', Leiden	Jan 30, 2009
EPS theme 1 Symposium 'Plant Developmental Biology', Wageningen	Jan 28, 2010
▶　NWO Lunteren days and other National Platforms	
ALW meeting Experimental Plant Sciences', Lunteren	Apr 02-03, 2007
ALW meeting Experimental Plant Sciences', Lunteren	Apr 07-08, 2008
ALW meeting Experimental Plant Sciences', Lunteren	Apr 19-20, 2010
▶　Seminars (series), workshops and symposia	
European flying seminars (Scott Poethig; Hiroo Fukuda; Richard Vierstra; Simon Gilroy; Zhenbiao Yang)	Sep 2007-Jul 2008
EPS workshop "Plant Endomembranes", Vrije Universiteit Amsterdam, Amsterdam, The Nethrlands	Jul 02, 2010
▶　Seminar plus	
▶　International symposia and congresses	
The Third Baltic Sea Region Symposium and PhD course AGRO-BIOTECHNOLOGY "Applied and fundamental aspects of responsens, signaling and developmental process in the root-microbe systems" St. Petersburg, Russia	Jun 25-Jul 02, 2007
Workshop on Endocytotic System: Mechanism and Function, Villars-sur-Ollon, Switzerland	Sep 18-23, 2007
8th European Nitrogen Fixation conference, Ghent, Belgium	Aug 30-Sep 03, 2008
IS-MPMI 2009. XIV International Congress on Molecular Plant-Microbe Interactions, Quebec City, Canada	Jul 19-23, 2009
International conference of young scientist «The biology - science of 21 century», Pushchino, Russia	2009
2nd joint retreat of PhD students in Plant Science, Cologne, Germany	Apr 15-17, 2010
9th European Nitrogen Fixation Conference, Geneva, Switzerland,	Sep 06-10, 2010
3rd joint retreat of PhD students in Plant Science, Paris, France	Jul 05-08, 2011
▶　Presentations	
Poster: The Third Baltic Sea Region Symposium; "Applied and fundamental aspects of responsens, signaling and developmental process in the root-microbe systems" St. Petersburg, Russia	Jun 25-Jul 02, 2007
Poster: ALW meeting, Lunteren, The Netherlands	Apr 07-08, 2008
Oral: EMBO Practical course: "Cell Biology of Host-Pathogens Interactions", Pasteur Institute, Paris, France	Aug 18-29, 2008
Poster: European Nitrogen Fixation conference, Ghent Belgium	Aug 30-Sep 03, 2008
Poster: IS-MPMI 2009. XIV International Congress on Molecular Plant-Microbe Interactions, Quebec City, Canada	Jul 19-23, 2009
Oral: International conference of young scientist «The biology - science of 21 century», Pushchino, Russia	27 September-2 October 2009
Oral: EPS theme 1 Symposium 'Plant Developmental Biology', Wageningen, The Netherlands	Jan 28, 2010
Oral ALW meeting Experimental Plant Sciences', Lunteren, The Netherlands	Apr 19-20, 2010
Oral: EPS workshop "Plant Endomembranes", Vrije Universiteit Amsterdam, Amsterdam, The Netherlands	Jul 02, 2010
Oral: 9th European Nitrogen Fixation Conference, Geneva, Switzerland	Sep 06-10, 2010
Oral: 3rd joint retriat of PhD students in Plant Science, Paris, France	Jul 05-08, 2011
▶　IAB Interview	Dec 04, 2009
▶　Excursions	
Subtotal Scientific Exposure	*26.4 credits**

3) In-Depth Studies	*date*
▶　EPS courses or other PhD courses	
PhD training course "Bioinformatics - A User's Approach" Wageningen University, Wageningen, The Netherlands	Mar 13-16, 2007
EMBO course: Workshop on Endocytotic System: Mechanism and Function, Villars-sur-Ollon, Switzerland	Sep 18-23, 2007
PhD training course "Metabolomics" Wageningen University, Wageningen, The Netherlands	Jun 06-08, 2007
EMBO Practical course: "Cell Biology of Host-Pathogens Interactions", Pasteur Institute, Paris, France	Aug 18-29, 2008
▶　Journal club	
Member of the literature discussion group of Mol. Biology	2008-2009
▶　Individual research training	
Paola Bonfante Lab, Torino University, Torino, Italy	Mar 16-Apr 11, 2009
Subtotal In-Depth Studies	*10.9 credits**

4) Personal development	*date*
▶　Skill training courses	
Academic Writing I	Jan 08-May 13, 2008
Career Perspectives	Mar-May 2010
Techniques for writing and presenting scientific papers	Oct 19-22, 2010
▶　Organisation of PhD students day, course or conference	
▶　Membership of Board, Committee or PhD council	
Subtotal Personal Development	*4.3 credits**

TOTAL NUMBER OF CREDIT POINTS*	**50.6**

Herewith the Graduate School declares that the PhD candidate has complied with the educational requirements set by the Educational Committee of
EPS which comprises of a minimum total of 30 ECTS credits

* A credit represents a normative study load of 28 hours of study.